8-1-2017

Numerical Methods for Option Pricing under the Two-Factor Models

Jiacheng Cai
University of Nevada, Las Vegas, caij@unlv.nevada.edu

NUMERICAL METHODS FOR OPTION PRICING UNDER THE TWO-FACTOR MODELS

by

Jiacheng Cai

Bachelor of Science - Mathematics
University of Science and Technology of China, China
2011

A dissertation submitted in partial fulfillment of
the requirements for the

Doctor of Philosophy - Mathematical Sciences

Department of Mathematical Sciences
College of Sciences
The Graduate College

University of Nevada, Las Vegas
August 2017

UNLV | GRADUATE COLLEGE

Dissertation Approval

The Graduate College
The University of Nevada, Las Vegas

August 2, 2017

This dissertation prepared by

Jiacheng Cai

entitled

Numerical Methods for Option Pricing under the Two-Factor Models

is approved in partial fulfillment of the requirements for the degree of

Doctor of Philosophy - Mathematical Sciences
Department of Mathematical Sciences

Hongtao Yang, Ph.D.
Examination Committee Chair

Michael Marcozzi, Ph.D.
Examination Committee Member

Monika Neda, Ph.D.
Examination Committee Member

Pengtao Sun, Ph.D.
Examination Committee Member

Jianzhong Zhang, Ph.D.
Graduate College Faculty Representative

Kathryn Hausbeck Korgan, Ph.D.
Graduate College Interim Dean

ABSTRACT

NUMERICAL METHODS FOR OPTION PRICING UNDER THE TWO-FACTOR MODELS

by

Jiacheng Cai

Dr. Hongtao Yang, Examination Committee Chair
Associate Professor of Mathematics
University of Nevada, Las Vegas, USA

Pricing options under multi-factor models are challenging and important problems for financial applications. In particular, the closed form solutions are not available for the American options and some European options, and the correlations between factors increase the complexity and difficulty for the formulations and implements of the numerical methods.

In this dissertation, we first introduce a general transformation to decouple correlated stochastic processes governed by a system of stochastic differential equations. Then we apply the transformation to the popular two-factor models: the two-asset model, the stochastic volatility model, and the stochastic interest rate models. Based on our new formulations, we develop a mixed Monte Carlo method, a lattice method, and a finite volume-alternating direction implicit method for pricing the European and American options under these models. The proposed methods can be easily implemented and need less memory. Numerical results are also presented to validate our C++ programs and to examine our methods. It shows that our methods are very accurate and efficient.

ACKNOWLEDGEMENTS

I would like to express my deepest gratitude to my advisor, Dr. Hongtao Yang for his guidance, support, and expertise. I would never have been able to finish my dissertation without his help. I am also very grateful to my committee members Dr. Michael Marcozzi, Dr. Monika Neda, Dr. Pengtao Sun, and Dr. Jianzhong Zhang for their time, expertise and support. I want to thank Dr. Jichun Li for his help.

I would also like to thank my friends Robert Ain, Moinak Bhaduri, Sean Breckling, Sharang Chaudhry, Min Chen, Daniel Corral, Zhiwei Fang, Zhanman He, Edward Huynh, Rihui Lan, Bowen Liu, John Nguyen, Wenxin Peng, Gary Phelps, Sidney Shield, Xudong Sun, Yuzhou Sun, Zhou Wang, Jianbo Xu, Lanxuan Yu, and Libo Zhou for their helps during this journey.

Finally I would like to show my gratitude and appreciation to my parents Mr. Jianxin Cai and Mrs. Lixuan Lin, my brother Jiarun Cai, and my entire family for their love. Their constant support and encouragement over the years motivated me to work more effectively and efficiently towards my goal.

TABLE OF CONTENTS

LIST OF TABLES

LIST OF FIGURES

CHAPTER 1

INTRODUCTION

In finance, an option is a contract that gives the buyer (owner) the right (no obligation) to buy or to sell an underlying asset at a specified strike price on or before a specified date. Whenever the buyer exercises the option, the seller of the option has the obligation to fulfill the transaction. The buyer pays a premium, which is the value of the option, to the seller for the right. The options that gives the right to buy the underlying asset is referred to as a call option, whereas a put option gives the right to sell the asset. There are two standard styles of options: the European and American options. The European options can only be exercised at the option expiration date, while the American options allow the owner to exercise at any time up to the option expiration date. The other styles such as the Asian options, Bermuda options, look-back options, etc. are referred as the exotic options.

The valuation problem of the options has been widely studied. The classical model (Black-Scholes Model) for stock options was first introduced by Fischer Black and Myron Scholes in 1973 ([5]). Since then, the extensions of their model to other financial derivatives have been investigated ([34][40]), for example, bonds and their options, futures, swaps, etc. Besides one factor models, various multi-factor models have been proposed in order to fit the real markets more accurately. These models include the jump diffusion models (the Merton model and Kuo model), stochastic volatility models (the Heston model), stochastic interest rate models (the Vasicek model and the CIR model for interest rate processes), the stochastic volatility with jump (the Bates model), etc.

Most of the European options under the multi-factor models cannot be evaluated analytically or efficiently, and the American options have to be evaluated numerically. Pricing of these options becomes one of the most challenging and important problems for financial applications. The difficulty is either due to the nonlinearity (the American option problems) or the correlation between the factors. Various numerical methods have been extensively studied such as Monte Carlo method, lattice method, finite difference/element/volume methods, and semi-analytic methods. We are referred to [28][34][40][54] and the references cites therein.

The objective of this dissertation is to develop several numerical methods to approximate option prices under popular two-factor models by decoupling the correlated two factors.

1.1 Option Pricing under Two-Factor Models

In this section, we review the existing works on option pricing under the two-asset model, the Heston model and the stochastic interest rate models.

1.1.1 The Two-Asset Model

The two-asset model is the extension of the Black-Scholes model from one asset to two. The price processes of the assets are governed by the following stochastic differential equations

$$\frac{dS_i(t)}{S_i(t)} = (r - q_i)dt + \sigma_i dB_i(t), \quad i = 1, 2,$$

where r is the risk-free interest rate, q_i is the dividend rate and σ_i is the volatility for the i-th asset, and the Wiener processes $B_1(t)$ and $B_2(t)$ are correlated with the correlation $dB_1(t)dB_2(t) = \rho dt$.

Let $V(s_1, s_2, t)$ be the value of the option when $S_1(t) = s_1$ and $S_2(t) = s_2$ at time $t \in [0, T)$. According to the no-arbitrage pricing theory, the rational price of the European option with the payoff $\Phi(s_1, s_2)$ (see Table 1.1) is given by

$$V(s_1, s_2, t) = \mathbb{E}\left[e^{-r(T-t)}\Phi(S_1(T), S_2(T)) \middle| S_1(t) = s_1, S_2(t) = s_2 \right].$$

For the American option, we have

$$V(s_1, s_2, t) = \sup_{t \le \tau \le T} \mathbb{E}\left[e^{-r(\tau-t)}\Phi(S_1(\tau), S_2(\tau)) \middle| S_1(t) = s_1, S_2(t) = s_2 \right],$$

where $\mathbb{E}$ is the expectation under the risk neutral measure and the τ is a stopping time. The most used payoff functions are

Type	Payoff
Spread	$\max(S_2 - S_1 - K, 0)$
Call on maximum	$\max(\max(S_1, S_2) - K, 0)$
Maximum call	$\max(\max(S_1 - K_1, 0), \max(S_2 - K_2, 0))$
Put on minimum	$\max(K - \min(S_1, S_2), 0)$
Maximum put	$\max(\max(K_1 - S_1, 0), \max(K_2 - S_2, 0))$

Table 1.1: Popular two-asset options

It is known that the European option price is the solution of the following partial differential equation

$$\frac{\partial V}{\partial t} + \mathcal{L}V = 0,$$

where

$$\mathcal{L}V = \frac{1}{2}\sum_{ij}^{2} \rho\sigma_i\sigma_j s_i s_j \frac{\partial^2 V}{\partial s_i \partial s_j} + \sum_{i}^{2}(r - q_i)s_i \frac{\partial V}{\partial s_i} - rV.$$

For the American option, we have the following variational inequality problem

$$\frac{\partial V}{\partial t} + \mathcal{L}V \le 0, \quad V \ge \Phi, \quad (V - \Phi)\left(\frac{\partial V}{\partial t} + \mathcal{L}V\right) = 0.$$

The expectation for the European option price can be expressed in term of the CDF of the normal and multi-variate normal distribution for the exchange option ([46]) and the options on the maximum or minimum ([56, 37]), respectively. For the spread option, we reformulate the expectation as the one with respect to two independent processes so that it can be also computed by numerical integration (see (3.14) of Example 3.1).

There are several numerical methods developed for the American options. Boyle, Evnine and Gibbs [7] applied the binomial tree methods in two and three underlying assets. Gamba and Trigeorgis [27] improved the lattice method by using a transformation to obtain uncorrelated processes. Monte Carlo methods are applied to the high dimensional European options valuation [8] and the upper and lower boundaries of the American option value. Details of Monte Carlo application are shown in Glasserman's book [28]. Kovalov, Linetsky and Marcozzi [41] developed a computational method for the valuation of multi-asset American-style options based on approximating partial differential variational inequality. We are also referred to [25] for a comprehensive survey of numerical methods in high dimensional American options.

1.1.2 The Stochastic Volatility Model

The Heston model, a commonly used stochastic volatility model, was proposed by Heston in 1993 [33]. It assumes the stochastic volatility v and underlying asset price S follow

$$\begin{aligned} dv(t) &= \kappa\left[\eta - v(t)\right]du + \sigma\sqrt{v(t)}dB_1(t), \\ \frac{dS(t)}{S(t)} &= (r-q)dt + \sqrt{v(t)}dB_2(t), \end{aligned}$$

where η is the long-term expectation of variance, $\kappa > 0$ is the speed of mean reversion, σ is the volatility of volatility, and the Wiener processes $B_1(t)$ and $B_2(t)$ are correlated with correlations $dB_1(t)dB_2(t) = \rho dt$. If $2\kappa\eta > \sigma^2$ (Feller condition), then $v(t)$ is strictly positive ([13]).

Let $V(s, v, t)$ be the value of the option when $v(t) = v$ and $S(t) = s$ at time t. It is known that the European option price is the solution of the following partial differential equation

$$\frac{\partial V}{\partial t} + \mathcal{L}V = 0,$$

where

$$\mathcal{L}V = \frac{1}{2}s^2 v\frac{\partial^2 V}{\partial s^2} + \rho\sigma s v\frac{\partial^2 V}{\partial s\partial v} + \frac{1}{2}\sigma^2 v\frac{\partial^2 V}{\partial v^2} + (r-q)s\frac{\partial V}{\partial s} + \kappa(\eta - v)\frac{\partial V}{\partial v} - rV.$$

For the American option, we have the following variational inequality problem:

$$\frac{\partial V}{\partial t} + \mathcal{L}V \leq 0, \quad V \geq \Phi, \quad (V - \Phi)\left(\frac{\partial V}{\partial t} + \mathcal{L}V\right) = 0.$$

The European option price can be computed by numerical integration with the characteristic function of $S(T)$ ([33]). Since there is no closed form solution for the American option problem under the Heston model, various numerical methods have been considered. For the Monte Carlo methods, we are referred to [28] and references cited therein. Loeper and

Pironneau [44] introduced a mixed PDE/Monte Carlo method for the European options with stochastic volatility. Longstaff and Schwartz [45] provided a Monte Carlo regression method for the American option. As to the lattice method, several papers [42][53] studied the application in this type of models. Beliaeva and Nawalkha [4] proposed a lattice scheme by using a transformation to generate path-independent tree. A detailed survey of lattice method application in the Heston model is presented in [4]. For the finite difference approaching, we are referred to Zvan, Forsyth and Vetzal[62], Oosterlee [50], Ikonen and Toivanen [36]. Haenetjens and in't Hout [31] presented a summary of ADI schemes for pricing the American option under the Heston model. However, the above works didn't avoid the mixed partial derivative terms raising from the correlation. Detail survey of finite difference scheme can be found in [31].

1.1.3 The Stochastic Interest Rate Models

Stochastic interest rate models assume that the asset price follows

$$\frac{dS(t)}{S(t)} = (r(t) - q)dt + \sigma dB_1(t).$$

The stochastic interest rate $r(t)$ follows the Vasicek model ([58])

$$dr(t) = \kappa(\theta - r(t))dt + v dB_2(t)$$

or the CIR model ([13])

$$dr(t) = \kappa\left(\theta - r(t)\right)du + v\sqrt{r(t)}dB_2(t).$$

Here θ is the long-term expectation of interest rate, $\kappa > 0$ is the speed of mean reversion, v is the volatility of the interest rate, and the Wiener processes $B_1(t)$ and $B_2(t)$ are correlated with the correlation $dB_1(t)dB_2(t) = \rho dt$.

Let $V(s, r, t)$ be the value of the option when $S(t) = s$ and $r(t) = r$ at time t. It is known that the European option price is the solution of the following partial differential equation

$$\frac{\partial V}{\partial t} + \mathcal{L}V = 0,$$

where for the Vasicek model,

$$\mathcal{L}V = \frac{1}{2}s^2\sigma^2\frac{\partial^2 V}{\partial s^2} + \rho\sigma s v\frac{\partial^2 V}{\partial s\partial r} + \frac{1}{2}v^2\frac{\partial^2 V}{\partial r^2} + (r-q)s\frac{\partial V}{\partial s} + \kappa(\theta - r)\frac{\partial V}{\partial r} - rV,$$

and for the CIR model,

$$\mathcal{L}V = \frac{1}{2}s^2\sigma^2\frac{\partial^2 V}{\partial s^2} + \rho\sigma s v\sqrt{r}\frac{\partial^2 V}{\partial s\partial r} + \frac{1}{2}v^2 r\frac{\partial^2 V}{\partial v^2} + (r-q)s\frac{\partial V}{\partial s} + \kappa(\theta - r)\frac{\partial V}{\partial r} - rV.$$

For the American option, we have the following variational inequality problem

$$\frac{\partial V}{\partial t} + \mathcal{L}V \le 0, \quad V \ge \Phi, \quad (V - \Phi)\left(\frac{\partial V}{\partial t} + \mathcal{L}V\right) = 0.$$

For the European options, we are referred to Kim and Kunitomo [38] for an analytic approximation for the CIR model and Fang [23] for an analytic formula for the Vasicek model. However, there are few papers about the numerical methods for the American options under the stochastic interest rate models.

1.2 Summary and Organization of this Dissertation

In this dissertation, we propose a transformation to decouple correlated stochastic processes governed by a system of stochastic differential equations. Then we apply the new transformation to the popular two-factor models: the two-asset model, the stochastic volatility model, and the stochastic interest rate models. Based on our new formulations, we develop a mixed Monte Carlo method, a lattice method, and a finite volume-alternating direction implicit method for pricing the European and American options under these models. The proposed methods can be easily implemented and need less memory. Numerical results are also presented to validate our C++ programs and to examine our methods. The numerical experiments show our methods are highly accurate and efficient.

The outlines of the remaining chapters are as follows:

- **Chapter 2: Decoupling Multi-factor models.**

  A transformation to decouple correlated stochastic processes is introduced and applied to the popular two-factor models.

- **Chapter 3: Mixed Monte Carlo Methods with Control Variates.**

  With the uncorrelated new processes, we are able to express the rational prices of the European contingent claims under the two-factor models as the nested expectations. The inner expectation is the price of the European contingent claim for an artificial asset and can be analytically evaluated by the Black-Scholes formula. Then we use the Monte Carlo method to estimate the outer expectation. We also employ the control variates technique to reduce the variances. Numerical results are presented to examine our methods.

- **Chapter 4: Lattice Methods.**

  We propose a new lattice method for the European and American options under the two-asset model and the stochastic interest rate models. Since our schemes are based on the uncorrelated stochastic differential equations, they need less nodes to generate the lattice and thus can be easily implemented. Numerical results are also presented to examine our methods and the early exercise boundaries for the American options.

- **Chapter 5: A Finite Volume - Alternative Direction Implicit Method.**

  We develop a finite volume - alternating direction implicit method for the transformed American option problem under the stochastic volatility model (the Heston model). Numerical results show that the method provides fast and accurate approximations of option prices for all the possible combinations of the model parameters.

- **Chapter 6: Conclusion.**

  We summarize the dissertation and propose several future research topics.

CHAPTER 2

DECOUPLING MULTI-FACTOR MODELS

In this chapter, we shall introduce a transformation to decouple correlated stochastic processes governed by a system of stochastic differential equations. Hence, the option prices can be evaluated by the nested expectations and the partial differential equations without the mixed terms.

2.1 Decoupling the Correlated Stochastic Processes

Consider the following system of stochastic differential equations

$$dX_i(t) = \phi_i\left(t, X(t)\right) dt + \psi_i\left(t, X(t)\right) dB_i(t), \quad i = 1, \ldots, n, \tag{2.1}$$

where $X(t) = \left(X_1(t), \ldots, X_n(t)\right)^T$ and $B_1(t), \ldots, B_n(t)$ are Wiener processes. Let

$$\Sigma = \begin{bmatrix} 1 & \rho_{12} & \rho_{13} & \cdots & \rho_{1n} \\ \rho_{21} & 1 & \rho_{23} & \cdots & \rho_{2n} \\ \rho_{31} & \rho_{32} & 1 & \cdots & \rho_{3n} \\ \vdots & \vdots & \vdots & \ddots & \vdots \\ \rho_{n1} & \rho_{n2} & \rho_{n3} & \cdots & 1 \end{bmatrix},$$

where

$$dB_i(t)dB_j(t) = \rho_{ij}dt.$$

It is known that Σ is a positive definite matrix. Thus it admits the following Cholesky decomposition

$$\Sigma = AA^T,$$

where $A = (a_{ij})$ is a lower triangular matrix with positive diagonal entries. For $n = 2$ and $n = 3$, we have

$$A = \begin{bmatrix} 1 & 0 \\ \rho_{12} & \sqrt{1-\rho_{12}^2} \end{bmatrix}, \tag{2.2}$$

and

$$A = \begin{bmatrix} 1 & 0 & 0 \\ \rho_{12} & \sqrt{1-\rho_{12}^2} & 0 \\ \rho_{13} & \frac{\rho_{23}-\rho_{12}\rho_{13}}{\sqrt{1-\rho_{12}^2}} & \sqrt{1-\rho_{13}^2-\left(\frac{\rho_{23}-\rho_{12}\rho_{13}}{\sqrt{1-\rho_{12}^2}}\right)^2} \end{bmatrix}. \tag{2.3}$$

Let

$$W(t) = \begin{bmatrix} W_1(t) \\ \vdots \\ W_n(t) \end{bmatrix} = A^{-1} \begin{bmatrix} B_1(t) \\ \vdots \\ B_n(t) \end{bmatrix}.$$

It is easy to verify that W is a n-dimensional Brownian motion. Assume that

$$\psi_i\left(t, X(t)\right) = \lambda_i \psi\left(t, X(t)\right), \quad i = 1, \dots, n, \tag{2.4}$$

where $\lambda_1, \dots, \lambda_n$ are constants. Then the system (2.1) can be rewritten to

$$dX(t) = \Phi\left(t, X(t)\right) dt + \psi(t, X(t)) \Lambda A dW(t), \tag{2.5}$$

where $\Phi\left(t, X(t)\right) = \left(\phi_1\left(t, X(t)\right), \dots, \phi_n\left(t, X(t)\right)\right)^T$ and $\Lambda = \operatorname{diag}\left(\lambda_1, \dots, \lambda_n\right)$. Let

$$Y(t) = \begin{bmatrix} Y_1(t) \\ \vdots \\ Y_n(t) \end{bmatrix} = BX(t), \tag{2.6}$$

where $B = \Lambda D(\Lambda A)^{-1}$ and $D = \operatorname{diag}\left(a_{11}, \dots, a_{nn}\right)$. Then we have by (2.5)

$$dY(t) = \Lambda D(\Lambda A)^{-1} \Phi\left(t, B^{-1}Y(t)\right) dt + \psi\left(t, B^{-1}Y(t)\right) \Lambda D dW(t). \tag{2.7}$$

It is apparent that the new processes $Y_1(t), \dots, Y_n(t)$ are mutually uncorrelated.

Remark 2.1. when $n = 2$, we may assume that λ_1 is a function of X_1 instead of a constant. Let

$$Y_1(t) = X_1(t), \quad Y_2(t) = X_2(t) - F(X_1(t)),$$

where

$$F(x) = a_{21} \int_0^x \lambda_1(u) du.$$

Then we have by (2.5)

$$\begin{aligned} dY_1(t) &= \phi_1(t, X(t))dt + \psi_1(t, X(t))dW_1(t), \\ dY_2(t) &= dX_2(t) - a_{21}\lambda_1(X_1(t))dX_1(t) - \frac{1}{2} a_{21} \left(\lambda_1'(X_1(t))\right)^2 \left(\psi_1(t, X(t))\right)^2 dt \\ &= \widetilde{\phi}_2(t, X(t))dt + a_{22}\sqrt{1-\rho_{12}^2}\psi_2(t, X(t))dW_2(t), \end{aligned}$$

where

$$\widetilde{\phi}_2(t, X(t)) = \phi_2(t, X(t)) - a_{21}\lambda_1(X_1(t))\phi_1(t, X(t)) - \frac{1}{2}\left(\lambda_1'(X_1(t))\right)^2 \left(\psi_1(t, X(t))\right)^2.$$

2.2 Two-Factor Models

In this section, we will apply the decoupling transformation in the previous section to the various popular two-factor models in asset pricing.

2.2.1 The Two-Asset Model

The two-asset model reads as follows

$$\frac{dS_i(t)}{S_i(t)} = (r - q_i)dt + \sigma_i dB_i(t), \quad i = 1, 2, \tag{2.8}$$

where r is the risk-free interest rate, q_i is the dividend rate for the i-th asset, σ_i is the volatility, and the Wiener processes $B_1(t)$ and $B_2(t)$ are correlated with the correlation

$dB_1(t)dB_2(t) = \rho dt$. Let

$$X_i(t) = \ln\left(\frac{S_i(t)}{S_i(0)}\right), \quad i = 1, 2. \tag{2.9}$$

where $S_i(0)$ is a given asset price. Then we have by Ito's Lemma

$$dX_i(t) = \left(r - q_i - \frac{1}{2}\sigma_i^2\right)dt + \sigma_i dB_i(t), \quad i = 1, 2.$$

Notice that

$$\psi(t, X(t)) \equiv 1, \quad \lambda_i = \sigma_i, \quad i = 1, 2.$$

Let

$$\widetilde{\sigma}_2 = \sqrt{1-\rho^2}\sigma_2, \quad \tilde{q}_2 = q_2 + \frac{1}{2}\rho^2\sigma_2^2 + \frac{\rho\sigma_2}{\sigma_1}\left(r - q_1 - \frac{1}{2}\sigma_1^2\right),$$
$$\mu_1 = r - q_1 - \frac{1}{2}\sigma_1^2, \quad \mu_2 = r - \widetilde{q}_2 - \frac{1}{2}\widetilde{\sigma}_2^2.$$

Then we have by (2.2), (2.6) and (2.7)

$$Y_1(t) = X_1(t), \tag{2.10}$$

$$Y_2(t) = -\frac{\rho\sigma_2}{\sigma_1}X_1(t) + X_2(t), \tag{2.11}$$

and

$$dY_1(t) = \mu_1 dt + \sigma_1 dW_1(t), \tag{2.12}$$

$$dY_2(t) = \mu_2 dt + \widetilde{\sigma}_2 dW_2(t). \tag{2.13}$$

Remark 2.2. We are referred to [27] for a similar transformation.

2.2.2 The Stochastic Volatility Model

The most popular stochastic volatility model is also known as the Heston model ([33]). It models one asset price process and its variance as follows

$$dv(t) = \kappa\left(\eta - v(t)\right)du + \sigma\sqrt{v(t)}dB_1(t), \tag{2.14}$$

$$\frac{dS(t)}{S(t)} = (r-q)dt + \sqrt{v(t)}dB_2(t), \tag{2.15}$$

where r is the risk-free interest rate, q is the dividend rate for the asset, σ is the volatility of volatility, and the Wiener processes $B_1(t)$ and $B_2(t)$ are correlated with the correlation $dB_1(t)dB_2(t) = \rho dt$. Let

$$X_1(t) = v(t), \quad X_2(t) = \ln\left(\frac{S(t)}{K}\right), \tag{2.16}$$

where K is the strike price. Then we have by Ito's Lemma

$$\begin{aligned} dX_1(t) &= \kappa\left(\eta - X_1(t)\right)du + \sigma\sqrt{X_1(t)}dB_1(t), \\ dX_2(t) &= \left(r - q - \frac{1}{2}X_1(t)\right)dt + \sqrt{X_1(t)}dB_2(t). \end{aligned}$$

Notice that

$$\psi(t, X(t)) = \sqrt{X_1(t)}, \quad \lambda_1 = \sigma, \quad \lambda_2 = 1.$$

We have by (2.6) and (2.7)

$$Y_1(t) = X_1(t), \quad Y_2(t) = -\frac{\rho}{\sigma}X_1(t) + X_2(t), \tag{2.17}$$

and

$$dY_1(t) = (a_1 + b_1 Y_1(t))dt + \sigma\sqrt{Y_1(t)}dW_1(t), \tag{2.18}$$

$$dY_2(t) = (a_2 + b_2 Y_1(t))dt + \sqrt{(1-\rho^2)Y_1(t)}dW_2(t), \tag{2.19}$$

where

$$\rho = \rho_{12}, \quad a_1 = \kappa\eta, \quad b_1 = -\kappa, \quad a_2 = r - q - \frac{\rho}{\sigma}\kappa\eta, \quad b_2 = \frac{\rho}{\sigma}\kappa - \frac{1}{2}.$$

Remark 2.3. We are referred to [4] for a similar transformation.

2.2.3 The Stochastic Interest Rate Model

The interest rates may be assumed to follow a stochastic process. Here we consider two popular interest rate models: the CIR model ([13]) and Vasicek model ([58]). The coupled stochastic differential equations for the asset price and interest rate are as follows

$$dr(t) = \kappa(\theta - r(t))dt + v(r(t))^p dB_1(t), \tag{2.20}$$

$$\frac{dS(t)}{S(t)} = (r(t) - q)dt + \sigma dB_2(t), \tag{2.21}$$

where q is the dividend rate, θ is the long-term expectation of interest rate, $\kappa > 0$ is the speed of mean reversion, σ is the volatility of the stock price, and $v > 0$. It is the Vasicek model and the CIR model when $p = 0$ and $p = \frac{1}{2}$, respectively.

Let

$$X_1(t) = (r(t))^{1-p}, \quad X_2(t) = \ln\left(\frac{S(t)}{K}\right), \tag{2.22}$$

where K is the strike price. Then we have by Ito's Lemma

$$dX_1(t) = \mu_1(X_1(t))dt + \sigma_1 dB_1(t),$$
$$dX_2(t) = \left((X_1(t))^{\frac{1}{1-p}} - q - \frac{1}{2}\sigma^2\right)dt + \sigma dB_2(t),$$

where

$$\mu_1(x) = (1-p)\kappa\left(\frac{\theta}{x^{\frac{p}{1-p}}} - x\right) - \frac{p(1-p)v^2}{2x}, \quad \sigma_1 = (1-p)v.$$

Since

$$\psi(t, X(t)) = 1, \quad \lambda_1 = (1-p)v, \quad \lambda_2 = \sigma,$$

we have by (2.6) and (2.7)

$$Y_1(t) = X_1(t), \quad Y_2(t) = -\frac{\rho\sigma}{(1-p)v}X_1(t) + X_2(t), \tag{2.23}$$

and

$$dY_1(t) = \mu_1\left(Y_1(t)\right)dt + \sigma_1 dW_1(t), \tag{2.24}$$

$$dY_2(t) = \mu_2\left(Y_1(t)\right)dt + \sigma_2 dW_2(t). \tag{2.25}$$

where

$$\mu_2(y) = y^{\frac{1}{1-p}} - q - \frac{1}{2}\sigma^2 - \frac{\rho\sigma}{(1-p)v}\mu_1(y). \quad \sigma_2 = \sigma\sqrt{1-\rho^2},$$

Remark 2.4. When $p = \frac{1}{2}$, using the transformation in Remark 2.1, we obtain

$$Y_1(t) = X_1(t), \quad Y_2(t) = X_2(t) - \frac{2\rho\sigma}{v}\sqrt{X_1(t)}, \tag{2.26}$$

and

$$dY_1(t) = \kappa(\theta - Y_1(t))dt + v\sqrt{Y_1(t)}dW_1(t), \tag{2.27}$$

$$dY_2(t) = g(Y_1(t))dt + \sigma\sqrt{1-\rho^2}dW_2(t), \tag{2.28}$$

where

$$g(Y_1(t)) = \left(Y_1(t) - q - \frac{1}{2}\sigma^2 - \frac{2\rho\sigma\kappa}{v\sqrt{Y_1(t)}}(\theta - Y_1(t)) + \frac{\rho\sigma v}{4\sqrt{Y_1(t)}}\right).$$

CHAPTER 3

MIXED MC METHODS WITH CONTROL VARIATES

The mixed Monte Carlo method was first introduced by Loeper and Pironneau[44] for s-tochastic volatility model. Cozma and Reisinger extended the method into Heston-CIR model [16]. In their paper, the stochastic volatility/interest rate process are simulated using Monte Carlo method, while the option values based on the the asset prices are computed via PDE/Analytic method. However, their simulation processes and asset price process are in fact not independent. In this chapter, the mixed Monte Carlo method is developed based on our decoupled stochastic processes in Chapter 2. We shall show that the rational prices of the European contingent claims under various two-factor models can be expressed as the nested expectations. The inner expectation is the price of the European contingent claim for an artificial asset and can be analytically evaluated by the Black-Scholes formula. We also use the method of control variates to reduce the variance.

3.1 The Two-Asset Model

Solving the stochastic differential equations (2.12) and (2.13), we get

$$Y_1(t,T) = \left(r - q_1 - \frac{1}{2}\sigma_1^2\right)(T-t) + \sigma_1(W_1(T) - W_1(t)),$$
$$Y_2(t,T) = \left(r - \tilde{q}_2 - \frac{1}{2}\widetilde{\sigma}_2^2\right)(T-t) + \widetilde{\sigma}_2(W_2(T) - W_2(t)).$$

Then we have by (2.9), (2.10) and (2.11)

$$S_1(T) = S_1(t)e^{Y_1(t,T)}, \quad S_2(T) = S_2(t)e^{\alpha Y_1(t,T)+Y_2(t,T)}, \tag{3.1}$$

where $\alpha = \frac{\rho\sigma_2}{\sigma_1}$. We introduce the artificial asset price process

$$\widetilde{S}_2(t) = \widetilde{S}_2(0)e^{Y_2(0,t)},$$

where

$$\widetilde{S}_2(0) = \frac{S_2(0)}{S_1^\alpha(0)},$$

which satisfies the SDE

$$\frac{d\widetilde{S}_2(t)}{\widetilde{S}_2(t)} = (r - \tilde{q}_2)dt + \widetilde{\sigma}_2 dW_2(t).$$

Then we have

$$S_2(t) = S_1^\alpha(t)\widetilde{S}_2(t), \quad t \in [0,T].$$

Let $\Phi(S_1(T), S_2(T))$ be the payoff of a European contingent claim. Then its price at time t is given by

$$\begin{aligned} V(S_1,S_2,t;T) &= \mathbb{E}\left[e^{-(T-t)r}\Phi(S_1(T),S_2(T))\middle|\, S_1(t)=S_1, S_2(t)=S_2\right] \qquad (3.2)\\ &= \mathbb{E}\left[e^{-(T-t)r}\Phi\left(S_1(T), S_1^\alpha(T)\widetilde{S}_2(T)\right)\middle|\, S_1(t)=S_1, \widetilde{S}_2(t)=S_1^{-\alpha}S_2\right]\\ &= \mathbb{E}\left[\mathbb{E}\left[e^{-(T-t)r}\Phi\left(S_1(T), S_1^\alpha(T)\widetilde{S}_2(T)\right)\middle|\, \widetilde{S}_2(t)=S_1^{-\alpha}S_2\right]\middle|\, S_1(t)=S_1\right]\\ &= \mathbb{E}\left[\widetilde{V}\left(S_1^{-\alpha}S_2, S_1(T), t, T\right)\middle|\, S_1(t)=S_1\right], \qquad (3.3) \end{aligned}$$

where

$$\widetilde{V}\left(\widetilde{S}_2, z, t, T\right) = \mathbb{E}\left[e^{-(T-t)r}\Phi\left(z, z^{\alpha}\widetilde{S}_2(T)\right)\middle|\,\widetilde{S}_2(t) = \widetilde{S}_2\right]. \tag{3.4}$$

In the appendix, we shall work out the analytic formulas for $\widetilde{V}$ for various payoff functions Φ.

Our mixed Monte Carlo method (MMC) is based on evaluating the expectations in (3.3) while $\widetilde{V}$ is computed by using the analytic formula (see the appendix). The first algorithm is the crude Monte Carlo method:

Algorithm 1. A MMC method for the two-asset European contingent claim

---

1. Initialize positive integer N as the number of simulations. Set $V = 0$.
2. For $n = 1, 2, \ldots, N$, do
   - Simulate $Y_1 = Y_1(t, T)$ and compute $\widetilde{S}_1 = S_1 e^{Y_1}$.
   - Compute $P = \widetilde{V}\left(S_1^{-\alpha} S_2, \widetilde{S}_1, t, T\right)$.
   - Let $V = V + P$.

   End do.
3. The approximate value of the price is $\overline{V} = V/N$.

To speed up the crude Monte Carlo method, we use the technique of control variates to reduce the variance of the random variable $\widetilde{V}\left(S_1^{-\alpha} S_2, S_1(T), t, T\right)$. It is apparent that $\widetilde{V}$ is highly correlated to $Y_1(T)$. Hence we naturally take it for the control variates. Our algorithm for the mixed Monte Carlo method with the control variates (MMCCV) is as follows:

Algorithm 2. A MMCCV method for the two-asset European contingent claim

1. Initialize positive integers N as the number of simulations. Set

$$V = b_1 = b_2 = b_3 = 0$$

and

$$\overline{Y}_1 = \mathbb{E}\left[Y_1(t,T)\right] = \left(r - q_1 - \frac{1}{2}\sigma_1\right)(T-t).$$

2. For $n = 1, 2, \ldots, N$, do

   – Simulate $Y_1 = Y_1(t,T)$ and let $\widetilde{S}_1 = S_1 e^{Y_1}$.

   – Compute $P = \widetilde{V}\left(S_1^{-\alpha} S_2, \widetilde{S}_1, t, T\right)$.

   – Let

$$\begin{aligned}
b_1 &= b_1 + P(Y_1 - \overline{Y}_1),\\
b_2 &= b_2 + (Y_1 - \overline{Y}_1),\\
b_3 &= b_3 + \left(Y_1 - \overline{Y}_1\right)^2,\\
V &= V + P.
\end{aligned}$$

   End do.

3. Let $\overline{V} = V/N$, $b = \left(b_1 - \overline{V} b_2\right)/b_3$. The approximate value of the option price is $V^* = \overline{V} - b b_3/N$.

Remark 3.1. We use control variates technique for variance reduction according to Glasserman's book [28]. There are other techniques for variance reduction, like stratified sampling and Latin hypercube sampling. It shall be pointed out that variance reduction techniques usually introduce dependence across replications, but the dependence from control variate technique becomes negligible as the number of simulation increases, compared with other techniques.

Remark 3.2. According to the central limit theorem, we expect that the error from Monte

Carlo simulations is $\mathcal{O}\left(N^{-\frac{1}{2}}\right)$.

3.2 The Stochastic Volatility Model

We only consider the European call option since the European put options can be treated similarly. Let K be the strike price and T be the expiration date of the option.

Using (2.16), (2.17), (2.18), and (2.19), we have

$$S(T) = S(t)e^{X(t,T)+Y(t,T)}, \tag{3.5}$$

where

$$X(t,T) = (r-q)(T-t) - \frac{1}{2}\lambda^2 \int_t^T v(s)ds + \lambda \int_t^T \sqrt{v(s)}dW_2(s), \tag{3.6}$$

$$Y(t,T) = -\frac{1}{2}\rho^2 \int_t^T v(s)ds + \rho \int_t^T \sqrt{v(s)}dW_1(s), \tag{3.7}$$

where $\lambda = \sqrt{1-\rho^2}$.

Consider the artificial asset price process $\widetilde{S}(t) = \widetilde{S}(0)e^{X(0,t)}$ which is the solution to the following stochastic differential equation

$$\frac{d\widetilde{S}(t)}{\widetilde{S}(t)} = (r-q)dt + \lambda\sqrt{v(t)}dW_2(t).$$

If a path $\{v(s): \ t \le s \le T\}$ of the volatility is given, then the European call option price for this stock is given by

$$\begin{aligned}\widetilde{V}\left(\widetilde{S},t,T\right) &= \mathbb{E}\left[e^{-(T-t)r}\left(\widetilde{S}(t)e^{X(t,T)} - K\right)^+ \middle| \widetilde{S}(t) = \widetilde{S}\right] \\ &= e^{-q(T-t)}\widetilde{S}N(d_1) - e^{-r(T-t)}KN(d_2), \end{aligned} \tag{3.8}$$

where

$$d_1 = \frac{\ln\left(\frac{\widetilde{S}}{K}\right) + \left(r - q + \frac{1}{2}\widetilde{\sigma}^2\right)(T-t)}{\widetilde{\sigma}\sqrt{T-t}},$$

$$d_2 = d_1 - \widetilde{\sigma}\sqrt{T-t}, \quad \widetilde{\sigma} = \left(\frac{\lambda}{T-t}\int_t^T v(s)ds\right)^{\frac{1}{2}}.$$

Then the European call option price for the Heston model is given by

$$\begin{aligned} V(S,v,t,T) &= \mathbb{E}\left[e^{-(T-t)r}\left(S(t)e^{X(t,T)+Y(t,T)} - K\right)^+ \middle| S(t) = S, v(t) = v\right] \\ &= \mathbb{E}\left[\mathbb{E}\left[e^{-(T-t)r}\left(\widetilde{S}(t)e^{X(t,T)} - K\right)^+ \middle| \widetilde{S}(t) = Se^{Y(t,T)}\right] \middle| v(t) = v\right] \\ &= \mathbb{E}\left[\widetilde{V}\left(Se^{Y(t,T)}, t, T\right) \middle| v(t) = v\right]. \end{aligned} \tag{3.9}$$

As in the previous section, we have the following crude Monte Carlo algorithm:

Algorithm 3. A MMC method for the Heston European call option

---

1. Initialize positive integer N as the number of simulations. Set $V = 0$.

2. For $n = 1, 2, \ldots, N$, do

   - Simulate $Y = Y(t,T)$ and compute $\widetilde{S} = Se^Y \& \widetilde{\sigma}$.
   - Compute $P = \widetilde{V}\left(\widetilde{S}, t, T\right)$.
   - Let $V = V + P$.

   End do.

3. The approximate value of the option price is $\overline{V} = V/N$.

In order to reduce the variance, we use $Y(t,T)$ for the control variates. To this purpose, we need $\overline{Y} = \mathbb{E}\left[Y(t,T)|v(t) = v\right]$. Taking the expected value on both sides of (3.7) and solving the resulting differential equation gives

$$\mathbb{E}\left[v(s)|v(t) = v\right] = \eta + (v - \eta)e^{-\kappa t}.$$

Then we have by (3.7)

$$\begin{aligned}\overline{Y} &= \mathbb{E}\left[-\frac{1}{2}\rho^2\int_t^T v(s)ds + \rho\int_t^T \sqrt{v(s)}dW_1(s)\right] = -\frac{1}{2}\rho^2\int_t^T \mathbb{E}\left[v(s)\right]ds \\ &= -\frac{1}{2}\left(\eta(T-t) + \frac{v-\eta}{\kappa}\left(1-e^{-\kappa(T-t)}\right)\right).\end{aligned}$$

Our algorithm for the mixed Monte Carlo method with the control variates (MMCCV) is as follows:

Algorithm 4. A MMCCV method for the Heston European call option

---

1. Initialize positive integer N as the number of simulations. Set $V = 0,\ b_1 = 0,\ b_2 = 0$, and $b_3 = 0$.

2. For $n = 1, 2, \ldots, N$, do

   - Simulate $Y = Y(t, T)$ and compute $\widetilde{S} = Se^Y \& \widetilde{\sigma}$.
   - Compute $P = \widetilde{V}\left(\widetilde{S}, t, T\right)$.
   - Let

$$\begin{aligned} b_1 &= b_1 + P(Y - \overline{Y}), \\ b_2 &= b_2 + (Y - \overline{Y}), \\ b_3 &= b_3 + \left(Y - \overline{Y}\right)^2, \\ V &= V + P. \end{aligned}$$

   End do.

3. Let $\overline{V} = V/N$, $b = \left(b_1 - \overline{V}b_2\right)/b_3$. The approximate value of the option price is $V^* = \overline{V} - bb_3/N$.

Remark 3.3. Consider the stochastic volatility model with jumps introduced by Bates in

1996 ([3])

$$\frac{dS(t)}{S(t)} = (r - q - \lambda\zeta)\, dt + \sqrt{v(t)} dB_1(t) + dZ(t),$$
$$dv(t) = \kappa(\theta - v(t))dt + \sigma\sqrt{v(t)} dB_2(t),$$

where $Z(t) = \sum_{n=1}^{N(t)} \left(e^{J_n} - 1\right)$, $N(t)$ is a Poisson process with intensity λ and independent of the Brownian motions $B_1(t)$ and $B_2(t)$, $\{J_n\}_1^\infty$ is a sequence of independent and identically distributed normal random variables with the mean $\ln(1+\zeta)$ and variance δ^2, and $\mu_J = \mathbb{E}\left[e^{J_1} - 1\right]$ is the expected jump percentage. By Itô's formula, we get

$$S(T) = S(t)e^{X(t,T)+Y(t,T)+Z(t,T)}, \tag{3.10}$$

where $X(t,T)$ and $Y(t,T)$ are defined in (3.7) and (3.7), and $Z(t,T) = \sum_{n=N(t)}^{N(T)} J_n - \lambda_J \mu_J (T - t)$. Hence, we can apply the above two algorithms to the call option under the Bates model while $Y(t,T)$ is replaced by $Y(t,T) + Z(t,T)$.

3.3 The Stochastic Interest Rate Model

We only consider the Vasicek model and the CIR model can be treated similarly. Using (2.22), (2.23), (2.24), and (2.25), we have

$$S(T) = S(t)e^{X(t,T)+Y(t,T)},$$

where

$$X(t,T) = \int_t^T (r(s) - q)ds - \frac{1}{2}\lambda^2\sigma^2(T-t) + \lambda\sigma(W_2(T) - W_2(t)), \tag{3.11}$$
$$Y(t,T) = -\frac{1}{2}\rho^2\sigma^2(T-t) + \rho\sigma(W_1(T) - W_1(t)). \tag{3.12}$$

Define artificial asset price process $\widetilde{S}(t) = \widetilde{S}(0)e^{X(0,t)}$ that follows the SDE

$$\frac{d\widetilde{S}(t)}{\widetilde{S}(t)} = (r(t) - q)dt + \lambda\sigma dW_2(t).$$

If a path $\{r(s) : \ t \le s \le T\}$ of the interest rate is given, then the European call option price for this asset is given by

$$\widetilde{V}\left(\widetilde{S}, t, T\right) = \mathbb{E}\left[e^{-\int_t^T r(s)ds} \left(\widetilde{S}(t)e^{X(t,T)} - K\right)^+ \middle| \widetilde{S}(T) = \widetilde{S} \right], \tag{3.13}$$

which can be computed by a closed form formula. Then the European call option price for the stochastic interest rate model is given by

$$\begin{aligned} V(S, r, t) &= \mathbb{E}\left[e^{-\int_t^T r(s)ds} \left(S(t)e^{X(t,T)+Y(t,T)} - K\right)^+ \middle| S(t) = S, r(t) = r \right] \\ &= \mathbb{E}\left[\mathbb{E}\left[e^{-\int_t^T r(s)ds} \left(\widetilde{S}(t)e^{X(t,T)} - K\right)^+ \middle| \widetilde{S}(t) = Se^{Y(t,T)} \right] \middle| r(t) = r \right] \\ &= \mathbb{E}\left[\widetilde{V}\left(Se^{Y(t,T)}, t, T\right) \middle| r(t) = r \right]. \end{aligned}$$

Hence, we have the algorithms similar to Algorithms 3 – 4 to compute the above expectation for the call price.

3.4 Numerical Results

In this section, we present numerical examples to examine the convergence and accuracy of the proposed MMC and MMCCV methods in the previous sections. We only consider the European call options due to the put-call parity. For convenience, we introduce the following notations.

Notation	Meaning
REF	Reference value
CV	Numerical result using MMCCV
MMC	Numerical result using MMC
RMSE	Root mean square error
AE	Absolute error
MAE	Maximum absolute error
N	Number of MC simulations
M	Number of time steps for each simulation

Table 3.1: Notations

Example 3.1. (*The two-asset model*) In this example, we consider the European spread option, a popular two-asset option with payoff $\Phi(S_1(T), S_2(T)) = (S_1(T) - S_2(T) - K)^+$. The parameters are given in Table 3.2.

Parameters	Values
K	\$15
r	0.05
T	1.0 year
q_1	0.03
q_2	0.02
σ_1	0.10
σ_2	0.15
ρ	0.8

Table 3.2: The parameters for the spread option

Using the processes $Y_1(t)$ and $Y_2(t)$, we have for the value of the European contingent claim in (3.2)

$$V(S_1, S_2, t; T) = \mathbb{E}\left[e^{-(T-t)r}\widetilde{\Phi}(Y_1(T), Y_2(T)) \middle| Y_1(t) = Y_1, Y_2(t) = Y_2 \right]. \tag{3.14}$$

Since Y_1 and Y_2 follow independent normal distributions, the above expectation can be computed by numerical integration and will be taken as the reference values.

We first examine the rate of convergence with respect to the number of simulations N.

We display the maximum absolute errors and root mean square errors for $S_1 = 100$ and $S_2 = 50 : 5 : 120$ in Figs. 3.1–3.2, respectively. We can observe that the rate of convergence is about $\frac{1}{2}$ as expected. It is also shown that the MMCCV method is about 10 times accurate as the MMC method, which is due to the variances have been reduced significantly (see Fig. 3.3 for $S = 100$, $N = 2000$, $M = 1000$). We display the option prices and their errors in Table 3.3, which shows that the MMCCV method provides very accurate approximations of option prices even with a small number of simulations.

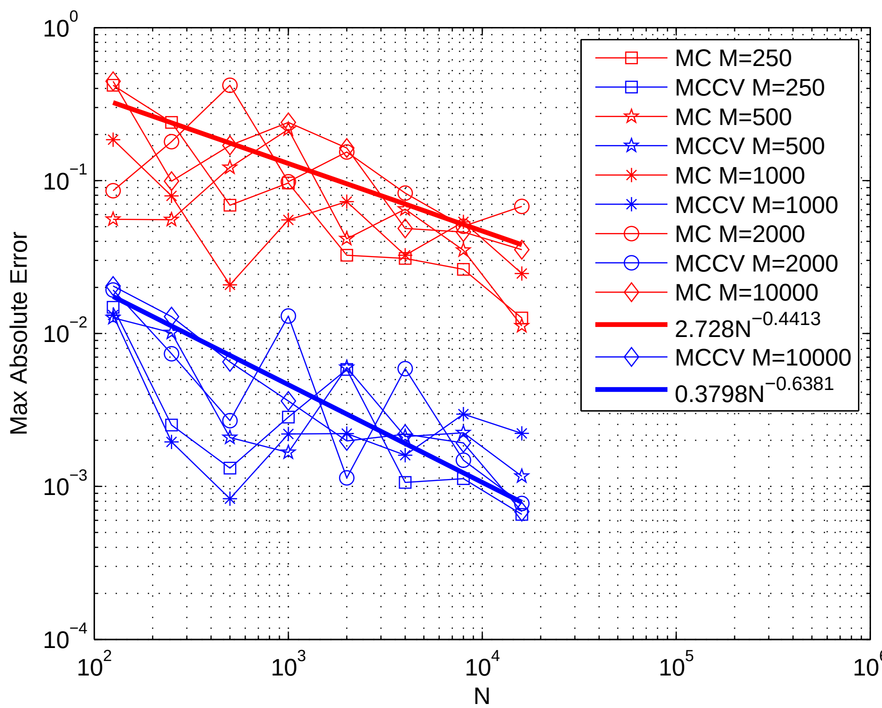

Figure 3.1: MAE vs N for the European spread option

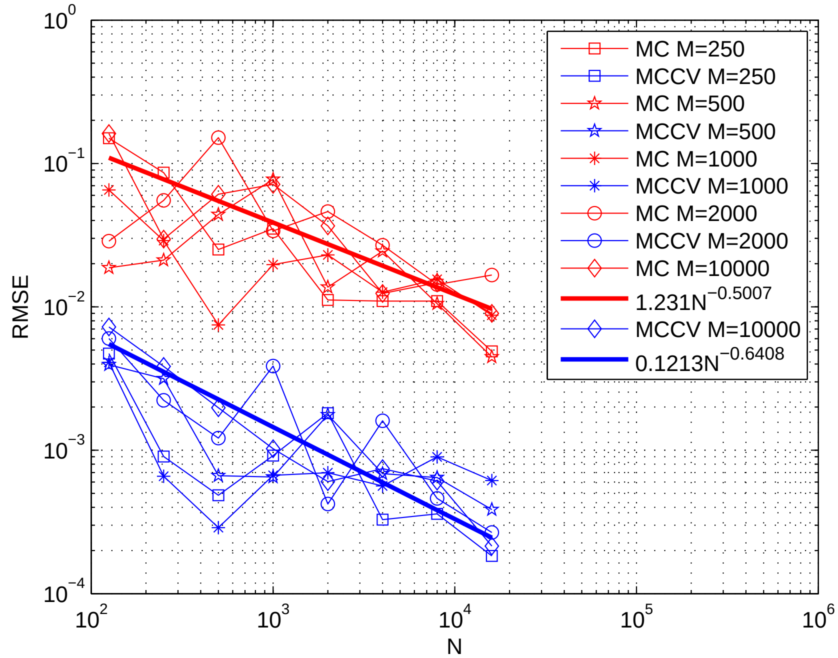

Figure 3.2: RMSE vs N for the European spread option

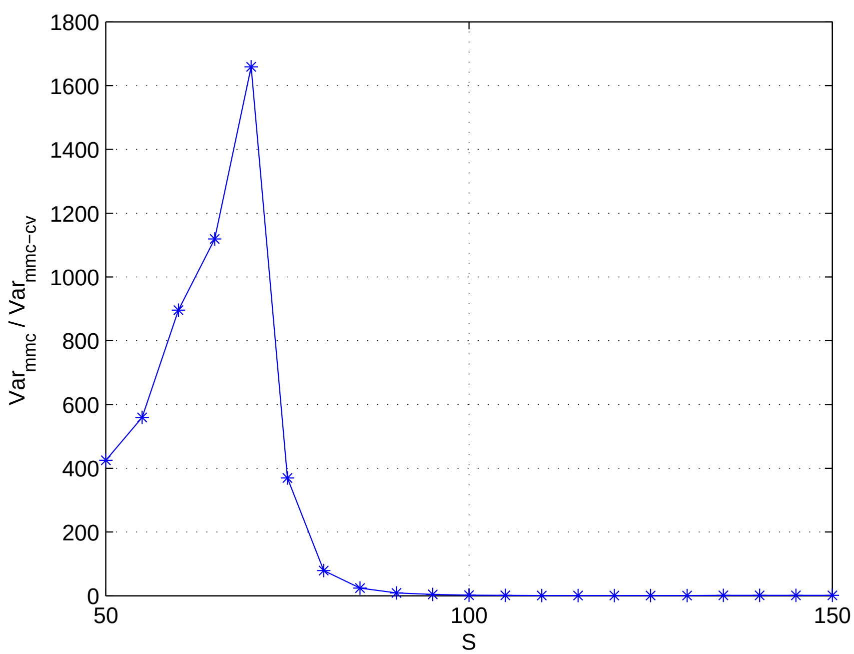

Figure 3.3: The variance ratios vs S_2 for the European spread option.

S_2	REF	CV	MMC	AE-CV	AE-MMC
50	33.766178	33.767729	33.800565	0.001551	0.034387
55	28.865186	28.866376	28.894166	0.001190	0.028980
60	23.964301	23.965129	23.987875	0.000828	0.023574
65	19.066659	19.066123	19.018384	0.000536	0.048275
70	14.208092	14.208159	14.173826	0.000067	0.034266
75	9.569087	9.569614	9.547782	0.000527	0.021305
80	5.581564	5.582259	5.570583	0.000695	0.010981
85	2.719943	2.719948	2.714905	0.000005	0.005038
90	1.085857	1.085859	1.084134	0.000002	0.001723
95	0.354055	0.354056	0.353592	0.000001	0.000463
100	0.095085	0.095085	0.094988	0.000000	0.000097
105	0.021342	0.021342	0.021326	0.000000	0.000016
110	0.004073	0.004071	0.004074	0.000002	0.000001
115	0.000672	0.000672	0.000672	0.000000	0.000000
120	0.000098	0.000098	0.000098	0.000000	0.000000
MAX				0.001551	0.048275

Table 3.3: The European spread option prices: $S_1 = 100,\ N = 2000,\ M = 1000.$

Example 3.2. (*The stochastic volatility model*) In this example, we consider the European call options under the Heston model with the parameters in Table 3.4. We use the option prices computed by the Bates' formula in [3] with numerical integration as the reference values.

Parameters	Values
K	100
r	0.05
t_0	0.0
T	1.0
q	0.00
κ	1.00
η	0.09
σ	0.9
ρ	0.3

Table 3.4: The parameters for the Heston model

We display the maximum absolute errors and root mean square errors for $v = 0.09$ and

$S = 50 : 5 : 150$ in Figs. 3.4–3.5, respectively. Again, we can observe that the rate of convergence is about $\frac{1}{2}$ as expected. It is also shown that the MMCCV method is about 10 times accurate as the MMC method due to the variance reduction (see Fig. 3.6 for $v = 0.09$, $N = 2000$, $M = 1000$). The option prices and their errors in Table 3.5 show that the MMCCV method provides very accurate approximations of option prices even with a small number of simulations.

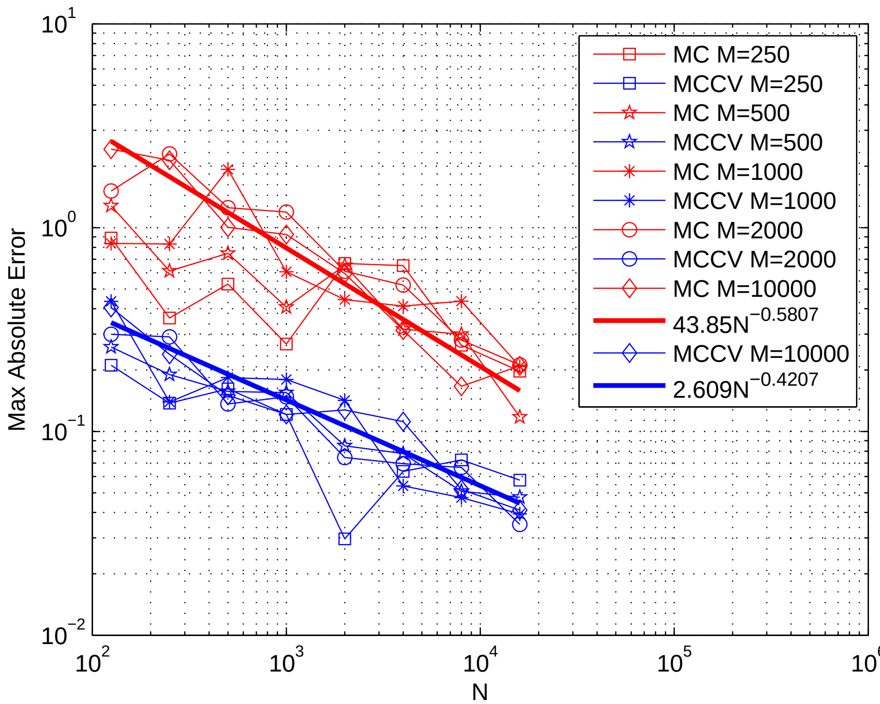

Figure 3.4: MAE vs N for the Heston model

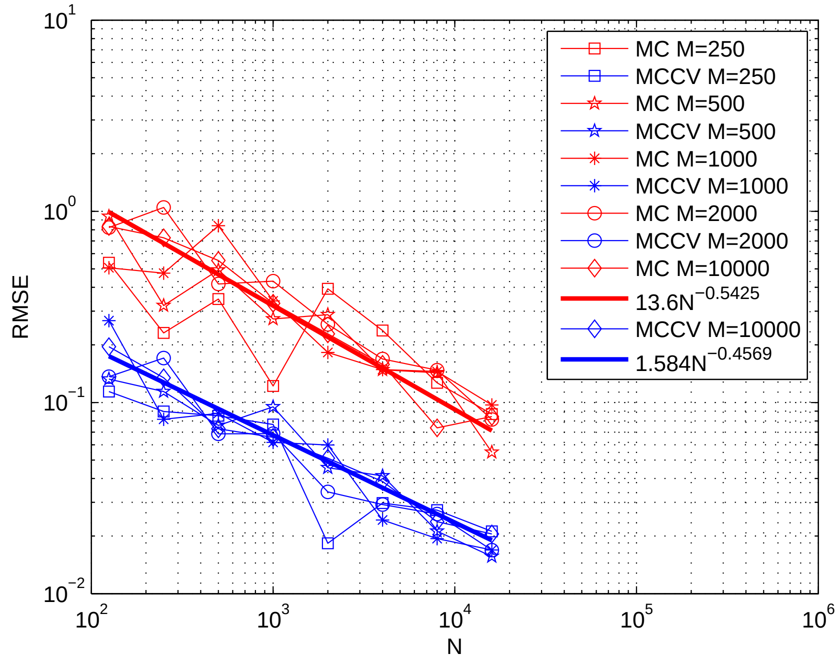

Figure 3.5: RMSE vs N for the Heston model

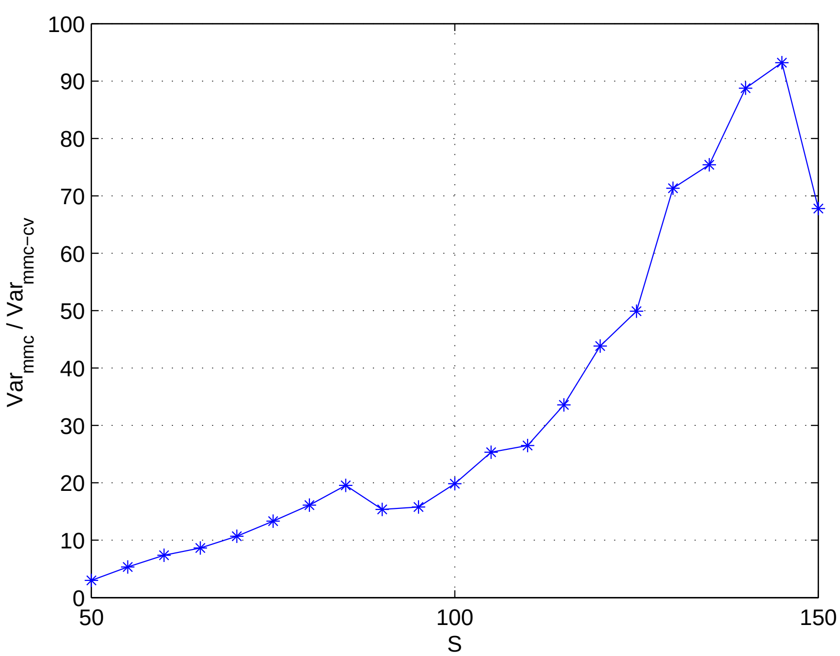

Figure 3.6: The variance ratios vs S for the Heston model

S	REF	CV	MMC	AE-CV	AE-MMC
65	1.935153	1.882274	1.822402	0.052879	0.112751
70	2.604112	2.579329	2.539507	0.024783	0.064605
75	3.458298	3.438213	3.409161	0.020085	0.049137
80	4.547084	4.520669	4.684157	0.026415	0.137073
85	5.934010	6.014273	5.946144	0.080263	0.012134
90	7.695986	7.680517	7.366249	0.015469	0.329737
95	9.912327	9.894834	9.548330	0.017493	0.363997
100	12.637215	12.662328	12.543154	0.025113	0.094061
105	15.866950	15.898040	16.087151	0.031090	0.220201
110	19.535526	19.493760	19.365479	0.041766	0.170047
115	23.546932	23.595580	23.958395	0.048648	0.411463
120	27.810157	27.885419	27.509502	0.075262	0.300655
125	32.254179	32.266008	31.715033	0.011829	0.539146
130	36.828075	36.790434	37.161237	0.037641	0.333162
135	41.496362	41.442971	41.244130	0.053391	0.252232
MAX				0.080263	0.539146

Table 3.5: The European option prices (Heston): $v = 0.09$, $N = 2000$, $M = 1000$.

Example 3.3. (*The stochastic interest rate model*) In this example, we consider the European call options under the stochastic interest rate model. We shall assume that the interest rate follows the Vasicek process and use the option prices computed by the analytic formula in Fang's paper [23] as the reference values. The parameters are given in Table 3.6. We display the maximum absolute errors and root mean square errors for $r = 0.11$ and $S = 50 : 5 : 150$ in Figs. 3.7–3.8, respectively. The variance ratios are displayed in Fig. 3.9 for $r = 0.11$, $N = 2000$, $M = 1000$. The option prices and their errors are presented in Table 3.7. Again, we have the same observations as in Examples 3.1–3.2.

Parameters	Values
S_0	Changing
K	100
r_0	0.11
t_0	0.0
T	1.0
q	0.00
σ	0.20
κ	2.00
θ	0.07
v	0.1
ρ	-0.5

Table 3.6: The parameters for the Vasicek model

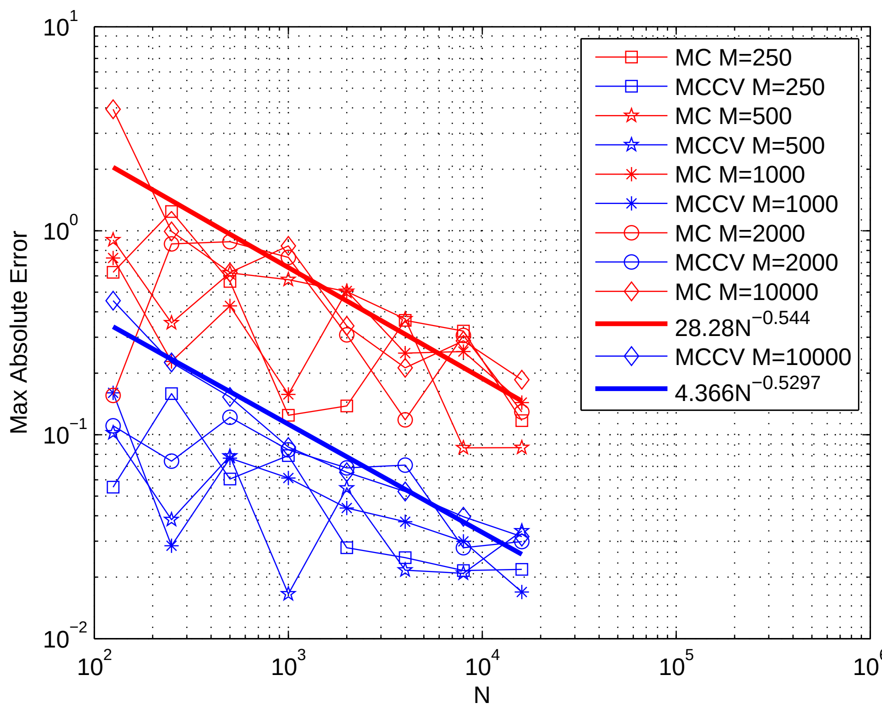

Figure 3.7: MAE vs N for the Vasicek model

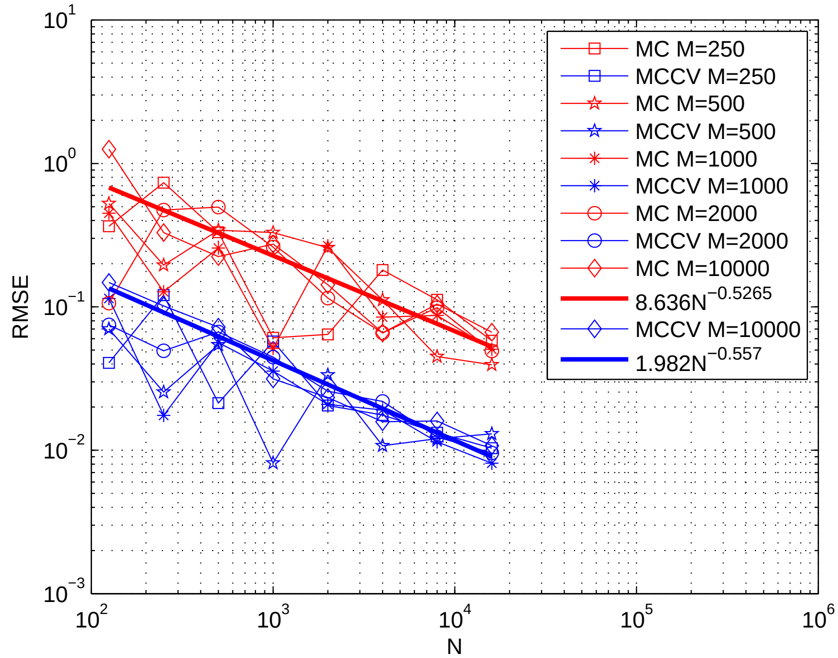

Figure 3.8: RMSE vs N for the Vasicek model

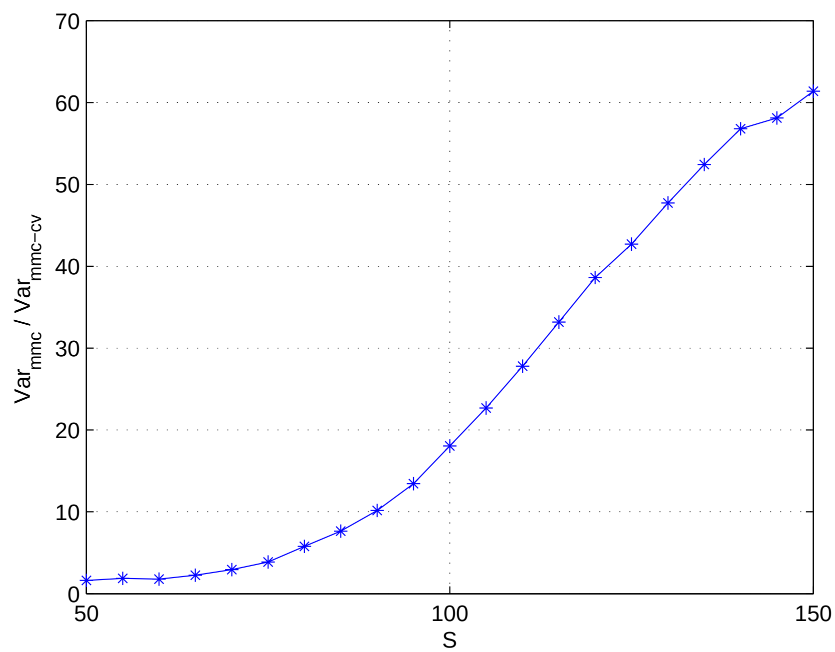

Figure 3.9: The variance ratios vs S for the Vasicek model

S	REF	CV	MMC	AE-CV	AE-MMC
65	0.190539	0.193729	0.197276	0.003190	0.006737
70	0.506896	0.512861	0.521067	0.005965	0.014171
75	1.131576	1.141477	1.157507	0.009901	0.025931
80	2.193787	2.207401	2.178983	0.013614	0.014804
85	3.795243	3.812772	3.769229	0.017529	0.026014
90	5.987420	6.008064	5.947071	0.020644	0.040349
95	8.765632	8.788288	8.708736	0.022656	0.056896
100	12.078444	12.022113	12.172700	0.056331	0.094256
105	15.845353	15.788699	15.966250	0.056654	0.120897
110	19.975172	19.919495	20.121899	0.055677	0.146727
115	24.380248	24.326120	24.551069	0.054128	0.170821
120	28.984916	28.932356	29.177691	0.052560	0.192775
125	33.728793	33.683015	33.411174	0.045778	0.317619
130	38.566558	38.521009	38.231306	0.045549	0.335252
135	43.465823	43.420008	43.113595	0.045815	0.352228
MAX				0.056654	0.352228

Table 3.7: The European option prices (Vasicek): $r = 0.11$, $N = 2000$, $M = 1000$

CHAPTER 4

LATTICE METHODS

In this chapter, we shall develop lattice methods for the European and American options under the two-asset model and the stochastic interest rate models. As usual, our lattice methods are based on simulating the solutions of the stochastic differential equations by lattice trees. Numerical results will be given to show the efficiency and accuracy of our methods.

4.1 The Two-Asset Model

Consider an option with expiration date T under the two-asset model (2.8). We want to compute the option price when $S_1(t_0) = S_{1,0}$ and $S_2(t_0) = S_{2,0}$.

We have from (2.9)–(2.11)

$$S_1(t) = S_1(t_0)e^{Y_1(t)}, \quad S_2(t) = (S_1(t))^{\alpha}\,\widetilde{S}_2(t), \tag{4.1}$$

$$\widetilde{S}_2(t) = \widetilde{S}_2(t_0)e^{Y_2(t)}, \quad \widetilde{S}_2(t_0) = S_2(t_0)\,(S_1(t_0))^{-\alpha}\,, \tag{4.2}$$

where $\alpha = \frac{\rho\sigma_2}{\sigma_1}$, and $Y_1(t)$ and $Y_2(t)$ are determined by the stochastic differential equations (2.12) and (2.13). Without loss of generality, we may assume that $\sigma_1 \geq \sigma_2$.

For a given positive integer M, let $t_m = t_0 + m\Delta t$ for $m = 0, 1, \ldots, M$, where $\Delta t = \frac{T-t_0}{M}$ is the step size in time. The tree for simulating the solution $Y_1(t)$ of the stochastic differential equation (2.12) consists of the following nodes

$$(y_{1,i}, t_m): \ i = -m, \dots, 0, \dots, m, \quad m = 0, 1, \dots, M,$$

where $y_{1,i} = ih_1$ and h_1 is the step size for the values of $Y_1(t)$. Let p_1 and q_1 be the probabilities by which the tree branches from $(y_{1,i}, t_m)$ to $(y_{1,i+1}, t_{m+1})$ and $(y_{1,i-1}, t_{m+1})$, respectively.

It follows from the stochastic differential equation (2.12) that

$$Y_1(t_{m+1}) = Y_1(t_m) + \mu_1 \Delta t + \sigma_1 \sqrt{\Delta t} Z_m,$$

where Z_m is a standard normal random variable. Then we have

$$\mathbb{E}\left[Y_1(t_{m+1}) \middle| Y_1(t_m) = y_{1,i}\right] = y_{1,i} + \mu_1 \Delta t,$$

and

$$\mathbb{V}\left[Y_1(t_{m+1}) \middle| Y_1(t_m) = y_{1,i}\right] = \sigma_1^2 \Delta t.$$

Matching the means and variances, we get

$$p_1(y_{1,i} + h_1) + q_1(y_{1,i} - h_1) = y_{1,i} + \mu_1 \Delta t,$$

$$p_1(h_1 - \mu_1 \Delta t)^2 + q_1(-h_1 - \mu_1 \Delta t)^2 = \sigma_1^2 \Delta t.$$

Solving the above equations together with $p_1 + q_1 = 1$, we obtain

$$h_1 = \left(\sigma_1^2 \Delta t + (\mu_1 \Delta t)^2\right)^{\frac{1}{2}}, \quad p_1 = \frac{1}{2}\left(1 + \frac{\mu_1 \Delta t}{h_1}\right), \quad q_1 = 1 - p_1.$$

Similarly, we can build the tree for simulating the solution $Y_2(t)$ of the stochastic differential equation (2.13) consists of the following nodes

$$(y_{2,j}, t_m): \ j = -m, \dots, 0, \dots, m, \quad m = 0, 1, \dots, M,$$

where

$$y_{2,j} = jh_2, \quad h_2 = \left(\widetilde{\sigma}_2^2 \Delta t + (\mu_2 \Delta t)^2\right)^{\frac{1}{2}}.$$

The probabilities by which the tree branches from $(y_{2,j}, t_m)$ to $(y_{2,j+1}, t_{m+1})$ and $(y_{2,j-1}, t_{m+1})$ are

$$p_2 = \frac{1}{2}\left(1 + \frac{\mu_2 \Delta t}{h_2}\right), \quad q_2 = 1 - p_2,$$

respectively.

Now the tree for simulating the two-dimensional process $(Y_1(t), Y_2(t))$ consists of the nodes

$$(y_{1,i}, y_{2,j}, t_m), \quad i, j = -m, \ldots, 0, \ldots, m, \quad m = 0, \ldots, M.$$

The tree for the process $(Y_1(t), Y_2(t))$ naturally branches from $(y_{1,i}, y_{2,j}, t_{m-1})$ to $(y_{1,i-1}, y_{2,j-1}, t_m)$, $(y_{1,i+1}, y_{2,j-1}, t_m)$, $(y_{1,i+1}, y_{2,j+1}, t_m)$, and $(y_{1,i-1}, y_{2,j+1}, t_m)$ with the probabilities

$$P_1 = q_1 q_2, \quad P_2 = p_1 q_2, \quad P_3 = p_1 p_2, \quad P_4 = q_1 p_2,$$

respectively. According to (4.1) and (4.2), the corresponding tree for the process $\left(S_1(t), \widetilde{S}_2(t)\right)$ consisting of the nodes

$$\left(S_{1,0} e^{ih_1}, \widetilde{S}_{2,0} e^{jh_2}, t_m\right), \quad i, j = -m, \ldots, 0, \ldots, m, \quad m = 0, \ldots, M.$$

For a given payoff $\Phi(S_1, S_2)$, we have the following algorithms to compute the prices of the European and American options.

Algorithm 5. A lattice method for the European option on two assets

1. Compute

$$S_{1,i} = S_{1,0} e^{(2.0*i-M)h_1}, \quad \widetilde{S}_{2,i} = \widetilde{S}_{2,0} e^{(2.0*i-M)h_2}, \quad i = 0, 1, \ldots, M.$$

2. Compute the payoff at the option expiration:

$$V_{i,j} = \Phi\left(S_{1,i}, (S_{1,i})^{\alpha}\, \widetilde{S}_{2,j}\right), \quad i, j = 0, 1, \ldots, M.$$

3. For $m = M-1, M-2, \ldots, 0$, do

   For $i = 0, \ldots, m$, do

   For $j = 0, \ldots, m$, do

$$V_{i,j} = e^{-r\Delta t}\left(P_1 V_{i,j} + P_2 V_{i+1,j} + P_3 V_{i+1,j+1} + P_4 V_{i,j+1}\right).$$

   End do.

   End do.

   End do.

4. Rerun $V_{0,0}$ for the approximate value of the option price.

Algorithm 6. A lattice method for the American option on two assets

1. Compute

$$S_{1,i} = S_{1,0} e^{(i-M)h_1}, \quad \widetilde{S}_{2,i} = \widetilde{S}_{2,0} e^{(i-M)h_2}, \quad i = 0, 1, \ldots, 2M.$$

2. Compute the payoff at the option expiration:

$$V_{i,j} = \Phi\left(S_{1,i}, (S_{1,2i})^{\alpha} \widetilde{S}_{2,2j}\right), \quad i, j = 0, 1, \ldots, M.$$

3. For $m = M-1, M-2, \ldots, 0$, do

   For $i = 0, \ldots, m$, do

   - Set $S_1 = S_{1,M-m+2*i}$.
   - For $j = 0, \ldots, m$, do
     * Compute

       $$V_{i,j} = e^{-r\Delta t}\left(P_1 V_{i,j} + P_2 V_{i+1,j} + P_3 V_{i+1,j+1} + P_4 V_{i,j+1}\right).$$

     * Check for early exercise:

       $$V_{i,j} = \max\left(V_{i,j}, \Phi\left(S_1, S_2\right)\right),$$

       where $S_2 = (S_1)^{\alpha} \widetilde{S}_{2,M-m+2*j}$.

     End do.

   End do.

   End do.

4. Return $V_{0,0}$ for the approximate value of the option price.

4.2 The Stochastic Interest Rate Model

Consider an option with expiration date T under the stochastic interest rate model (2.20) – (2.21). We want to compute the option price V when $S(t_0) = S_0$ and $r(t_0) = r_0$.

We have from (2.22) and (2.23)

$$S(t) = Ke^{\alpha Y_1(t)+Y_2(t)}, \quad r(t) = (Y_1(t))^{1/(1-p)}, \tag{4.3}$$

where $\alpha = \frac{\rho\sigma}{(1-p)v}$, and $Y_1(t)$ and $Y_2(t)$ are determined by the stochastic differential equations (2.24) and (2.25) with the initial conditions $Y_1(t_0) = y_{1,0}$ and $Y_2(t_0) = y_{2,0}$, where

$$y_{1,0} = r_0^{1-p}, \quad y_{2,0} = \log(S_0/K) - \alpha r_0^{1-p}.$$

For a given positive integer M, let $t_m = t_0 + m\Delta t$ for $m = 0, 1, \ldots, M$, where $\Delta t = \frac{T-t_0}{M}$ is the step size in time. The tree for simulating the solution $Y_1(t)$ of the stochastic differential equation (2.24) consists of the following nodes

$$(y_{1,i}, t_m): \ i = -m, \ldots, 0, \ldots, m, \quad m = 0, 1, \ldots, M,$$

where $y_{1,i} = y_{1,0} + ih_1$ and h_1 is the step size for the values of $Y_1(t)$. Let p_1 and q_1 be the probabilities by which the tree branches from $(y_{1,i}, t_m)$ to $(y_{1,i+1}, t_{m+1})$ and $(y_{1,i-1}, t_{m+1})$, respectively.

We can approximate the stochastic differential equation (2.24) by the Euler scheme:

$$Y_1(t_{jm+1}) \approx Y_1(t_m) + \mu_1(Y_1(t_m))\Delta t + \sigma_1\sqrt{\Delta t}Z_m,$$

where Z_m is a standard normal random variable. Then we have

$$\mathbb{E}\left[Y_1(t_{m+1}) | Y_1(t_m) = y_{1,i}\right] \approx y_{1,i} + \mu_1(y_{1,i})\Delta t,$$

and

$$\mathbb{V}\left[Y_1\left(t_{m+1}\right)\middle|\, Y_1\left(t_m\right)=y_{1,i}\right]\approx \sigma_1^2\Delta t.$$

Matching the variances, we get

$$p_1\left(h_1-\mu_1\left(y_{1,i}\right)\Delta t\right)^2+q_1\left(-h_1-\mu_1\left(y_{1,i}\right)\Delta t\right)^2=\sigma_1^2\Delta t.$$

Since $p_1+q_1=1$, we have from the above equation

$$h_1=\left(\sigma_1^2\Delta t+\left(\mu_1\left(y_{1,i}\right)\Delta t\right)^2\right)^{\frac{1}{2}},$$

which depends on $y_{1,i}$. After dropping the higher order term $\left(\mu_1\left(y_{1,i}\right)\Delta t\right)^2$, we get

$$h_1=\sigma_1\sqrt{dt}.$$

We have by matching the means

$$p_1\left(y_i+h_1\right)+q_1\left(y_j-h_1\right)=y_{1,i}+\mu_1\left(y_{1,i}\right)\Delta t,$$

which implies

$$p-q=\frac{\mu_1\left(y_{1,i}\right)}{h_1}.$$

Thus we have

$$p_1=\frac{1}{2}\left(1+\frac{\mu_1\left(y_{1,i}\right)\Delta t}{h_1}\right),\quad q_1=1-p_1.$$

Notice that p_1 may not be between 0 and 1. We shall artificially set

$$p_1=\begin{cases}0, & \text{if } p_1<0;\\ \\ 1, & \text{if } p_1>1.\end{cases}$$

Since $Y_1(t)$ should be always positive for the CIR model, we also set

$$p_1=1.0,\quad \text{if } y_{1,i}\leq 0$$

to make the value of $Y_1(t_{m+1})$ positive.

Similarly, we can build the tree for simulating the solution $Y_2(t)$ of the stochastic differential equation (2.25) when $Y_1(t) = y_{1,i}$ is given. It consists of the following nodes

$$(y_{2,j}, t_m): \ j = -m, \ldots, 0, \ldots, m, \quad m = 0, 1, \ldots, M,$$

where

$$y_{2,j} = y_{2,0} + jh_2, \quad h_2 = \sigma_2 \sqrt{\Delta t}.$$

The probabilities by which the tree branches from $(y_{2,j}, t_m)$ to $(y_{2,j+1}, t_{m+1})$ and $(y_{2,j-1}, t_{m+1})$ are

$$p_2 = \frac{1}{2}\left(1 + \frac{\mu_2(y_{1,i})\,\Delta t}{h_2}\right), \quad q_2 = \frac{1}{2}\left(1 - \frac{\mu_2(y_{1,i})\,\Delta t}{h_2}\right),$$

respectively. As for probability p_1, we shall artificially set

$$p_2 = \begin{cases} 0, & \text{if } p_2 < 0; \\ \\ 1, & \text{if } p_2 > 1. \end{cases}$$

Now the tree for simulating the two-dimensional process $(Y_1(t), Y_2(t))$ consists of the nodes

$$(y_{1,i}, y_{2,j}, t_m), \quad i, j = -m, \ldots, 0, \ldots, m, \quad m = 0, \ldots, M.$$

The tree for the process $(Y_1(t), Y_2(t))$ naturally branches from from $(y_{1,i}, y_{2,j}, t_m)$ to $(y_{1,i-1}, y_{2,j-1}, t_m)$, $(y_{1,i+1}, y_{2,j-1}, t_m)$, $(y_{1,i+1}, y_{2,j+1}, t_m)$, and $(y_{1,i-1}, y_{2,j+1}, t_m)$ with the probabilities

$$P_1 = q_1 q_2, \quad P_2 = p_1 q_2, \quad P_3 = p_1 p_2, \quad P_4 = q_1 p_2,$$

respectively. It follows from (4.3) that the corresponding tree for the process $(S(t), r(t))$ consisting of the nodes

$$\left(Ke^{\alpha y_{1,i} + y_{2,j}}, (y_{1,i})^{1/(1-p)}, t_m\right), \quad i, j = -m, \ldots, 0, \ldots, m, \quad m = 0, \ldots, M.$$

For a given payoff $\Phi(S)$, we have the following algorithms to compute the prices of the European and American options.

Algorithm 7. A lattice method for the European option (stochastic interest rate)

---

1. Compute

$$y_{1,i} = y_{1,0} + (i - M)h_1, \quad y_{2,i} = y_{2,0} + (i - M)h_2, \quad i = 0, 1, \ldots, 2M.$$

2. Compute the payoff at the option expiration:

$$V_{i,j} = \Phi\left(K \exp\left(y_{2,2j} + \alpha y_{1,2i}\right)\right), \quad i, j = 0, 1, \ldots, M.$$

3. For $m = M-1, M-2, \ldots, 0$, do

   For $i = 0, \ldots, m$, do

   - Compute $p_1 = \frac{1}{2}\left(1 + \frac{\mu_1\left(y_{1,M-m+2i}\right)\Delta t}{dz}\right)$.
   - If $p_1 < 0$, set $p_1 = 0$; if $p_1 > 1$, set $p_1 = 1$; if $y_{1,M-m+2i} \le 0$, set $p_1 = 1$.
   - Set $q_1 = 1 - p_1$.
   - Compute $p_2 = \frac{1}{2}\left(1 + \frac{\mu_2\left(y_{1,M-m+2i}\right)\Delta t}{dz}\right)$.
   - If $p_2 < 0$, set $p_2 = 0$; if $p_2 > 1$, set $p_2 = 1$.
   - Set $q_2 = 1 - p_2$.
   - Compute the discount factor $D = \exp\left(-\left(y_{1,M-m+2i}\right)^{1/(1-p)}\Delta t\right)$.
   - For $j = 0, \ldots, m$, do

$$V_{i,j} = D\left(P_1 V_{i,j} + P_2 V_{i+1,j} + P_3 V_{i+1,j+1} + P_4 V_{i,j+1}\right).$$

     End do.

   End do.

   End do.

4. Rerun $V_{0,0}$ for the approximate value of the option price.

Algorithm 8. A lattice method for the American option (stochastic interest rate)

1. Compute

$$y_{1,i} = y_{1,0} + (i - M)h_1, \quad y_{2,i} = y_{2,0} + (i - M)h_2, \quad i = 0, 1, \ldots, 2M.$$

2. Compute the payoff at the option expiration:

$$V_{i,j} = \Phi\left(K \exp\left(y_{2,2j} + \alpha y_{1,2i}\right)\right), \quad i, j = 0, 1, \ldots, M.$$

3. For $m = M - 1, M - 2, \ldots, 0$, do

   For $i = 0, \ldots, m$, do

   - Compute $p_1 = \frac{1}{2}\left(1 + \frac{\mu_1\left(y_{1,M-m+2i}\right)\Delta t}{dz}\right)$;
   - If $p_1 < 0$, set $p_1 = 0$; if $p_1 > 1$, set $p_1 = 1$; if $y_{1,M-m+2i} \leq 0$, set $p_1 = 1$.
   - Set $q_1 = 1 - p_1$.
   - Compute $p_2 = \frac{1}{2}\left(1 + \frac{\mu_2\left(y_{1,M-m+2i}\right)\Delta t}{dz}\right)$;
   - If $p_2 < 0$, set $p_2 = 0$; if $p_2 > 1$, set $p_2 = 1$.
   - Set $q_2 = 1 - p_2$.
   - Compute the discount factor $D = \exp\left(-\left(y_{1,M-m+2i}\right)^{1/(1-p)} \Delta t\right)$.
   - For $j = 0, \ldots, m$, do
     * $V_{i,j} = D\left(P_1 V_{i,j} + P_2 V_{i+1,j} + P_3 V_{i+1,j+1} + P_4 V_{i,j+1}\right)$.
     * $S = K \exp\left(y_{2,M-m+2j} + \alpha y_{1,M-m+2i}\right)$.
     * $V_{i,j} = \max\left(V_{i,j}, \Phi\left(S\right)\right)$.

     End do.

   End do.

   End do.

4. Rerun $V_{0,0}$ for the approximate value of the option price.

4.3 Numerical Results

In this section, we present numerical examples to examine the convergence and accuracy of the proposed lattice methods in the previous sections. We will focus on the accuracy of the method, especially for the European options. We will also examine the early exercise boundaries for the American options. For convenience, we introduce the following abbreviations.

Notation	Meaning
REF	Reference value
LAT	Numerical result using lattice
MMC	Numerical result using mixed Monte Carlo method
AE	Absolute error between the numerical results of LAT and MMC
N	Number of MC simulations
M	Number of time steps

Table 4.1: Notations

Example 4.1. (*The European Spread Option*) In this example, we consider the European spread options whose payoff is $\Phi(S_1(T), S_2(T)) = (S_1(T) - S_2(T) - K)^+$. The reference values are computed the same as in example 3.1. The parameters for the two-asset model are given in Table 4.2.

Parameters	Values
K	\$10
T	1.0 year
t_0	0.0
q_1	0.05
q_2	0.07
r	0.08
σ_1	0.3
σ_2	0.2

Table 4.2: Parameters for the European spread option

In order to examine the rate of convergence of our lattice method, we plot the maximum absolute errors (MAE) against the time step sizes in Figs. 4.1. The MAEs are computed at the points $S1 = 60 : 5 : 120 \times S2 = 60 : 5 : 120$ with different correlations $\rho = -0.8, -0.4, 0.4, 0.8$ and different interest rates $r = 0.04, 0.05, 0.06, 0.07, 0.08$. We can observe that the rate of convergence of our lattice method is about 1. For the accuracy of the lattice scheme, we display the option prices and the absolute errors (AE) in Tables 4.3–4.6. We can see that the AEs is $\mathcal{O}(10^{-3})$ when the number of time steps $M = 1000$. All of these numerical results are as expected since the theoretical rate of convergence of the lattice method is $\mathcal{O}(M^{-1})$.

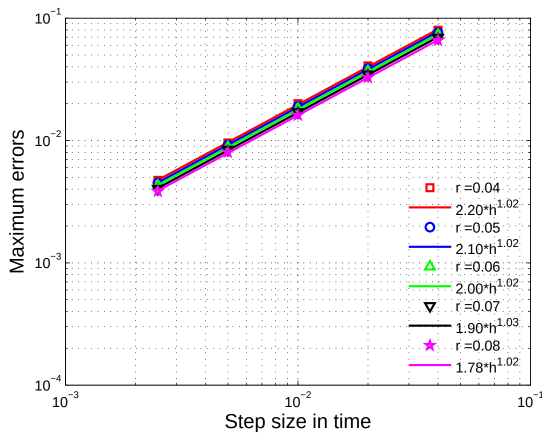

(a) $\rho = -0.8$

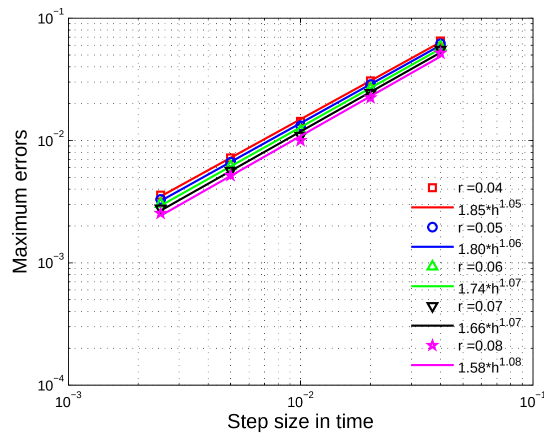

(b) $\rho = -0.4$

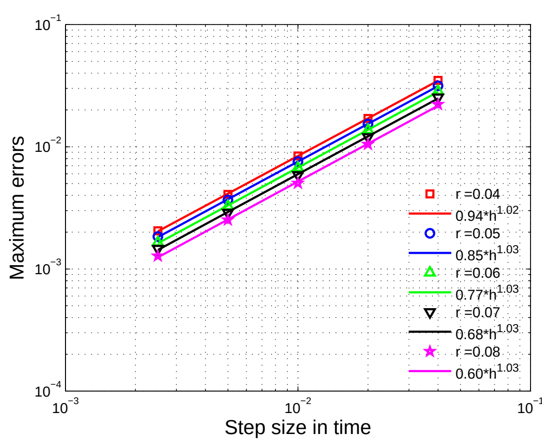

(c) $\rho = 0.4$

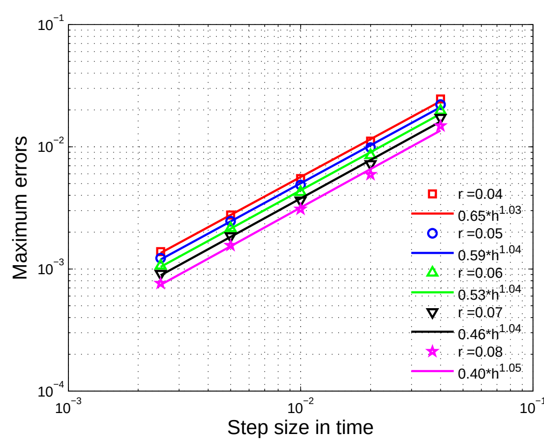

(d) $\rho = 0.8$

Figure 4.1: The maximum absolute errors of the European spread options

S_2	60			80			100		
S_1	LAT	REF	AE	LAT	REF	AE	LAT	REF	AE
85	22.2686	22.2679	0.0007	13.3697	13.3687	0.0010	7.9117	7.9110	0.0007
90	25.9780	25.9775	0.0005	16.1528	16.1518	0.0011	9.8719	9.8710	0.0009
95	29.8525	29.8521	0.0004	19.1589	19.1579	0.0011	12.0595	12.0584	0.0010
100	33.8675	33.8672	0.0002	22.3679	22.3669	0.0010	14.4650	14.4638	0.0012
105	38.0013	38.0012	0.0001	25.7598	25.7589	0.0009	17.0770	17.0757	0.0013
110	42.2353	42.2353	0.0000	29.3158	29.3150	0.0008	19.8830	19.8817	0.0013
115	46.5535	46.5536	0.0001	33.0180	33.0173	0.0007	22.8701	22.8687	0.0013

Table 4.3: The European spread option prices: $\rho = -0.8$

S_2	60			80			100		
S_1	LAT	REF	AE	LAT	REF	AE	LAT	REF	AE
85	21.0588	21.0583	0.0005	11.7873	11.7866	0.0007	6.3837	6.3834	0.0003
90	24.8238	24.8234	0.0004	14.5188	14.5180	0.0008	8.1943	8.1938	0.0005
95	28.7665	28.7663	0.0003	17.5018	17.5010	0.0008	10.2562	10.2556	0.0007
100	32.8575	32.8573	0.0001	20.7130	20.7122	0.0008	12.5617	12.5609	0.0008
105	37.0710	37.0710	0.0000	24.1286	24.1279	0.0007	15.0994	15.0985	0.0009
110	41.3855	41.3856	0.0001	27.7260	27.7254	0.0006	17.8562	17.8553	0.0009
115	45.7825	45.7827	0.0002	31.4835	31.4830	0.0005	20.8173	20.8163	0.0009

Table 4.4: The European spread option prices: $\rho = -0.4$

S_2	60			80			100		
S_1	LAT	REF	AE	LAT	REF	AE	LAT	REF	AE
85	18.2373	18.2372	0.0002	7.7912	7.7909	0.0003	2.8506	2.8507	0.0001
90	22.2524	22.2523	0.0001	10.3870	10.3866	0.0004	4.1612	4.1611	0.0001
95	26.4707	26.4707	0.0000	13.3485	13.3481	0.0004	5.8014	5.8012	0.0002
100	30.8415	30.8416	0.0001	16.6365	16.6362	0.0003	7.7789	7.7786	0.0003
105	35.3246	35.3247	0.0001	20.2080	20.2078	0.0003	10.0897	10.0893	0.0004
110	39.8890	39.8891	0.0002	24.0198	24.0196	0.0002	12.7201	12.7197	0.0005
115	44.5115	44.5116	0.0002	28.0310	28.0309	0.0001	15.6490	15.6486	0.0005

Table 4.5: The European spread option prices: $\rho = 0.4$

S_2	60			80			100		
S_1	LAT	REF	AE	LAT	REF	AE	LAT	REF	AE
85	16.6045	16.6045	0.0000	4.8703	4.8702	0.0002	0.8598	0.8600	0.0002
90	20.9474	20.9474	0.0001	7.3589	7.3587	0.0002	1.6120	1.6121	0.0001
95	25.4668	25.4669	0.0001	10.3863	10.3861	0.0002	2.7493	2.7493	0.0000
100	30.0922	30.0923	0.0001	13.8772	13.8770	0.0002	4.3335	4.3334	0.0001
105	34.7782	34.7783	0.0001	17.7410	17.7409	0.0001	6.3951	6.3949	0.0002
110	39.4977	39.4978	0.0001	21.8885	21.8885	0.0000	8.9317	8.9315	0.0003
115	44.2351	44.2352	0.0001	26.2417	26.2418	0.0001	11.9132	11.9129	0.0003

Table 4.6: The European spread option prices: $\rho = 0.8$

Example 4.2. (*The American options on two assets*) In this example, we examine the early exercise boundaries of the 1-year American options with the popular payoffs as listed in Table 1.1. The volatilities for the two-asset model and the parameters for the payoffs are given in Table 4.7. The other parameters (the interest rate r, correlation ρ, and dividend rates q_1, q_2) will be specified later. All the early exercise boundaries are computed via bisection method while the option prices are computed by using Algorithm 6 in section 4.1 with the number of time steps $M = 500$.

Parameters	Spread	Call on max	Max call	Put on min	Max put
K	\$10	\$100	N/A	\$50	N/A
K_1	N/A	N/A	\$80	N/A	\$5
K_2	N/A	N/A	\$120	N/A	\$12
σ_1	0.3	0.3	0.3	0.3	0.3
σ_2	0.2	0.2	0.2	0.2	0.2

Table 4.7: Parameters for the American options with two-asset

In the following, we will use S_t^i $(i = 1, 2)$ for the spot price of the i-th asset at time $t \in [0, T)$, E for the immediate exercise region, and B_t^i for the exercise boundary for a standard American option on the i-th asset.

We first consider the spread options and list the properties of the exercise region proved in [10] as follows:

(1) $(S_t^1, S_t^2, t) \in E$ implies $S_t^2 > S_t^1 + K$.

(2) $(S_t^1, S_t^2, t) \in E$ implies $(S_t^1, S_t^2, s) \in E$ for all $t \leq s \leq T$.

(3) $(S_t^1, S_t^2, t) \in E$ implies $(S_t^1, \lambda S_t^2, t) \in E$ for all $\lambda \geq 1$.

(4) $(S_t^1, S_t^2, t) \in E$ implies $(\lambda S_t^1, S_t^2, t) \in E$ for all $0 \leq \lambda \leq 1$.

(5) $(0, S_t^2, t) \in E$ implies $S_t^2 \geq B_t^2$; $S_t^2 \geq B_t^2$ and $S_t^1 = 0$ implies $(0, S_t^2, t) \in E$.

(6) $(S_t^1, S_t^2, t) \in E$ and $(\widetilde{S}_t^1, \widetilde{S}_t^2, t) \in E$ implies $(S_t^1(\lambda), S_t^2(\lambda), t) \in E$ for all $0 \leq \lambda \leq 1$, where $S_t^i(\lambda) = \lambda S_t^i + (1-\lambda)\widetilde{S}_t^i$ for $i = 1, 2$.

(7) The S_2 intercept of the early exercise boundary at time t is $(0, B_t^2)$. And $\lim_{t \to T^-} B_t^2 = \max\left(\frac{r}{q_2}K, K\right)$.

(8) When $t \to T^-$, the early exercise boundary is given by

$$S_T^2 = \max\left(\frac{q_1}{q_2}S_T^1 + \frac{r}{q_2}K, S_T^1 + K\right).$$

Our numerical results in Fig. 4.2 agree with the above theoretical properties. In addition, we can observe that the early exercise boundaries of different times are more dispersive when the correlation is negative.

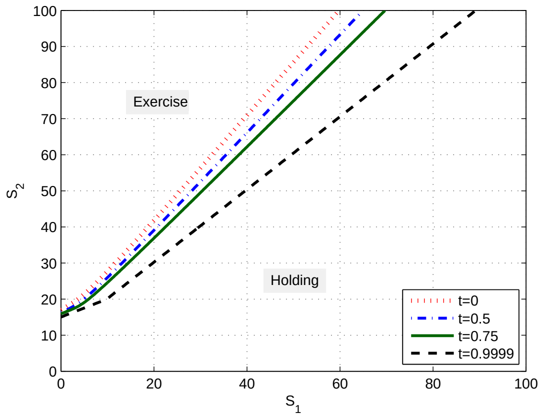

(a) $\rho = 0.5, q_1 = 0.02, q_2 = 0.04, r = 0.06$

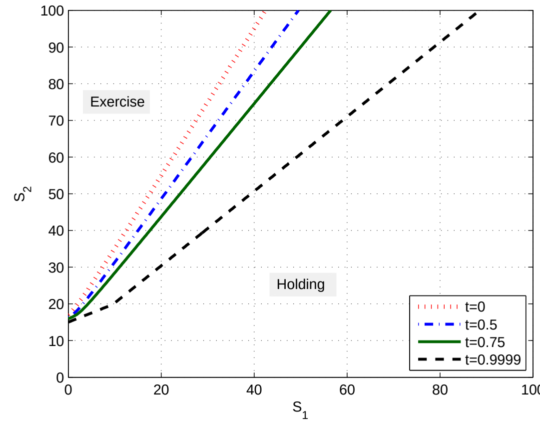

(b) $\rho = -0.5, q_1 = 0.02, q_2 = 0.04, r = 0.06$

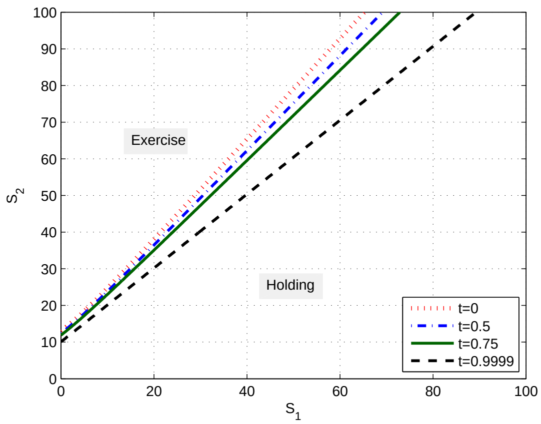

(c) $\rho = 0.5, q_1 = 0.02, q_2 = 0.06, r = 0.04$

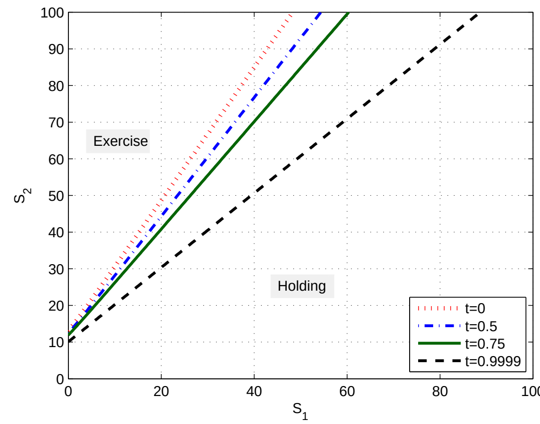

(d) $\rho = -0.5, q_1 = 0.02, q_2 = 0.06, r = 0.04$

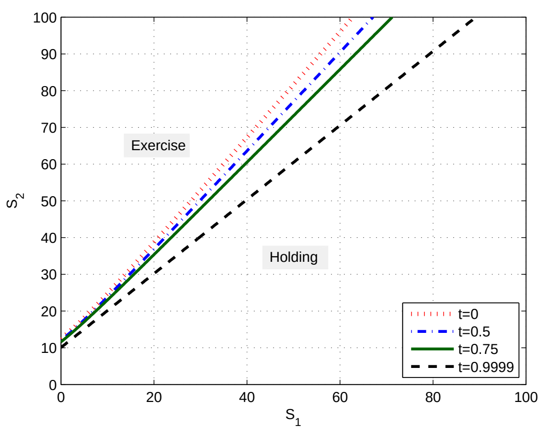

(e) $\rho = 0.5, q_1 = 0.04, q_2 = 0.06, r = 0.02$

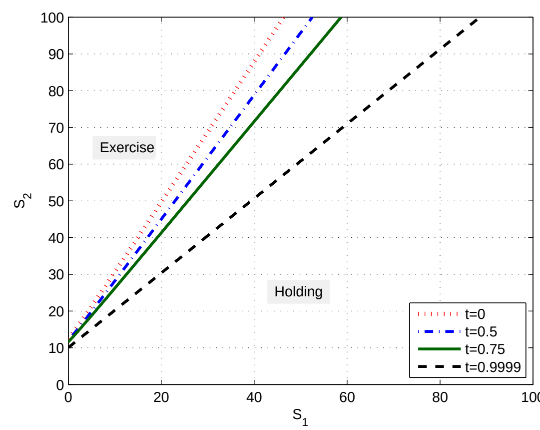

(f) $\rho = -0.5, q_1 = 0.04, q_2 = 0.06, r = 0.02$

Figure 4.2: The early exercise boundaries of the spread options

Secondly, we consider the call option on the maximum. Define $E^i = E \cap G^i, i = 1,2$ where $G^i \equiv \{(S_t^1, S_t^2, t) : S_t^i = \max(S_t^1, S_t^2)\}$. We list the properties of the exercise region proved in [10]:

(1) $(S_t^1, S_t^2, t) \in E$ implies $(S_t^1, S_t^2, s) \in E$ for all $t \le s \le T$.

(2) $(S_t^1, S_t^2, t) \in E^1$ implies $(\lambda S_t^1, S_t^2, t) \in E^1$ for all $\lambda \ge 1$. $(S_t^1, S_t^2, t) \in E^2$ implies $(S_t^1, \lambda S_t^2, t) \in E^2$ for all $\lambda \ge 1$.

(3) $(S_t^1, S_t^2, t) \in E^1$ implies $(S_t^1, \lambda S_t^2, t) \in E^1$ for all $0 \le \lambda \le 1$. $(S_t^1, S_t^2, t) \in E^2$ implies $(\lambda S_t^1, S_t^2, t) \in E^2$ for all $0 \le \lambda \le 1$.

(4) $(S_t^1, 0, t) \in E^1$ implies $S_t^1 \ge B_t^1$. $(0, S_t^2, t) \in E^2$ implies $S_t^2 \ge B_t^2$.

(5) $(S_t^1, S_t^2, t) \in E^j$ and $(\widetilde{S}_t^1, \widetilde{S}_t^2, t) \in E^j$ implies $(S_t^1(\lambda), S_t^2(\lambda), t) \in E^j$ for j=1,2 and all $0 \le \lambda \le 1$, where $S_t^i(\lambda) = \lambda S_t^i + (1-\lambda)\widetilde{S}_t^i$ for $i = 1, 2$.

(6) The S_1 intercept of the early exercise boundary at time t is $(B_t^1, 0)$. The S_2 intercept of the early exercise boundary at time t is $(0, B_t^2)$ .And $\lim_{t \to T^-} B_t^i = \max\left(\frac{r}{q_i}K, K\right)$.

(7) When $t \to T^-$, the early exercise boundary is given by

$$S_T^1 = \max\left(\max\left(\frac{r}{q_1}K, K\right), S_T^2\right) for E^1,$$

$$S_T^2 = \max\left(\max\left(\frac{r}{q_2}K, K\right), S_T^1\right) for E^2.$$

Our numerical results in Fig. 4.3 agree with the above theoretical properties. In addition, we can observe that the early exercise boundaries of different times are more dispersive when the correlation is negative.

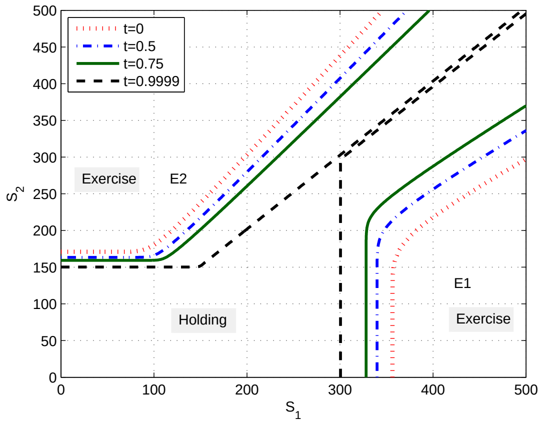

(a) $\rho = 0.5, q_1 = 0.02, q_2 = 0.04, r = 0.06$

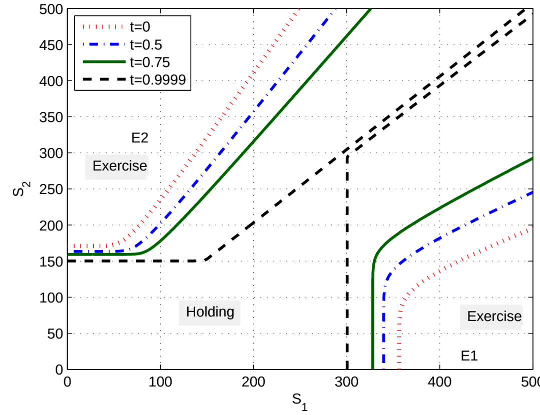

(b) $\rho = -0.5, q_1 = 0.02, q_2 = 0.04, r = 0.06$

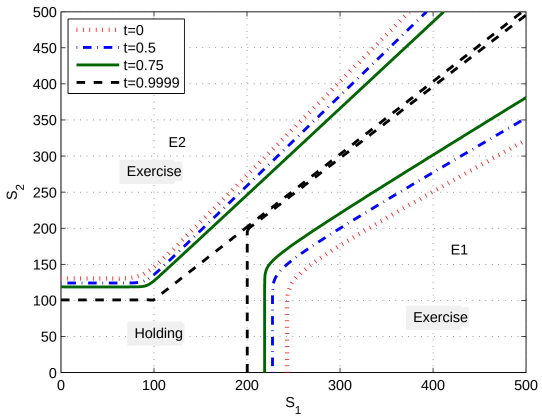

(c) $\rho = 0.5, q_1 = 0.02, q_2 = 0.06, r = 0.04$

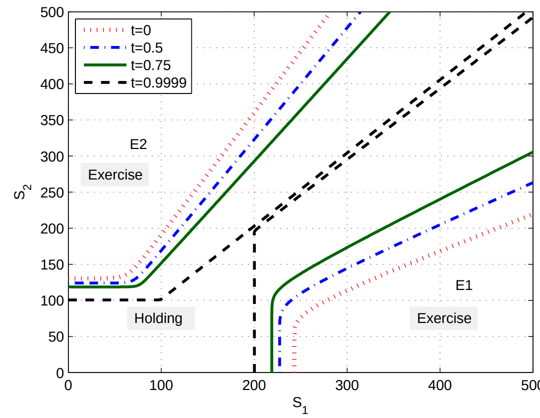

(d) $\rho = -0.5, q_1 = 0.02, q_2 = 0.06, r = 0.04$

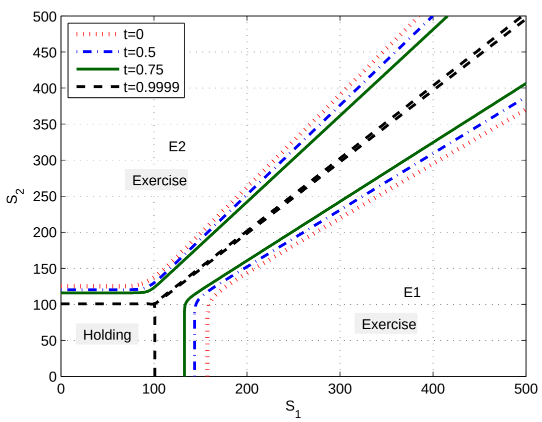

(e) $\rho = 0.5, q_1 = 0.04, q_2 = 0.06, r = 0.02$

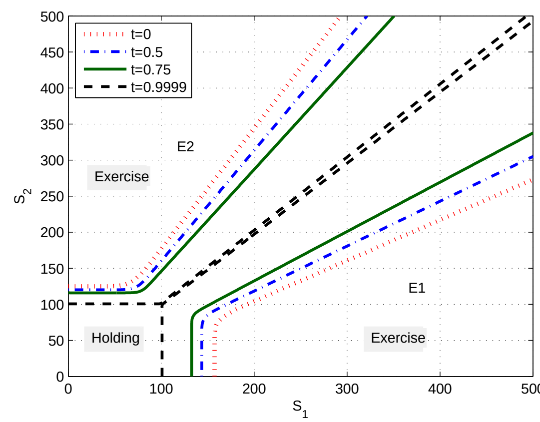

(f) $\rho = -0.5, q_1 = 0.04, q_2 = 0.06, r = 0.02$

Figure 4.3: The early exercise boundaries of the call option on the maximum

Thirdly, we consider the maximum call option. Define $E^i = E \cap G^i, i = 1,2$ where $G^i \equiv \{(S_t^1, S_t^2, t) : S_t^i - K_i = \max(S_t^1 - K_1, S_t^2 - K_2)\}$. We list the properties of the exercise region proved in [10]:

(1) $(S_t^1, S_t^2, t) \in E$ implies $(S_t^1, S_t^2, s) \in E$ for all $t \le s \le T$.

(2) $(S_t^1, S_t^2, t) \in E^1$ implies $(\lambda S_t^1, S_t^2, t) \in E^1$ for all $\lambda \ge 1$. $(S_t^1, S_t^2, t) \in E^2$ implies $(S_t^1, \lambda S_t^2, t) \in E^2$ for all $\lambda \ge 1$.

(3) $(S_t^1, S_t^2, t) \in E^1$ implies $(S_t^1, \lambda S_t^2, t) \in E^1$ for all $0 \le \lambda \le 1$. $(S_t^1, S_t^2, t) \in E^2$ implies $(\lambda S_t^1, S_t^2, t) \in E^2$ for all $0 \le \lambda \le 1$.

(4) $(S_t^1, 0, t) \in E^1$ implies $S_t^1 \ge B_t^1$. $(0, S_t^2, t) \in E^2$ implies $S_t^2 \ge B_t^2$.

(5) $(S_t^1, S_t^2, t) \in E^j$ and $(\widetilde{S}_t^1, \widetilde{S}_t^2, t) \in E^j$ implies $(S_t^1(\lambda), S_t^2(\lambda), t) \in E^j$ for j=1,2 and all $0 \le \lambda \le 1$, where $S_t^i(\lambda) = \lambda S_t^i + (1-\lambda)\widetilde{S}_t^i$ for $i = 1,2$.

(6) The S_1 intercept of the early exercise boundary at time t is $(B_t^1, 0)$. The S_2 intercept of the early exercise boundary at time t is $(0, B_t^2)$ .And $\lim_{t \to T^-} B_t^i = \max\left(\frac{r}{q_i} K_i, K_i\right)$.

(7) When $t \to T^-$, the early exercise boundary is given by

$$S_T^1 = \max\left(\max\left(\frac{r}{q_1} K_1, K_1\right), S_T^2\right) for E^1,$$

$$S_T^2 = \max\left(\max\left(\frac{r}{q_2} K_2, K_2\right), S_T^1\right) for E^2.$$

Our numerical results in Fig. 4.4 agree with the above theoretical properties. In addition, we can observe that the early exercise boundaries of different times are more dispersive when the correlation is negative.

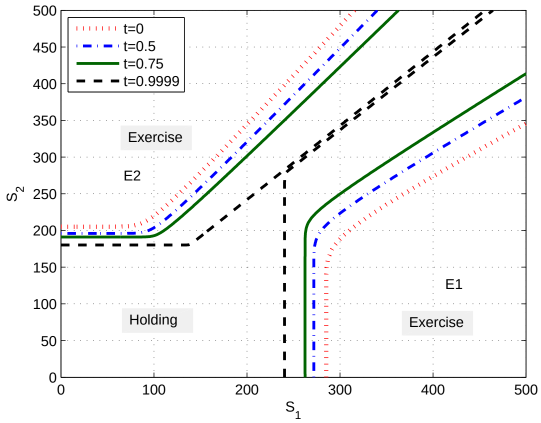

(a) $\rho = 0.5, q_1 = 0.02, q_2 = 0.04, r = 0.06$

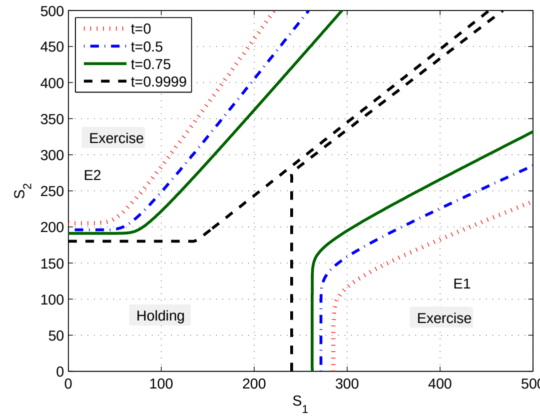

(b) $\rho = -0.5, q_1 = 0.02, q_2 = 0.04, r = 0.06$

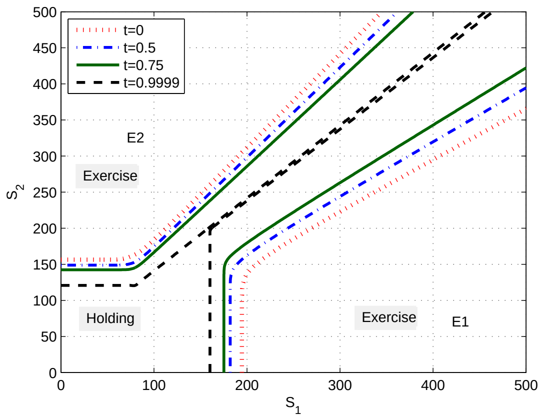

(c) $\rho = 0.5, q_1 = 0.02, q_2 = 0.06, r = 0.04$

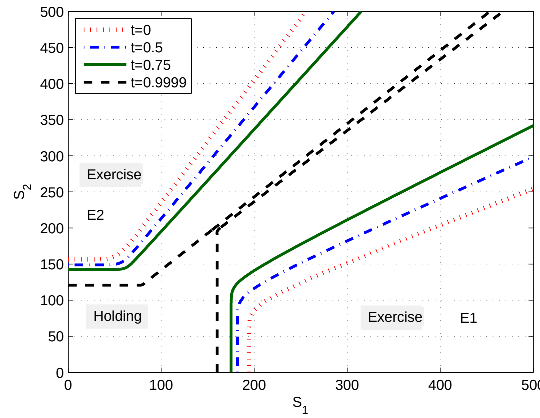

(d) $\rho = -0.5, q_1 = 0.02, q_2 = 0.06, r = 0.04$

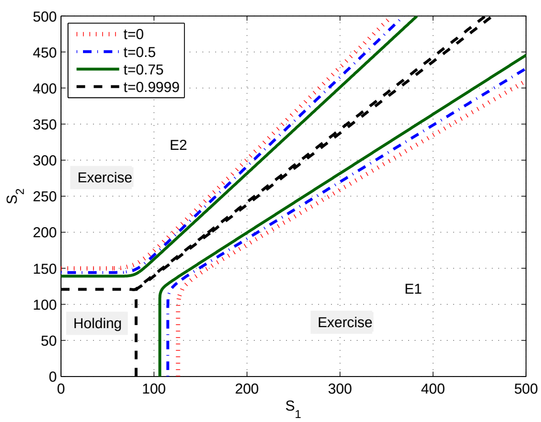

(e) $\rho = 0.5, q_1 = 0.04, q_2 = 0.06, r = 0.02$

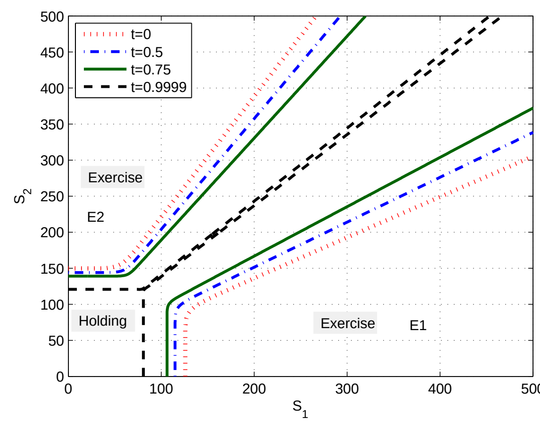

(f) $\rho = -0.5, q_1 = 0.04, q_2 = 0.06, r = 0.02$

Figure 4.4: The early exercise boundaries of the maximum call option

Fourthly, we consider the put option on the minimum. Define $E^i = E \cap G^i, i = 1, 2$ where $G^i \equiv \{(S_t^1, S_t^2, t) : S_t^i = \min(S_t^1, S_t^2)\}$. We have the following observation from the Fig. 4.5:

(1) $(S_t^1, S_t^2, t) \in E$ implies $(S_t^1, S_t^2, s) \in E$ for all $t \le s \le T$.

(2) $(S_t^1, S_t^2, t) \in E^1$ implies $(\lambda S_t^1, S_t^2, t) \in E^1$ for all $0 \le \lambda \le 1$. $(S_t^1, S_t^2, t) \in E^2$ implies $(S_t^1, \lambda S_t^2, t) \in E^2$ for all $0 \le \lambda \le 1$.

(3) $(S_t^1, S_t^2, t) \in E^1$ implies $(S_t^1, \lambda S_t^2, t) \in E^1$ for all $\lambda \ge 1$. $(S_t^1, S_t^2, t) \in E^2$ implies $(\lambda S_t^1, S_t^2, t) \in E^2$ for all $\lambda \ge 1$.

(4) $(S_t^1, S_t^2, t) \in E^j$ and $(\widetilde{S}_t^1, \widetilde{S}_t^2, t) \in E^j$ implies $(S_t^1(\lambda), S_t^2(\lambda), t) \in E^j$ for j=1,2 and all $0 \le \lambda \le 1$, where $S_t^i(\lambda) = \lambda S_t^i + (1-\lambda)\widetilde{S}_t^i$ for $i = 1, 2$.

(5) When $t \to T^-$, the early exercise boundary is given by

$$S_T^1 = \min\left(\min\left(\frac{r}{q_1}K, K\right), S_T^2\right) \, for E^1,$$

$$S_T^2 = \min\left(\min\left(\frac{r}{q_2}K, K\right), S_T^1\right) \, for E^2.$$

(6) The early exercise boundaries of different times are more dispersive when the correlation is negative.

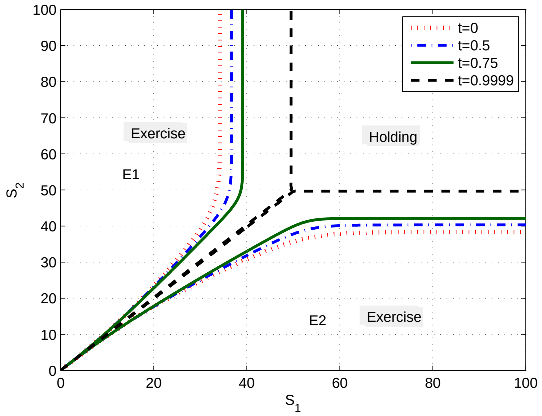

(a) $\rho = 0.5, q_1 = 0.02, q_2 = 0.04, r = 0.06$

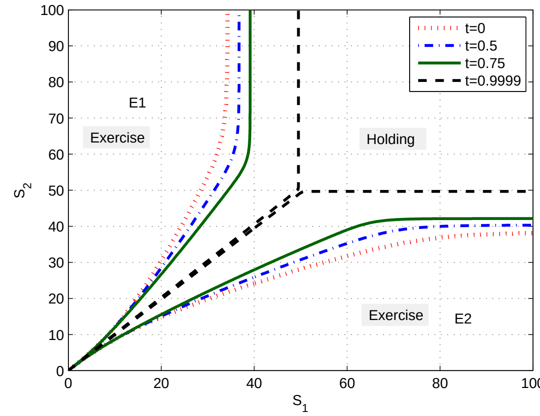

(b) $\rho = -0.5, q_1 = 0.02, q_2 = 0.04, r = 0.06$

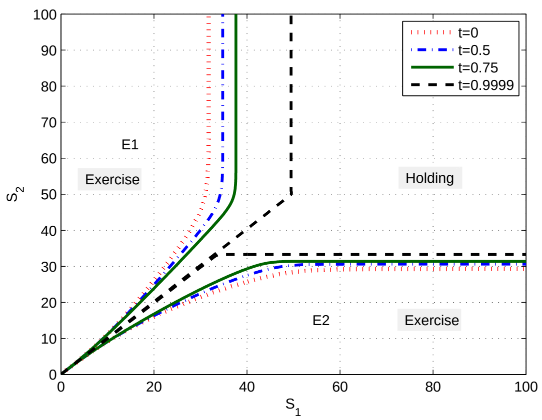

(c) $\rho = 0.5, q_1 = 0.02, q_2 = 0.06, r = 0.04$

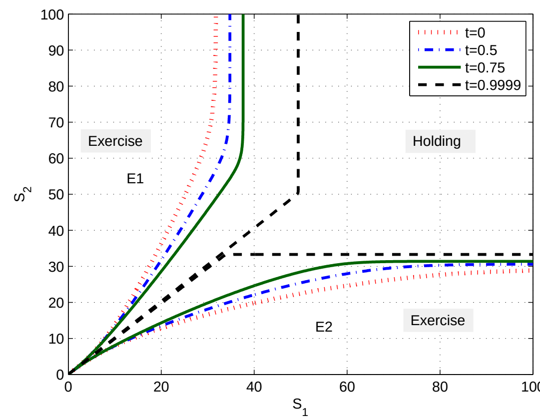

(d) $\rho = -0.5, q_1 = 0.02, q_2 = 0.06, r = 0.04$

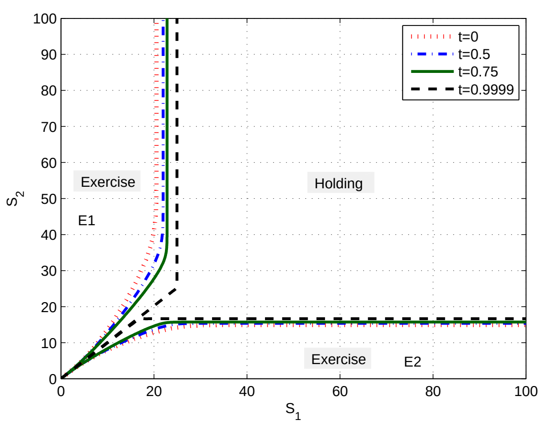

(e) $\rho = 0.5, q_1 = 0.04, q_2 = 0.06, r = 0.02$

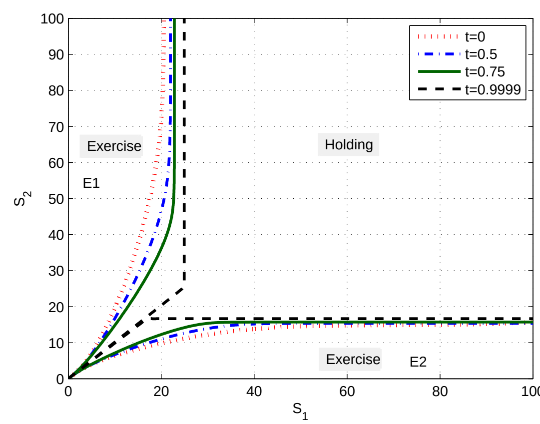

(f) $\rho = -0.5, q_1 = 0.04, q_2 = 0.06, r = 0.02$

Figure 4.5: The early exercise boundaries of the put option on the minimum

Finally, we consider the maximum put option. Without lose of generality, assume that $K_1 < K_2$. Define $E^i = E \cap G^i, i = 1,2$ where $G^i \equiv \{(S_t^1, S_t^2, t) : K_i - S_t^i = \max(K_1 - S_t^1, K_2 - S_t^2)\}$. We have the following observation form the Fig. 4.6:

(1) $(S_t^1, S_t^2, t) \in E$ implies $(S_t^1, S_t^2, s) \in E$ for all $t \leq s \leq T$.

(2) $(S_t^1, S_t^2, t) \in E^1$ implies $(\lambda S_t^1, S_t^2, t) \in E^1$ for all $0 \leq \lambda \leq 1$. $(S_t^1, S_t^2, t) \in E^2$ implies $(S_t^1, \lambda S_t^2, t) \in E^2$ for all $0 \leq \lambda \leq 1$.

(3) $(S_t^1, S_t^2, t) \in E^1$ implies $(S_t^1, \lambda S_t^2, t) \in E^1$ for all $\lambda \geq 1$. $(S_t^1, S_t^2, t) \in E^2$ implies $(\lambda S_t^1, S_t^2, t) \in E^2$ for all $\lambda \geq 1$.

(4) $(S_t^1, S_t^2, t) \in E^j$ and $(\widetilde{S}_t^1, \widetilde{S}_t^2, t) \in E^j$ implies $(S_t^1(\lambda), S_t^2(\lambda), t) \in E^j$ for j=1,2 and all $0 \leq \lambda \leq 1$, where $S_t^i(\lambda) = \lambda S_t^i + (1-\lambda)\widetilde{S}_t^i$ for $i = 1,2$.

(5) When $t \to T^-$, the early exercise boundary is given by

$$S_T^1 = \min\left(\min\left(\frac{r}{q_1}K_1, K_1\right), \max(S_T^2 - K_2 + K_1, 0)\right) for E^1,$$
$$S_T^2 = \min\left(\min\left(\frac{r}{q_2}K_2, K_2\right), S_T^1 + K_2 - K_1\right) for E^2.$$

(6) The early exercise boundaries of different times are more dispersive when the correlation is negative.

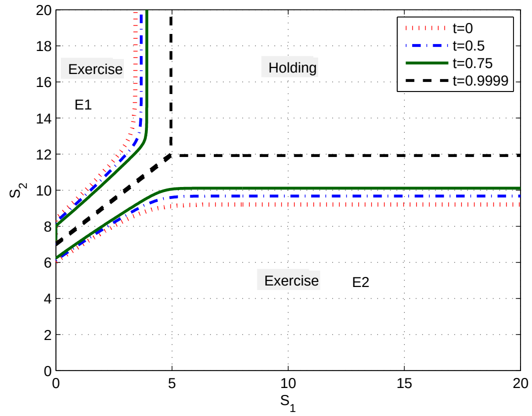

(a) $\rho = 0.5, q_1 = 0.02, q_2 = 0.04, r = 0.06$

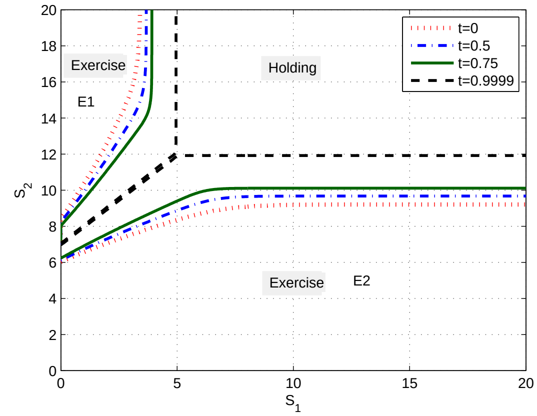

(b) $\rho = -0.5, q_1 = 0.02, q_2 = 0.04, r = 0.06$

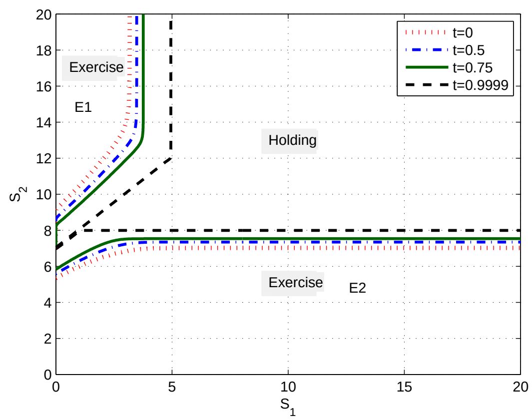

(c) $\rho = 0.5, q_1 = 0.02, q_2 = 0.06, r = 0.04$

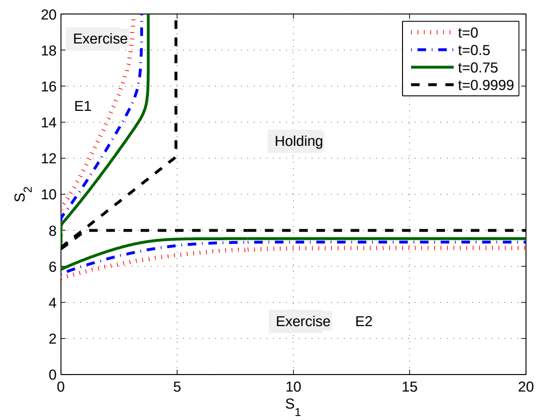

(d) $\rho = -0.5, q_1 = 0.02, q_2 = 0.06, r = 0.04$

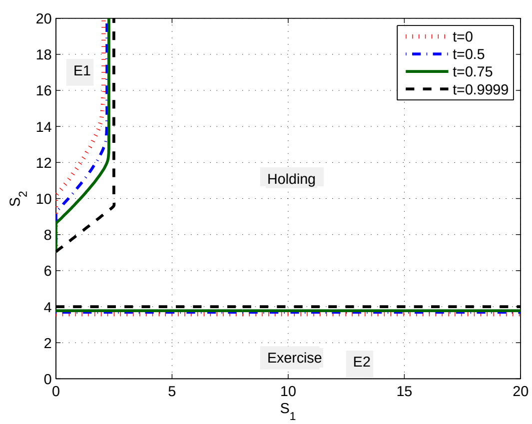

(e) $\rho = 0.5, q_1 = 0.04, q_2 = 0.06, r = 0.02$

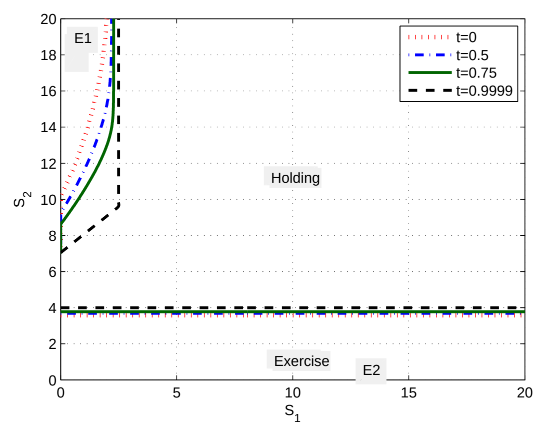

(f) $\rho = -0.5, q_1 = 0.04, q_2 = 0.06, r = 0.02$

Figure 4.6: The early exercise boundaries of the maximum put option

Example 4.3. (*The European option under the Vasicek model*) In this example, we consider the European call option under the Vasicek model using lattice method. The reference values are computed using analytic formula in Fang' paper [23]. The parameters are given in Table 4.8. Other parameters (ρ,θ) will be specified later.

Parameters	Values
K	100
t_0	0.0
T	1.0
q	0.05
σ	0.2
υ	0.2
κ	1.0

Table 4.8: Parameters for the European call option: the Vasicek model

In order to examine the rate of convergence of our lattice method, we plot the maximum absolute errors (MAE) against the time step sizes in Figs. 4.7. The MAEs are computed at the points $S = 60 : 5 : 120 \times r = 0.01 : 0.01 : 0.2$ with different correlations $\rho = -0.8, -0.4, 0.4, 0.8$ and different long-term expectations of interest rates $\theta = 0.04, 0.05, 0.06, 0.07, 0.08$. We can observe that the rate of convergence of our lattice method is about 1. For the accuracy of the lattice scheme, we display the option prices and the absolute errors (AE) in Tables 4.9–4.12. We can see that the AEs is $\mathcal{O}\left(10^{-3}\right)$ when the number of time steps $M = 1000$. All of these numerical results are as expected since the theoretical rate of convergence of the lattice method is $\mathcal{O}\left(M^{-1}\right)$.

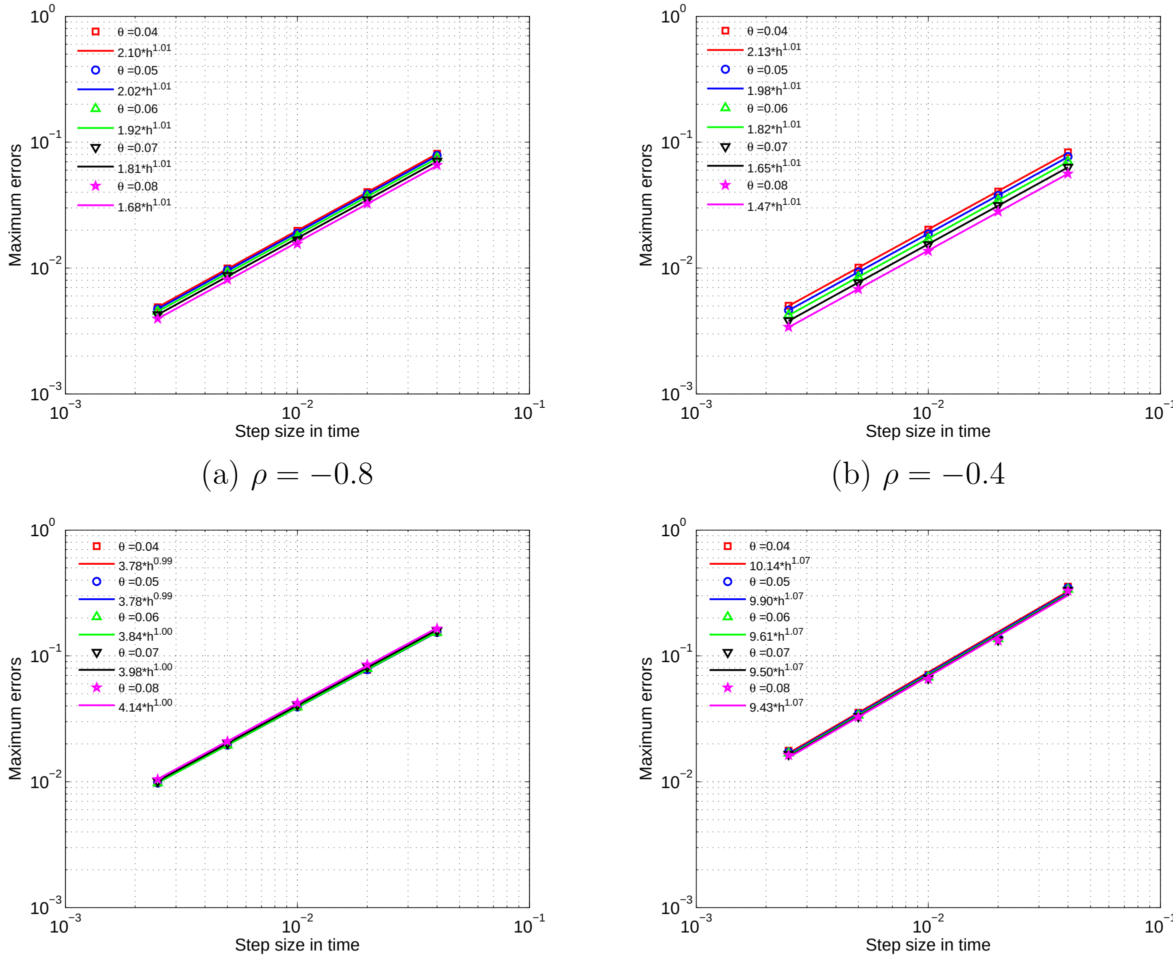

(a) $\rho = -0.8$ (b) $\rho = -0.4$

(c) $\rho = 0.4$ (d) $\rho = 0.8$

Figure 4.7: The maximum absolute errors of the European nall of Vasicek

r	0.02			0.06			0.10		
S	LAT	REF	AE	LAT	REF	AE	LAT	REF	AE
85	0.7346	0.7344	0.0002	1.0113	1.0110	0.0003	1.3646	1.3641	0.0005
90	1.5569	1.5565	0.0003	2.0500	2.0494	0.0006	2.6492	2.6484	0.0008
95	2.8927	2.8923	0.0004	3.6626	3.6619	0.0007	4.5581	4.5571	0.0010
100	4.8262	4.8259	0.0003	5.9057	5.9051	0.0006	7.1146	7.1136	0.0009
105	7.3760	7.3757	0.0003	8.7644	8.7637	0.0007	10.2692	10.2682	0.0010
110	10.4972	10.4971	0.0001	12.1644	12.1639	0.0005	13.9232	13.9223	0.0009
115	14.1024	14.1026	0.0002	16.0007	16.0004	0.0003	17.9598	17.9590	0.0008

Table 4.9: The European call prices (Vasicek): $\theta = 0.05$, $\rho = -0.8$

r	0.02			0.06			0.10		
S	LAT	REF	AE	LAT	REF	AE	LAT	REF	AE
85	1.4073	1.4074	0.0001	1.7845	1.7845	0.0000	2.2338	2.2337	0.0001
90	2.5025	2.5025	0.0000	3.0838	3.0836	0.0002	3.7546	3.7542	0.0004
95	4.0684	4.0683	0.0001	4.8880	4.8877	0.0003	5.8071	5.8065	0.0006
100	6.1414	6.1414	0.0001	7.2156	7.2152	0.0004	8.3902	8.3895	0.0007
105	8.7188	8.7189	0.0000	10.0450	10.0447	0.0003	11.4636	11.4629	0.0008
110	11.7644	11.7646	0.0003	13.3242	13.3240	0.0002	14.9613	14.9606	0.0007
115	15.2194	15.2199	0.0005	16.9838	16.9837	0.0000	18.8061	18.8056	0.0006

Table 4.10: The European call prices (Vasicek): $\theta = 0.05$, $\rho = -0.4$

r	0.02			0.06			0.10		
S	LAT	REF	AE	LAT	REF	AE	LAT	REF	AE
85	2.7313	2.7331	0.0018	3.2229	3.2248	0.0019	3.7749	3.7771	0.0022
90	4.1606	4.1625	0.0019	4.8295	4.8314	0.0019	5.5665	5.5686	0.0021
95	5.9893	5.9914	0.0021	6.8505	6.8524	0.0019	7.7837	7.7857	0.0020
100	8.2224	8.2247	0.0023	9.2816	9.2836	0.0020	10.4122	10.4141	0.0019
105	10.8463	10.8489	0.0026	12.1003	12.1025	0.0021	13.4211	13.4230	0.0019
110	13.8333	13.8361	0.0029	15.2717	15.2740	0.0023	16.7687	16.7706	0.0020
115	17.1459	17.1491	0.0032	18.7531	18.7556	0.0025	20.4083	20.4104	0.0020

Table 4.11: The European call prices (Vasicek): $\theta = 0.05$, $\rho = 0.4$

r	0.02			0.06			0.10		
S	LAT	REF	AE	LAT	REF	AE	LAT	REF	AE
85	3.3544	3.3575	0.0031	3.8814	3.8847	0.0033	4.4637	4.4675	0.0039
90	4.8977	4.9010	0.0033	5.5910	5.5945	0.0034	6.3454	6.3493	0.0039
95	6.8137	6.8173	0.0036	7.6843	7.6879	0.0035	8.6185	8.6223	0.0038
100	9.1012	9.1053	0.0040	10.1527	10.1564	0.0038	11.2668	11.2707	0.0039
105	11.7455	11.7498	0.0043	12.9746	12.9784	0.0039	14.2624	14.2663	0.0039
110	14.7208	14.7255	0.0047	16.1189	16.1231	0.0041	17.5692	17.5732	0.0040
115	17.9953	18.0004	0.0051	19.5498	19.5542	0.0044	21.1480	21.1521	0.0041

Table 4.12: The European call prices (Vasicek): $\theta = 0.05$, $\rho = 0.8$

Example 4.4. (*The early exercise boundaries of the American options under the Vasicek model*) In this example, we consider the early exercise boundaries of the American call and put options under the Vasicek stochastic interest rate model with the following parameters:

$$K = 100, t = 0, T = 1, \sigma = 0.3, \kappa = 2.0, v = 0.2.$$

The other parameters (correlation ρ, dividend rate q, and long term mean θ) will be specified later. All the early exercise boundaries are computed via bisection methods using Algorithm 4 in section 4.2 with number of time steps $M = 500$.

Firstly, we consider the call option. Figures 4.8 show the early exercise boundaries with fixed q and changing θ, while figures 4.9 are with changing q and fixed θ. Figures 4.10 are plotted with extreme case (r up to 1.0). Denote S_t, r_t as the spot asset price and interest rate at time t, and let E be the immediate exercise region. From the above figures, we have the following observations:

(1) $(S_t, r_t, t) \in E$ implies $S_t > K$.

(2) $(S_t, r_t, t) \in E$ does not implies $(S_t, r_t, s) \in E$ for all $t \leq s \leq T$.

(3) $(S_t, r_t, t) \in E$ implies $(\lambda S_t, r_t, t) \in E$ for all $\lambda \geq 1$.

(4) $(S_t, r_t, t) \in E$ implies $(S_t, \lambda r_t, t) \in E$ for all $0 \leq \lambda \leq 1$.

(5) $(S_t, r_t, t) \in E$ and $(\widetilde{S}_t, \widetilde{r}_t, t) \in E$ does not implies $(S_t(\lambda), r_t(\lambda), t) \in E$ for some $0 \leq \lambda \leq 1$, where $S_t(\lambda) = \lambda S_t + (1-\lambda)\widetilde{S}_t, r_t(\lambda) = \lambda r_t + (1-\lambda)\widetilde{r}_t$ for $i = 1, 2$.

(6) When $t \to T^-$, the early exercise boundary is given by $S_T = \max\left(\frac{r_T}{q}K, K\right)$.

(7) θ does not significantly change the shape of early exercise region.

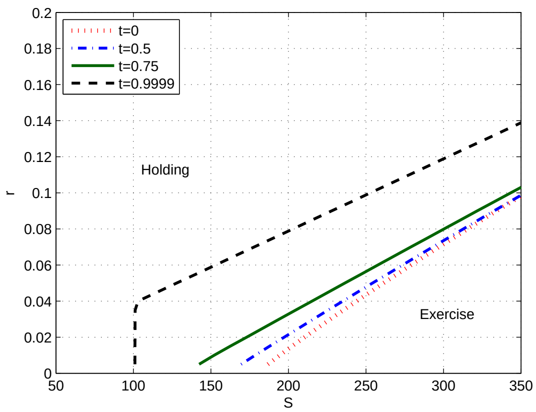

(a) $\rho = 0.5, q = 0.04, \theta = 0.02$

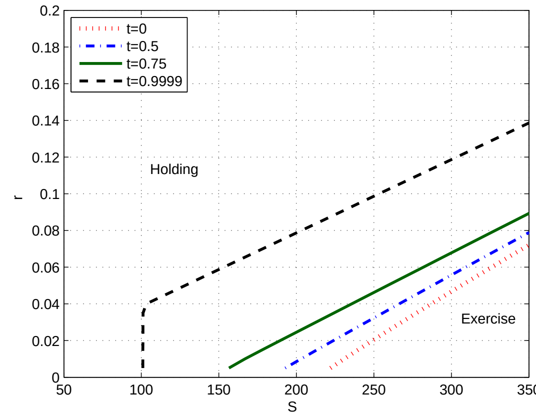

(b) $\rho = -0.5, q = 0.04, \theta = 0.02$

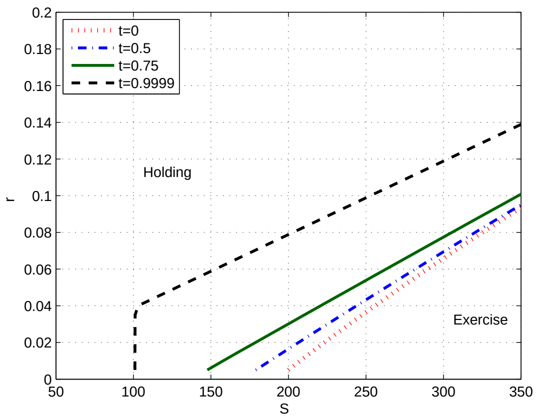

(c) $\rho = 0.5, q = 0.04, \theta = 0.04$

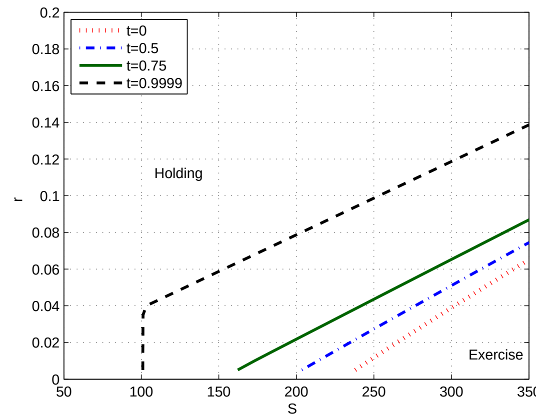

(d) $\rho = -0.5, q = 0.04, \theta = 0.04$

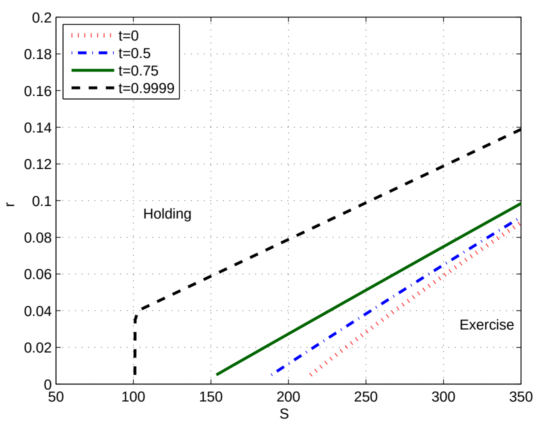

(e) $\rho = 0.5, q = 0.04, \theta = 0.06$

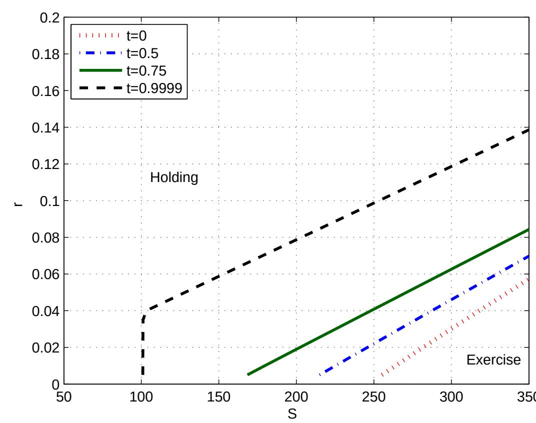

(f) $\rho = -0.5, q = 0.04, \theta = 0.06$

Figure 4.8: The early exercise boundaries of call option (Vasicek, ρ, θ)

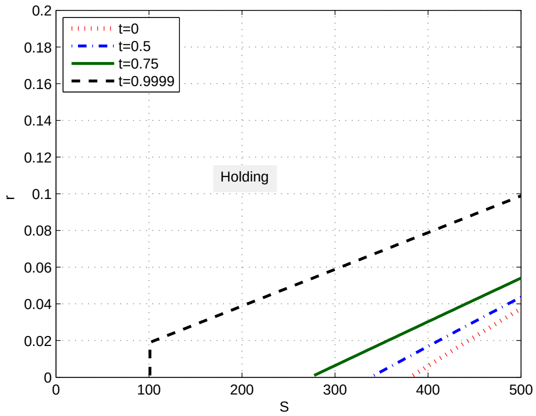

(a) $\rho = 0.5, q = 0.02, \theta = 0.04$

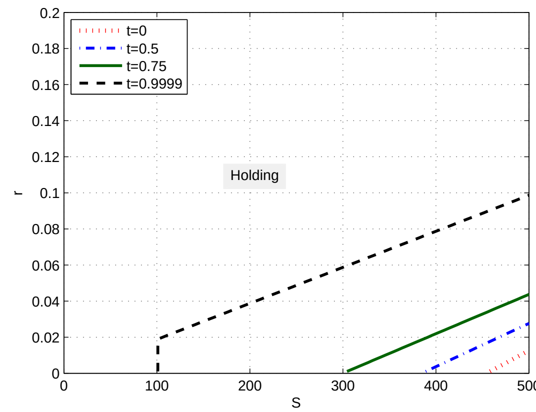

(b) $\rho = -0.5, q = 0.02, \theta = 0.04$

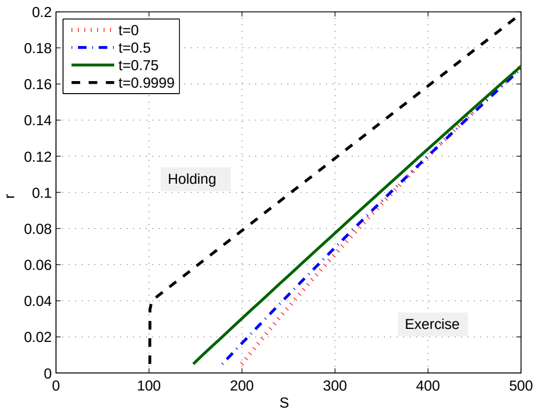

(c) $\rho = 0.5, q = 0.04, \theta = 0.04$

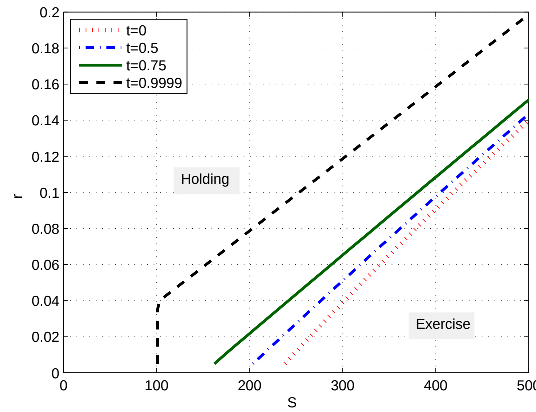

(d) $\rho = -0.5, q = 0.04, \theta = 0.04$

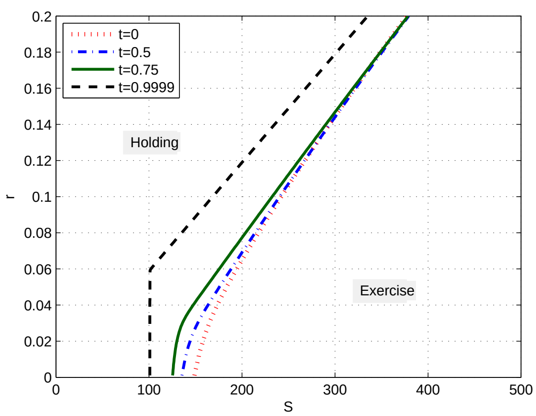

(e) $\rho = 0.5, q = 0.06, \theta = 0.04$

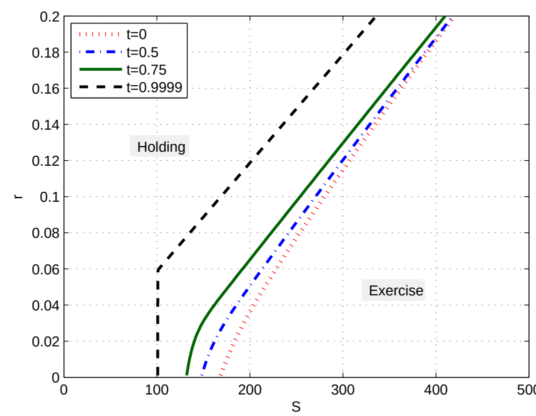

(f) $\rho = -0.5, q = 0.06, \theta = 0.04$

Figure 4.9: The early exercise boundaries of call option (Vasicek, ρ, q)

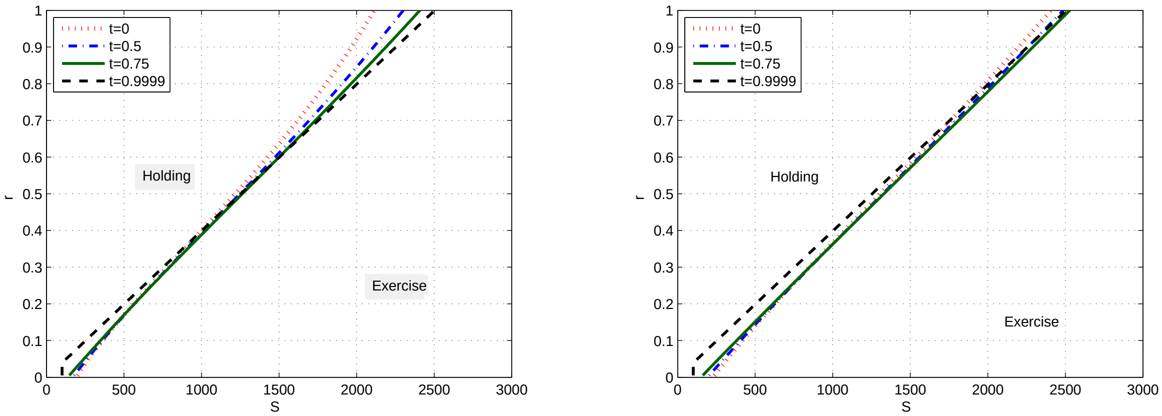

(a) $\rho = 0.5, q = 0.04, \theta = 0.04$ (b) $\rho = -0.5, q = 0.04, \theta = 0.04$

Figure 4.10: The early exercise boundaries of call option with Vasicek (extreme)

Next, we consider the put option. Fig. 4.11 show the early exercise boundaries with fixed q and changing θ, while Fig. 4.12 are with changing q and fixed θ. Denote S_t, r_t as the spot asset price and interest rate at time t, and let E be the immediate exercise region. From the above figures, we have the following observations:

(1) $(S_t, r_t, t) \in E$ implies $S_t < K$.

(2) $(S_t, r_t, t) \in E$ implies $(S_t, r_t, s) \in E$ for all $t \leq s \leq T$.

(3) $(S_t, r_t, t) \in E$ implies $(S_t, \lambda r_t, t) \in E$ for all $\lambda \geq 1$.

(4) $(S_t, r_t, t) \in E$ implies $(\lambda S_t, r_t, t) \in E$ for all $0 \leq \lambda \leq 1$.

(5) $(S_t, r_t, t) \in E$ and $(\widetilde{S}_t, \widetilde{r}_t, t) \in E$ implies $(S_t(\lambda), r_t(\lambda), t) \in E$ for all $0 \leq \lambda \leq 1$, where $S_t(\lambda) = \lambda S_t + (1-\lambda)\widetilde{S}_t, r_t(\lambda) = \lambda r_t + (1-\lambda)\widetilde{r}_t$ for $i = 1, 2$.

(6) When $t \to T^-$, the early exercise boundary is given by $S_T = \min\left(\frac{r_T}{q}K, K\right)$.

(7) θ does not significantly change the shape of early exercise region.

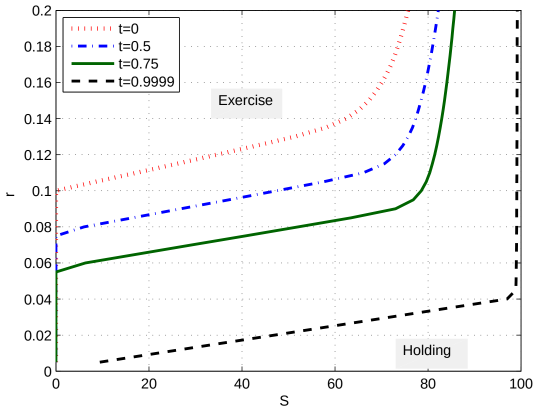

(a) $\rho = 0.5, q = 0.04, \theta = 0.02$

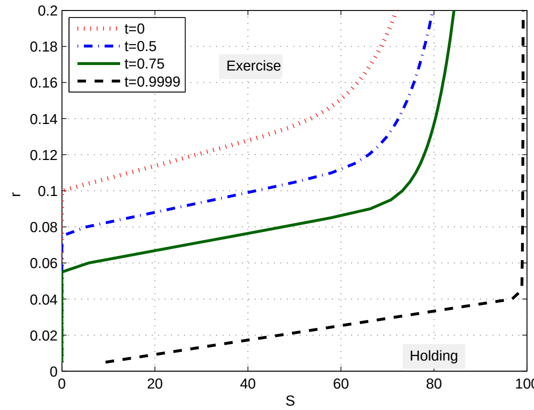

(b) $\rho = -0.5, q = 0.04, \theta = 0.02$

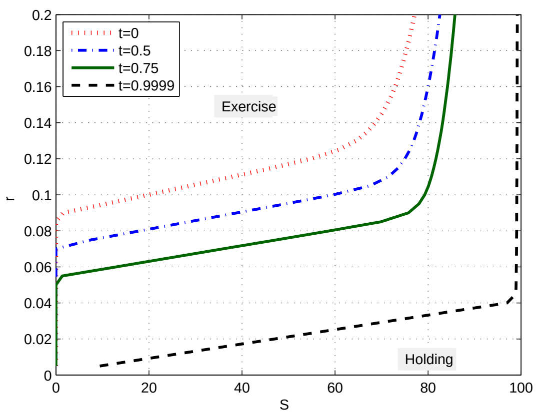

(c) $\rho = 0.5, q = 0.04, \theta = 0.04$

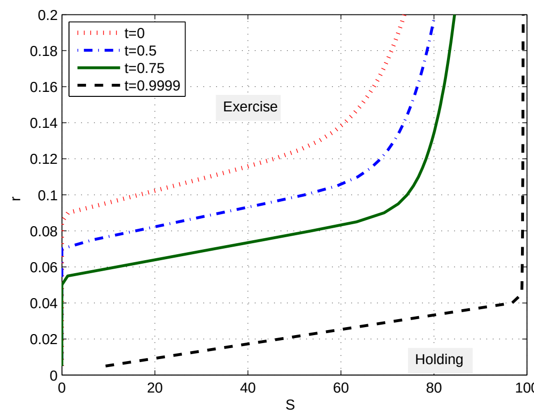

(d) $\rho = -0.5, q = 0.04, \theta = 0.04$

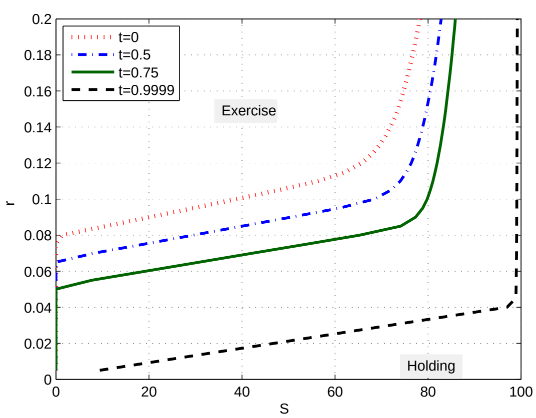

(e) $\rho = 0.5, q = 0.04, \theta = 0.06$

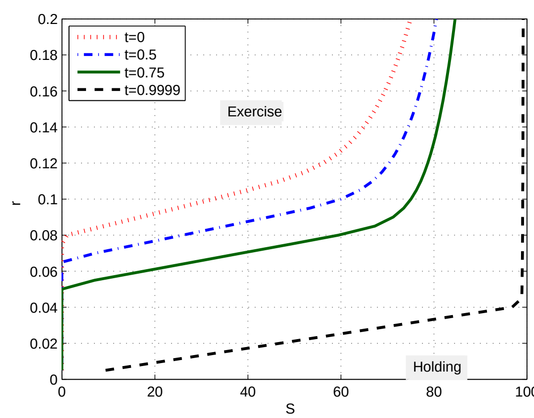

(f) $\rho = -0.5, q = 0.04, \theta = 0.06$

Figure 4.11: The early exercise boundaries of put option (Vasicek, ρ, θ)

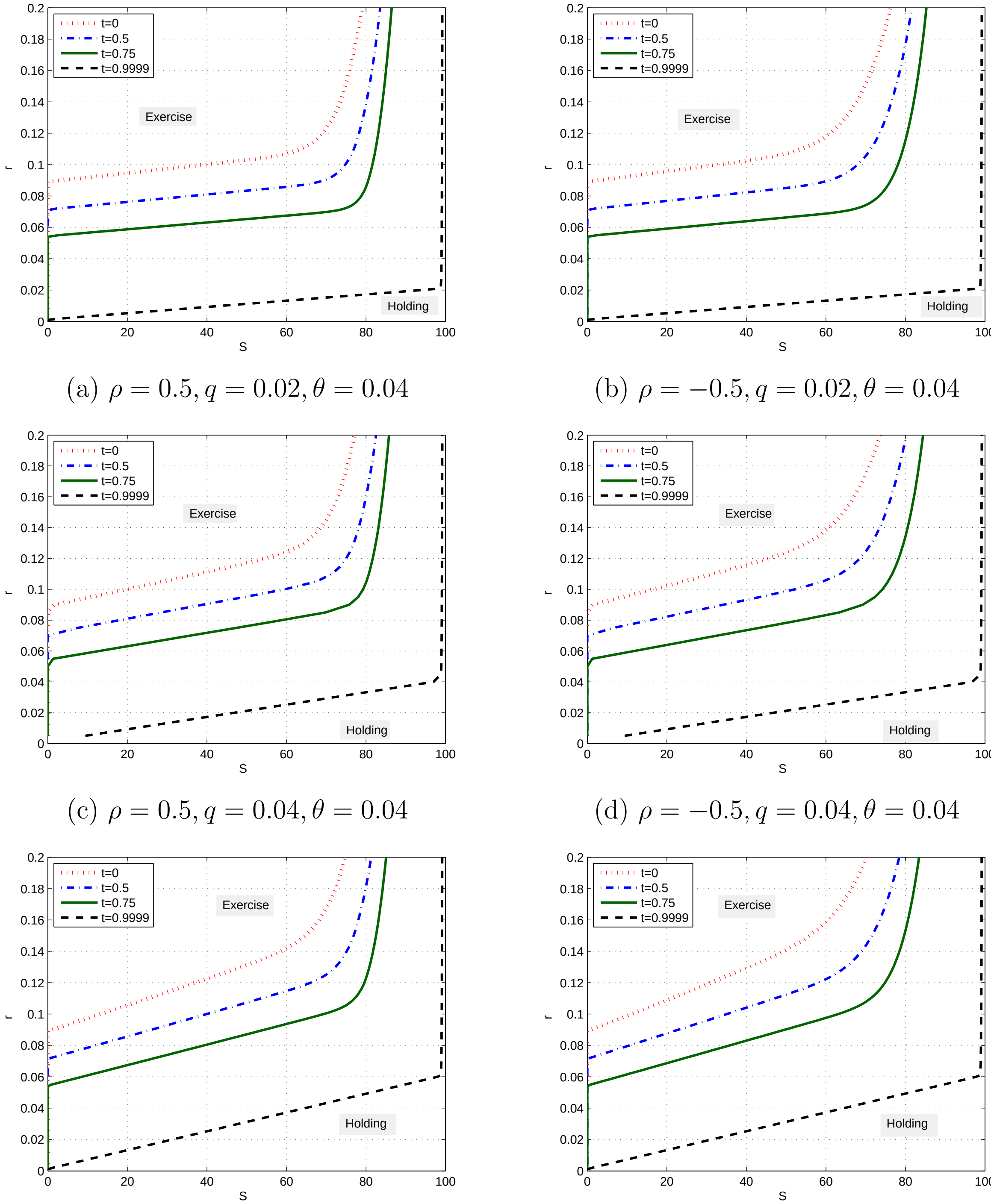

(a) $\rho = 0.5, q = 0.02, \theta = 0.04$

(b) $\rho = -0.5, q = 0.02, \theta = 0.04$

(c) $\rho = 0.5, q = 0.04, \theta = 0.04$

(d) $\rho = -0.5, q = 0.04, \theta = 0.04$

(e) $\rho = 0.5, q = 0.06, \theta = 0.04$

(f) $\rho = -0.5, q = 0.06, \theta = 0.04$

Figure 4.12: The early exercise boundaries of put option (Vasicek, ρ, q)

Example 4.5. (*The European options under the CIR model*) In this example, we consider the European call options under the CIR model using lattice method with the parameters in table 4.13. Other parameters (ρ,θ) will be specified later. The parameters are chosen to satisfy the Feller condition $2\kappa\theta > v^2$. Notice that there is no analytic solution for the European options, we compute the result using mixed Monte Carlo method with the control variates from previous chapter with $M = 1000$, $N = 1000000$ as reference values.

Parameters	Values
K	100
t_0	0.0
T	1.0
q	0.05
σ	0.2
v	0.2
κ	1.0

Table 4.13: Parameters for the European call option: the CIR model

In order to examine the rate of convergence of our lattice method, we plot the maximum absolute errors (MAE) against the time step sizes in Figs. 4.13. Since there is no analytic solutions, we investigating the rate of convergence by examining the errors between the approximate solutions for numbers of steps M and $2M$. The MAEs are computed at the points $S = 60 : 5 : 120 \times r = 0.01 : 0.01 : 0.2$ with different correlations $\rho = -0.8, -0.4, 0.4, 0.8$ and different long-term means of interest rates $\theta = 0.04, 0.05, 0.06, 0.07, 0.08$. We can observe that the rate of convergence of our lattice method is about 1. For the accuracy, we display the option prices and the absolute errors (AE) in Tables 4.14–4.17. We can see that the AEs is $\mathcal{O}\left(10^{-3}\right)$ when the number of time steps $M = 1000$. All of these numerical results are as expected since the theoretical rate of convergence of the lattice method is $\mathcal{O}\left(M^{-1}\right)$.

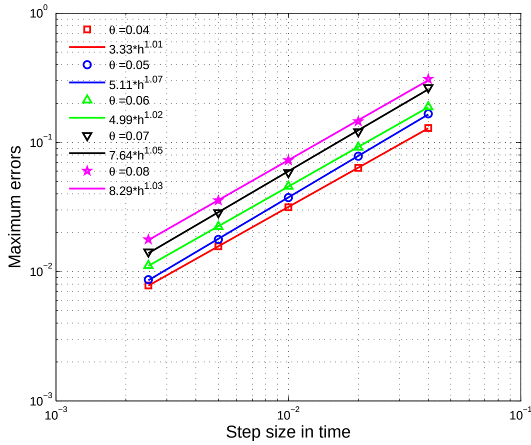

(a) $\rho = -0.8$

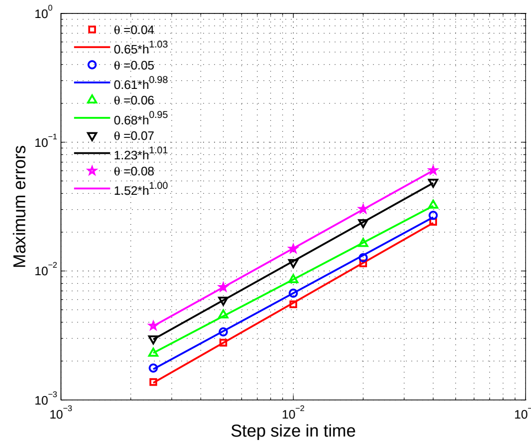

(b) $\rho = -0.4$

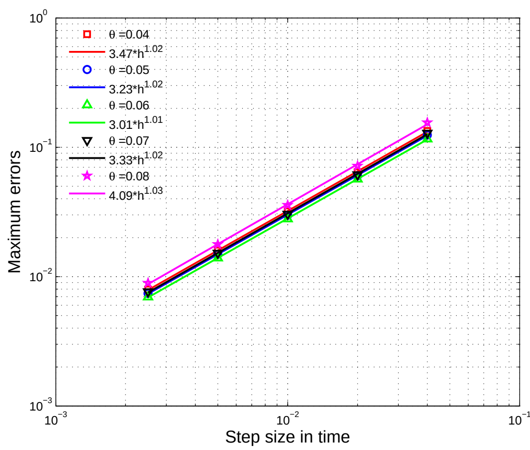

(c) $\rho = 0.4$

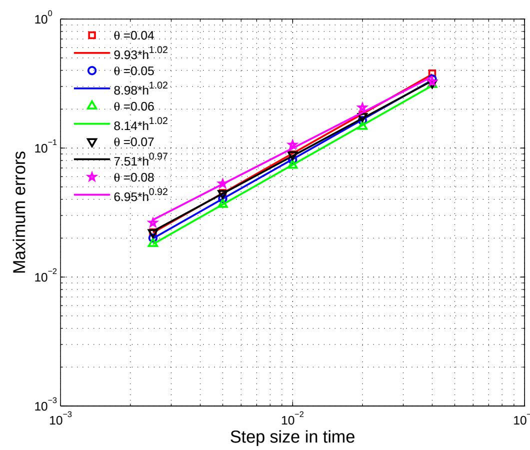

(d) $\rho = 0.8$

Figure 4.13: The maximum absolute errors of the European Call of CIR

r	0.02			0.06			0.10		
S	LAT	MMC	AE	LAT	MMC	AE	LAT	MMC	AE
85	1.5586	1.5666	0.0080	1.8590	1.8591	0.0001	2.2365	2.2397	0.0032
90	2.7038	2.7104	0.0067	3.1801	3.1862	0.0061	3.7605	3.7594	0.0012
95	4.3146	4.3214	0.0068	5.0054	5.0065	0.0011	5.8224	5.8269	0.0045
100	6.4232	6.4298	0.0067	7.3533	7.3515	0.0018	8.4223	8.4235	0.0012
105	9.0255	9.0225	0.0030	10.2026	10.2059	0.0033	11.5198	11.5221	0.0022
110	12.0858	12.0921	0.0063	13.5011	13.5089	0.0078	15.0469	15.0492	0.0022
115	15.5475	15.5506	0.0030	17.1797	17.1825	0.0029	18.9238	18.9306	0.0069

Table 4.14: The European call prices (CIR): $\theta = 0.05$, $\rho = -0.8$

r	0.02			0.06			0.10		
S	LAT	MMC	AE	LAT	MMC	AE	LAT	MMC	AE
85	1.6515	1.6526	0.0010	2.0163	2.0159	0.0004	2.4580	2.4581	0.0000
90	2.8314	2.8325	0.0011	3.3869	3.3866	0.0003	4.0394	4.0389	0.0005
95	4.4737	4.4731	0.0006	5.2520	5.2517	0.0003	6.1409	6.1400	0.0009
100	6.6056	6.6053	0.0003	7.6236	7.6234	0.0002	8.7568	8.7584	0.0015
105	9.2198	9.2207	0.0010	10.4779	10.4777	0.0001	11.8466	11.8484	0.0018
110	12.2800	12.2801	0.0001	13.7644	13.7644	0.0000	15.3468	15.3460	0.0008
115	15.7314	15.7322	0.0008	17.4179	17.4194	0.0015	19.1845	19.1836	0.0009

Table 4.15: The European call prices (CIR): $\theta = 0.05$, $\rho = -0.4$

r	0.02			0.06			0.10		
S	LAT	MMC	AE	LAT	MMC	AE	LAT	MMC	AE
85	1.8771	1.8763	0.0009	2.3718	2.3731	0.0013	2.9283	2.9294	0.0010
90	3.1180	3.1199	0.0019	3.8228	3.8229	0.0001	4.5956	4.5944	0.0011
95	4.8073	4.8090	0.0017	5.7427	5.7421	0.0006	6.7462	6.7485	0.0023
100	6.9659	6.9668	0.0009	8.1371	8.1358	0.0013	9.3704	9.3702	0.0002
105	9.5846	9.5876	0.0030	10.9825	10.9864	0.0039	12.4316	12.4341	0.0025
110	12.6294	12.6312	0.0018	14.2341	14.2321	0.0020	15.8760	15.8765	0.0005
115	16.0501	16.0537	0.0035	17.8350	17.8357	0.0007	19.6416	19.6433	0.0017

Table 4.16: The European call prices (CIR): $\theta = 0.05$, $\rho = 0.4$

r	0.02			0.06			0.10		
S	LAT	MMC	AE	LAT	MMC	AE	LAT	MMC	AE
85	2.0066	2.0153	0.0087	2.5638	2.5632	0.0006	3.1702	3.1722	0.0020
90	3.2731	3.2832	0.0101	4.0467	4.0501	0.0034	4.8695	4.8704	0.0009
95	4.9786	4.9766	0.0020	5.9847	5.9858	0.0010	7.0346	7.0339	0.0007
100	7.1423	7.1439	0.0016	8.3820	8.3856	0.0036	9.6554	9.6622	0.0068
105	9.7559	9.7610	0.0051	11.2168	11.2133	0.0035	12.6987	12.6985	0.0002
110	12.7871	12.7976	0.0105	14.4474	14.4473	0.0001	16.1146	16.1109	0.0037
115	16.1887	16.1944	0.0057	18.0209	18.0224	0.0015	19.8462	19.8538	0.0076

Table 4.17: The European call prices (CIR): $\theta = 0.05$, $\rho = 0.8$

Example 4.6. (*The American options under the CIR model*) In this example, we consider the early exercise boundaries (with respect to S and r) of the American call and put options under the CIR stochastic interest rate model with the following parameters:

$$K = 100, t = 0, T = 1, \sigma = 0.3, \kappa = 2.0, v = 0.2.$$

The other parameters (correlation ρ, dividend rate q, and long term mean θ) will be specified later. All the early exercise boundaries are computed via bisection methods using Algorithm 4 in section 4.2 with number of time steps $M = 500$.

Firstly, we consider the call option. Fig. 4.14 show the early exercise boundaries with fixed q and changing θ, while Fig. 4.15 are with changing q and fixed θ. Fig. 4.16 are plotted with extreme case (r up to 1.0). Denote S_t, r_t as the spot asset price and interest rate at time t, and let E be the immediate exercise region. We have the following observations:

(1) $(S_t, r_t, t) \in E$ implies $S_t > K$.

(2) $(S_t, r_t, t) \in E$ does not implies $(S_t, r_t, s) \in E$ for all $t \leq s \leq T$.

(3) $(S_t, r_t, t) \in E$ implies $(\lambda S_t, r_t, t) \in E$ for all $\lambda \geq 1$.

(4) $(S_t, r_t, t) \in E$ implies $(S_t, \lambda r_t, t) \in E$ for all $0 \leq \lambda \leq 1$.

(5) $(S_t, r_t, t) \in E$ and $(\widetilde{S}_t, \widetilde{r}_t, t) \in E$ does not implies $(S_t(\lambda), r_t(\lambda), t) \in E$ for some $0 \leq \lambda \leq 1$, where $S_t(\lambda) = \lambda S_t + (1-\lambda)\widetilde{S}_t, r_t(\lambda) = \lambda r_t + (1-\lambda)\widetilde{r}_t$ for $i = 1, 2$.

(6) When $t \to T^-$, the early exercise boundary is given by $S_T = \max\left(\frac{r_T}{q}K, K\right)$.

(7) θ does not significantly change the shape of early exercise region.

(8) The early exercise boundaries at different times in each case are closer to each other, compare with Vasicek model.

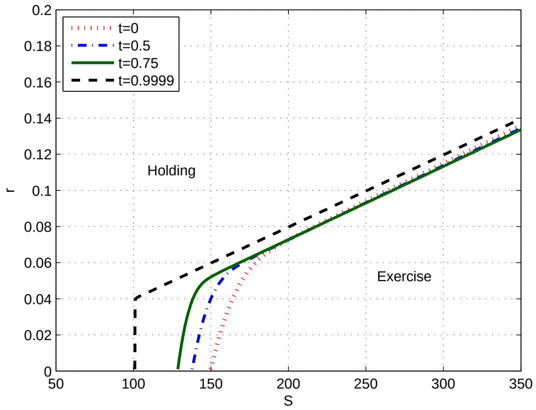

(a) $\rho = 0.5, q = 0.04, \theta = 0.02$

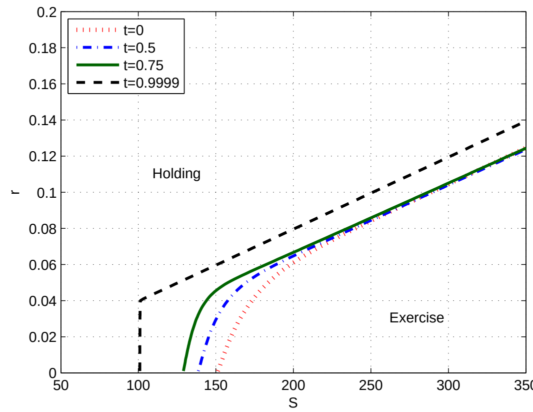

(b) $\rho = -0.5, q = 0.04, \theta = 0.02$

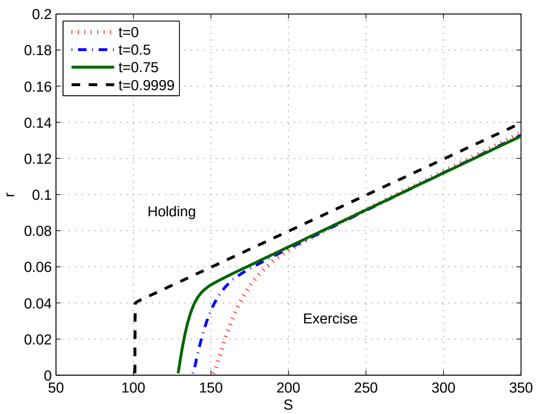

(c) $\rho = 0.5, q = 0.04, \theta = 0.04$

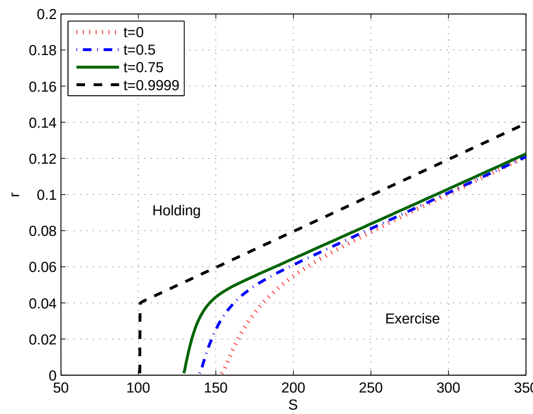

(d) $\rho = -0.5, q = 0.04, \theta = 0.04$

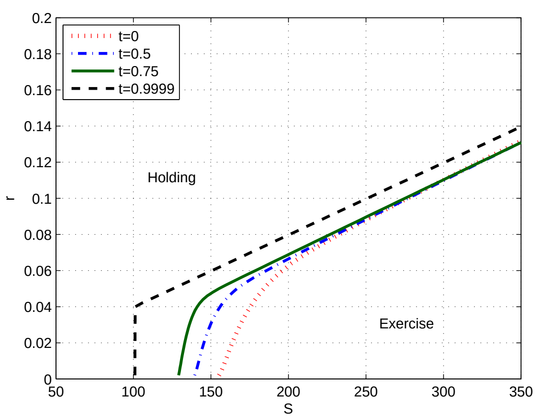

(e) $\rho = 0.5, q = 0.04, \theta = 0.06$

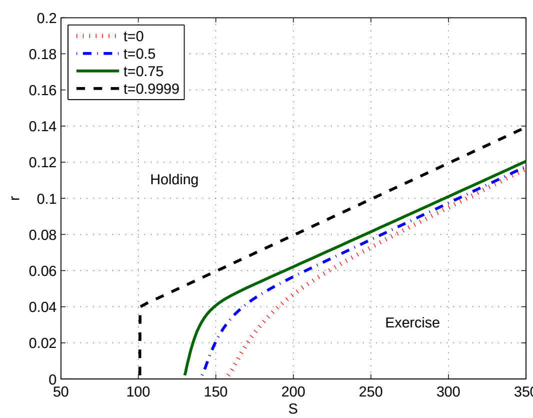

(f) $\rho = -0.5, q = 0.04, \theta = 0.06$

Figure 4.14: The early exercise boundaries of call option (CIR, ρ, θ)

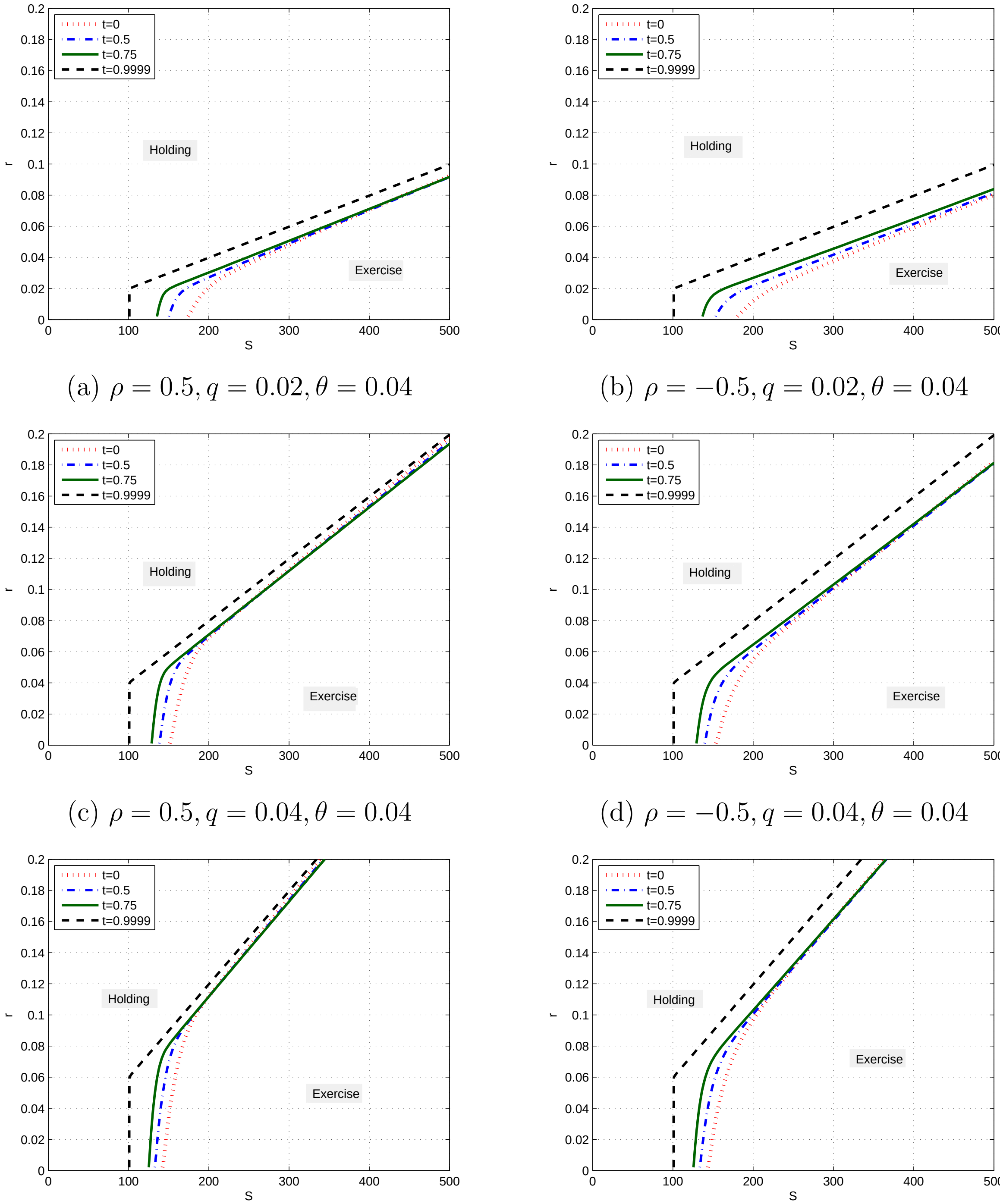

(a) $\rho = 0.5, q = 0.02, \theta = 0.04$

(b) $\rho = -0.5, q = 0.02, \theta = 0.04$

(c) $\rho = 0.5, q = 0.04, \theta = 0.04$

(d) $\rho = -0.5, q = 0.04, \theta = 0.04$

(e) $\rho = 0.5, q = 0.06, \theta = 0.04$

(f) $\rho = -0.5, q = 0.06, \theta = 0.04$

Figure 4.15: The early exercise boundaries of call option (CIR, ρ, q)

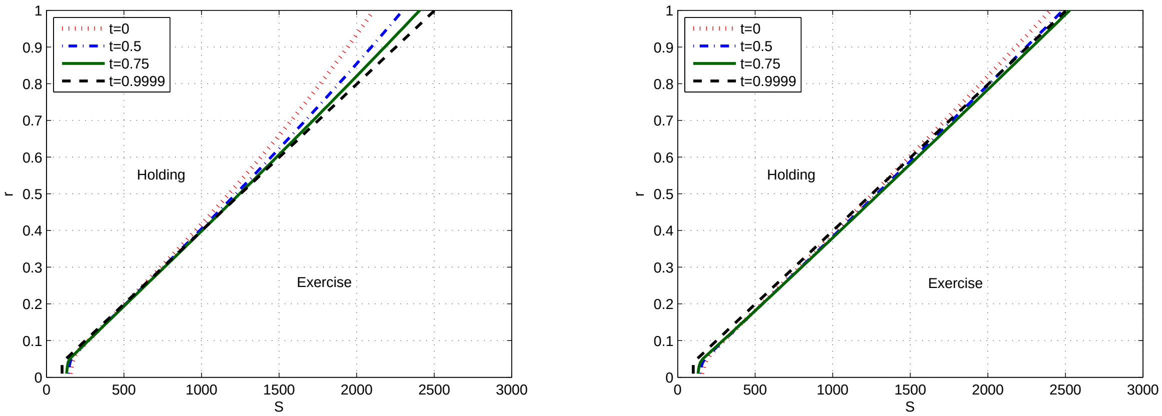

(a) $\rho = 0.5, q = 0.04, \theta = 0.04$ (b) $\rho = -0.5, q = 0.04, \theta = 0.04$

Figure 4.16: The early exercise boundaries of call option with CIR (extreme)

Next, we consider the put option. Fig. 4.17 show the early exercise boundaries with fixed q and changing θ, while Fig. 4.18 are with changing q and fixed θ. We have the following observations:

(1) $(S_t, r_t, t) \in E$ implies $S_t < K$.

(2) $(S_t, r_t, t) \in E$ implies $(S_t, r_t, s) \in E$ for all $t \leq s \leq T$.

(3) $(S_t, r_t, t) \in E$ implies $(S_t, \lambda r_t, t) \in E$ for all $\lambda \geq 1$.

(4) $(S_t, r_t, t) \in E$ implies $(\lambda S_t, r_t, t) \in E$ for all $0 \leq \lambda \leq 1$.

(5) $(S_t, r_t, t) \in E$ and $(\widetilde{S}_t, \widetilde{r}_t, t) \in E$ implies $(S_t(\lambda), r_t(\lambda), t) \in E$ for all $0 \leq \lambda \leq 1$, where $S_t(\lambda) = \lambda S_t + (1-\lambda)\widetilde{S}_t, r_t(\lambda) = \lambda r_t + (1-\lambda)\widetilde{r}_t$ for $i = 1, 2$.

(6) When $t \to T^-$, the early exercise boundary is given by $S_T = \min\left(\frac{r_T}{q}K, K\right)$.

(7) θ does not significantly change the shape of early exercise region.

(8) The early exercise boundaries at different times in each case are closer to each other, compare with Vasicek model.

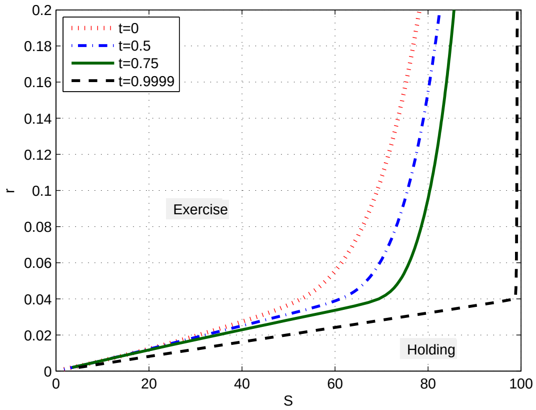

(a) $\rho = 0.5, q = 0.04, \theta = 0.02$

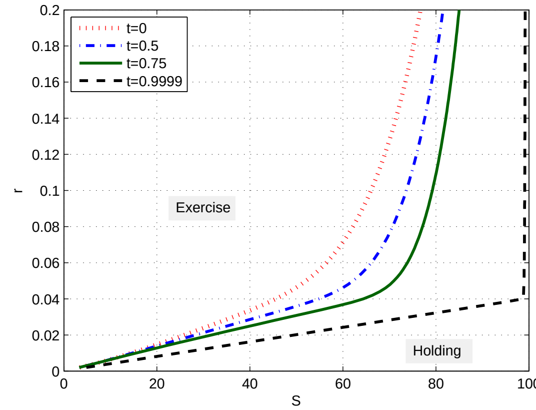

(b) $\rho = -0.5, q = 0.04, \theta = 0.02$

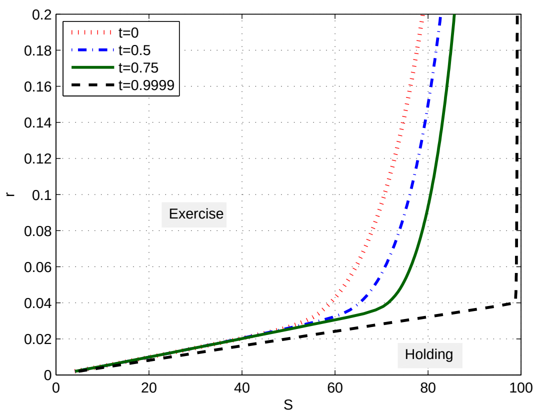

(c) $\rho = 0.5, q = 0.04, \theta = 0.04$

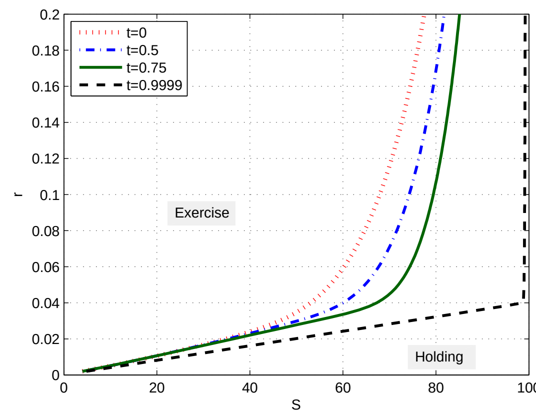

(d) $\rho = -0.5, q = 0.04, \theta = 0.04$

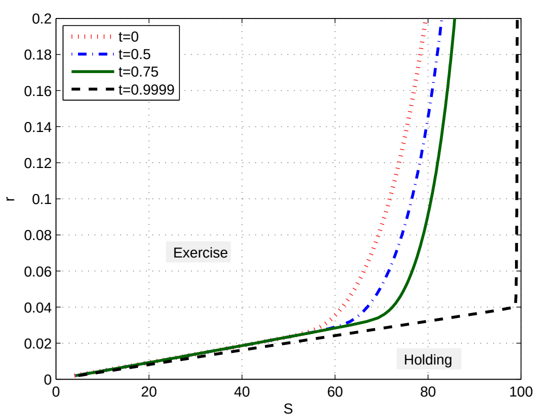

(e) $\rho = 0.5, q = 0.04, \theta = 0.06$

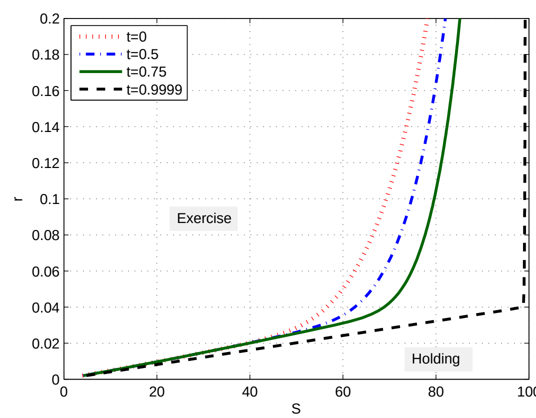

(f) $\rho = -0.5, q = 0.04, \theta = 0.06$

Figure 4.17: The early exercise boundaries of put option (CIR, ρ, θ)

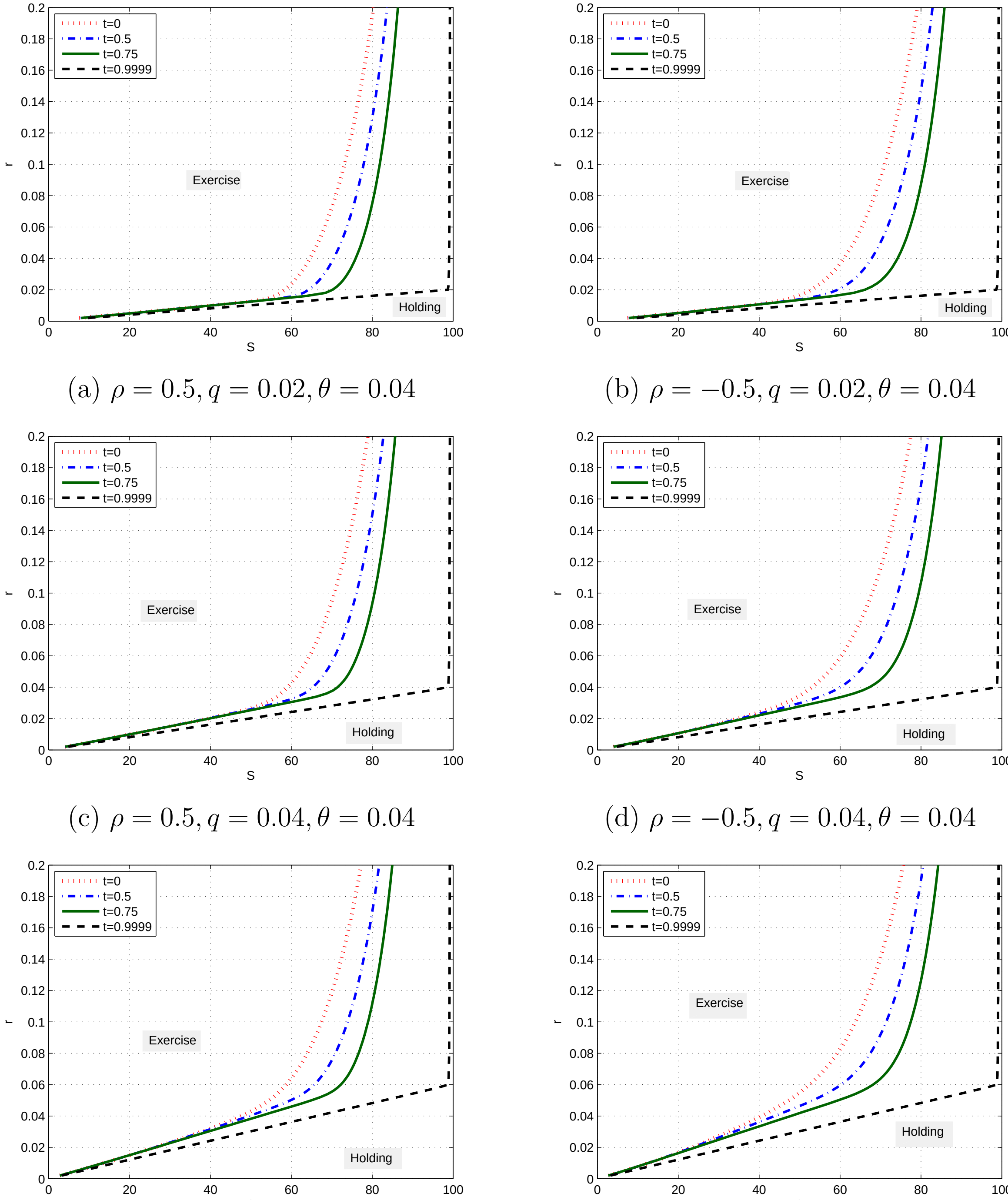

(a) $\rho = 0.5, q = 0.02, \theta = 0.04$

(b) $\rho = -0.5, q = 0.02, \theta = 0.04$

(c) $\rho = 0.5, q = 0.04, \theta = 0.04$

(d) $\rho = -0.5, q = 0.04, \theta = 0.04$

(e) $\rho = 0.5, q = 0.06, \theta = 0.04$

(f) $\rho = -0.5, q = 0.06, \theta = 0.04$

Figure 4.18: The early exercise boundaries of put option (CIR, ρ, q)

CHAPTER 5

A FINITE VOLUME - ADI METHOD

The alternating direction implicit (ADI) method was first introduced by Peaceman and Rachford in 1955[51]. It uses the idea of splitting the finite difference equations into two, one taking x-derivative implicitly and the other taking y-derivative implicitly. We are referred to the book from W. Hundsdorfer and J. Verwer [35].

For multi-asset options, Villeneuve and Zanette [61] performed a coordinate transformation to get an operator that is essentially the standard two-dimensional Laplacian, then Peaceman-Rachford ADI scheme can be applied. Dang, Christara, and Jackson developed an Alternating Direction Implicit Approximate Factorization (ADI-AF) techniques based on Graphics Processing Units (GPUs) in 2010[18]. They used a combination of an efficient GPU-based parallelization of ADI-AF techniques with a penalty approach for the pricing of multi-asset American options in the Black-Scholes framework. For Stochastic Volatility models (especially Heston model), Haentjens and in't Hout [31] developed an effective adaptation of ADI time discretization schemes to the semi-discretized Heston partial differential complementarity problem for American-style options in 2015. The method is applied to the PDE directly without transformation of variables. For models with both stochastic volatility and stochastic interest rate, Haentjens and in in't Hout [30] applied ADI for the Heston

Hull White model. Grzelak and Oosterlee [29] applied ADI for the Heston-Hull-White and Heston-CIR models, Donnelly, Jaimungal, and Rubisov[22] valued guaranteed withdrawal benefits with stochastic interest rates and volatility. Since the the mixed partial derivatives are not removed in these papers, the schemes are complicated and thus inefficient.

In this chapter, we applied the ADI method to the partial differential equations derived under the uncorrelated processes in Chapter 2. The partial differential operator will be discretized by a finite volume method and thus the Neumann boundary conditions can be treated more accurately. Since there is not mixed partial derivatives, our scheme is numerically simplest and very fast. Here we only consider the stochastic volatility model (the Heston model) and it is not difficult to extend our method to the other models in Chapter 2.

5.1 The Partial Differential Variational Inequalities

Consider the European contingent claim with expiration date T and payoff function $\Phi(S)$ under the the Heston model (2.14)–(2.15). Its rational price at time t is given by

$$p(s,v,t) = \mathbb{E}\left[e^{-r(T-t)}\Phi(S(T)) \middle| S(t) = s, v(t) = v \right].$$

Since $e^{-rt}p(S(t), v(t), t)$ is a martingale, it follows from Ito's Lemma that function $p(s,v,t)$ solves the parabolic partial differential equation

$$\frac{\partial p}{\partial t} + \mathcal{K}p = 0, \tag{5.1}$$

where

$$\mathcal{K}p = \frac{1}{2}s^2 v p_{ss} + \rho\sigma s v p_{sv} + \frac{1}{2}\sigma^2 v p_{vv} + (r-q)sp_s + \kappa(\eta - v)p_v - rV. \tag{5.2}$$

The rational price of the American contingent claim is given by

$$q(s,v,t) = \sup_{t \le t^* \le T} \mathbb{E}\left[e^{-r(t^*-t)} \Phi(S(t^*)) \middle| S(t) = s, v(t) = v \right],$$

where t^* is the stopping time. It is known that function $q(S,v,t)$ solves the parabolic partial differential variational inequalities (PDVIs)

$$\frac{\partial q}{\partial t} + \mathcal{K}q \le 0, \quad q \ge \Phi, \quad (q - \Phi)\left(\frac{\partial q}{\partial t} + \mathcal{K}q\right) = 0.$$

It should be pointed out that the operator $\mathcal{K}$ has a mixed partial derivative term. These PDVIs are widely used by many papers, like Ikonen and Toivanen [36], Haentjens and in in't Hout [31].

Under the transformed processes $Y_1(t)$ and $Y_2(t)$ defined by the SDEs (2.18)–(2.19), the rational price of the European contingent claim is given by

$$P(x,y,t) = \mathbb{E}\left[e^{-r(T-t)} \Psi\left(Y_1(T), Y_2(T)\right) \middle| Y_1(t) = x, Y_2(t) = y \right],$$

where

$$\Psi(x,y) = \Phi\left(K e^{x + \frac{\rho}{\sigma} y}\right).$$

Since $e^{-rt}P(Y_1(t), Y_2(t), t)$ is also a martingale, we have by Ito's Lemma

$$\frac{\partial P}{\partial t} + \mathcal{L}P = 0, \tag{5.3}$$

where

$$\mathcal{L}P = \frac{1}{2}\lambda^2 y P_{xx} + \frac{1}{2}\sigma^2 y P_{yy} + (a_1 + b_1 y)P_x + (a_2 + b_2 y)P_y - rP. \tag{5.4}$$

For the American option, the price is given by

$$Q(x,y,t) = \sup_{t \le t^* \le T} \mathbb{E}\left[e^{-r(t^*-t)} \Psi\left(Y_1(T), Y_2(T)\right) \middle| Y_1(t) = x, Y_2(t) = y \right],$$

which satisfies the parabolic partial differential variational inequalities

$$\frac{\partial Q}{\partial t} + \mathcal{L}Q \leq 0, \quad Q \geq \Psi, \quad (Q - \Psi)\left(\frac{\partial Q}{\partial t} + \mathcal{L}Q\right) = 0. \tag{5.5}$$

Now there is no mixed partial derivative term in the operator $\mathcal{L}$.

Let

$$U(x, y, \tau) = \begin{cases} P(x, y, T - \tau), & \text{for the European contingent claim,} \\ \\ Q(x, y, T - \tau), & \text{for the American contingent claim.} \end{cases}$$

Then the backward partial differential equation (5.3) and variational inequalities (5.5) becomes

$$\frac{\partial U}{\partial \tau} - \mathcal{L}U = 0, \tag{5.6}$$

and

$$\frac{\partial U}{\partial \tau} - \mathcal{L}U \geq 0, \quad U \geq \Psi, \quad (U - \Psi)\left(\frac{\partial U}{\partial \tau} - \mathcal{L}U\right) = 0. \tag{5.7}$$

The boundary conditions will be specified in the next section in order to solve the problems on a bounded domain.

5.2 The Boundary Conditions

From now on, we only consider the put option with expiration date T and strike price K. The call option can be evaluated according to the put-call parity or the put-call symmetry ([1][11][19][55]). The payoff function of the put is

$$\Phi(S) = (K - S)^+.$$

The partial differential equation (5.6) and the partial differential variational inequalities (5.7) are posed on the unbounded domain $(-\infty, +\infty) \times (0, +\infty) \times (0, T)$. We need to solve them numerically on a bounded domain $(X_{\text{min}}, X_{\text{max}}) \times (0, Y_{\text{max}}) \times (0, T)$ for sufficiently small negative number X_{min} and sufficiently large positive numbers X_{max} and Y_{max}.

For the European put, when $S = 0$, we have from (5.1)

$$\frac{\partial p}{\partial t} - rp = 0,$$

which means that

$$p(0, v, t) = p(0, v, T)e^{-r(T-t)}.$$

It is apparent that $p(0, v, T) = \Phi(0) = K$. Thus the boundary condition at $S = 0$ is

$$p(0, v, t) = Ke^{-r(T-t)}.$$

Notice that

$$U(x, y, \tau) = p\left(Ke^{x+\frac{\rho}{\sigma}y}, y\right) \to p(0, y, t) = Ke^{-r(T-t)}, \quad x \to -\infty.$$

We set the boundary condition at $x = X_{\text{min}}$ for the European put option as

$$U\left(X_{\text{min}}, y, \tau\right) = Ke^{-r\tau}. \tag{5.8}$$

It is known that the American put price is equal to its payoff when S is sufficiently small. The boundary condition at $x = X_{\text{min}}$ for the American put option is naturally set as

$$U\left(X_{\text{min}}, y, \tau\right) = K - K\exp\left(X_{\text{min}} + \frac{\rho}{\sigma}y\right). \tag{5.9}$$

Since the put price goes to zero as $S \to \infty$, we can set the boundary condition at $x = X_{\text{max}}$ as follows:

$$U\left(X_{\text{max}}, y, \tau\right) = 0. \tag{5.10}$$

Since we have degenerate partial differential operator $\mathcal{L}$ with respect to v, the boundary condition at $v = 0$ is the partial differential equation for the European put option and the partial differential variational inequalities for the American put option obtained from (5.6) and (5.7) by letting $v = 0$: for the European option

$$\frac{dU}{d\tau} - a_1 U_x - a_2 U_y + rU = 0,$$

and for the American option

$$\begin{cases} \dfrac{dU}{d\tau} - a_1 U_x - a_2 U_y + rU \geq 0, \quad U \geq \Psi, \\ (U - \Psi)\left(\dfrac{dU}{d\tau} - a_1 U_x - a_2 U_y + rU\right) = 0. \end{cases} \tag{5.11}$$

As pointed in [12], [36] and [62], the put price would be expected be insensitive to volatility change as $v \to \infty$. Hence, we use the following artificial Neumann boundary conditions:

$$\frac{\partial p}{\partial v} = 0 \quad \text{and} \quad \frac{\partial q}{\partial v} = 0.$$

The above Neumann boundary conditions for U become

$$U_y - \frac{\rho}{\sigma} U_x = 0. \tag{5.12}$$

5.3 The Semi-discretization by a Finite Volume Method

Let $X_{\text{min}} = x_0 < x_1 < x_2 < \cdots < x_{N_1-1} < x_{N_1} = X_{\text{max}}$ and $0 = y_0 < y_1 < y_2 < \cdots < y_{N_2-1} < y_{N_2} = Y_{\text{max}}$ be the partitions of intervals $[X_{\text{min}}, X_{\text{max}}]$ and $[0, Y_{\text{max}}]$, respectively. The dual nodal points for the partitions are

$$x_{i-\frac{1}{2}} = \frac{1}{2}\left(x_{i-1} + x_i\right), i = 1, \ldots, N_1,$$

and

$$y_{j-\frac{1}{2}} = \frac{1}{2}\left(y_{j-1} + y_i\right), j = 1, \ldots, N_2.$$

For a given positive integer M, let

$$\tau_m = m\Delta\tau, \quad m = 0, 1, \ldots, M,$$

where $\Delta\tau = \frac{T}{M}$ is the step size in time. The approximation of $U(x_i, y_j, \tau_m)$ will be denoted by $U_{i,j}^m$. For simplicity, we shall drop the superscript m. In the following, we consider a finite volume method to discretize the spatial differential operator $\mathcal{L}$. The full discretization will be given in the next section.

We first rewrite the spatial differential operator $\mathcal{L}$ in divergent form

$$\begin{aligned}\mathcal{L}U &= \frac{\partial}{\partial x}\left((a_1 + b_1 y)U\right) + \frac{\partial}{\partial y}\left(\left(a_2 - \frac{1}{2}\sigma^2 + b_2 y\right)U\right) \\ &\quad + \frac{\partial}{\partial x}\left(\frac{1}{2}\lambda^2 y \frac{\partial U}{\partial x}\right) + \frac{\partial}{\partial y}\left(\frac{1}{2}\sigma^2 y \frac{\partial U}{\partial y}\right) - (b_2 + r)U \\ &= \frac{\partial M_1}{\partial x} - \frac{\partial L_1}{\partial y} + \frac{\partial M_2}{\partial x} - \frac{\partial L_2}{\partial y} - (b_2 + r)U, \end{aligned} \tag{5.13}$$

where

$$\begin{aligned} M_1 &= (a_1 + b_1 y)U, \quad L_1 = -\left(a_2 - \frac{1}{2}\sigma^2 + b_2 y\right)U, \\ M_2 &= \frac{1}{2}\lambda^2 y \frac{\partial U}{\partial x}, \quad L_2 = -\frac{1}{2}\sigma^2 y \frac{\partial U}{\partial y}. \end{aligned}$$

5.3.1 The Interior Nodes

For an interior node (x_i, y_j) ($1 \le i \le N_1 - 1$ and $1 \le j \le N_2 - 1$), let R be the dual rectangle $ABCD$ as shown in Fig. 5.1.

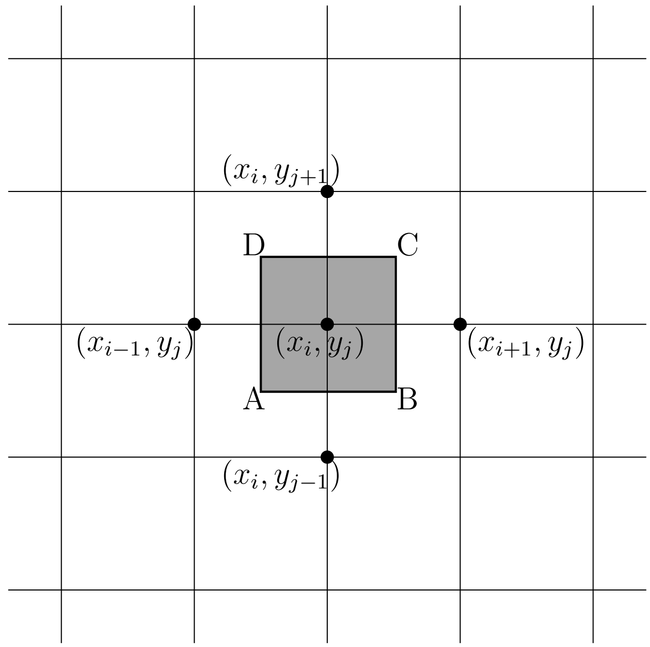

Figure 5.1: An interior node

By the Green's formula, we have

$$
\begin{aligned}
\iint\limits_R \mathcal{L}U\,dxdy &= \iint\limits_R \frac{\partial M_1}{\partial x} - \frac{\partial L_1}{\partial y} + \frac{\partial M_2}{\partial x} - \frac{\partial L_2}{\partial y} - (b_2 + r)U \\
&= \oint\limits_{\partial R} (L_1 dx + M_1 dy) + \oint\limits_{\partial R} (L_2 dx + M_2 dy) - \iint\limits_R (b_2 + r)U\,dxdy \\
&= \int\limits_{\overrightarrow{AB}} (L_1 + L_2)dx + \int\limits_{\overrightarrow{BC}} (M_1 + M_2)dy + \int\limits_{\overrightarrow{CD}} (L_1 + L_2)dx \\
&+ \int\limits_{\overrightarrow{DA}} (M_1 + M_2)dy - \iint\limits_R (b_2 + r)U\,dxdy.
\end{aligned}
$$

For the integrals in x direction, we have

$$\int\limits_{\overrightarrow{BC}} M_1 dy = \int_{y_{j-\frac{1}{2}}}^{y_{j+\frac{1}{2}}} (a_1 + b_1 y) U dy \approx \frac{1}{2}\left(y_{j+\frac{1}{2}} - y_{j-\frac{1}{2}}\right)(a_1 + b_1 y_j)(U_{i,j} + U_{i+1,j}),$$

$$\int\limits_{\overrightarrow{DA}} M_1 dy = \int_{y_{j+\frac{1}{2}}}^{y_{j-\frac{1}{2}}} (a_1 + b_1 y) U dy \approx -\frac{1}{2}\left(y_{j+\frac{1}{2}} - y_{j-\frac{1}{2}}\right)(a_1 + b_1 y_j)(U_{i-1,j} + U_{i,j}),$$

$$\int\limits_{\overrightarrow{BC}} M_2 dy = \int_{y_{j-\frac{1}{2}}}^{y_{j+\frac{1}{2}}} \frac{1}{2}\lambda^2 y \frac{\partial U}{\partial x} dy \approx \frac{1}{2}\lambda^2 y_j \left(y_{j+\frac{1}{2}} - y_{j-\frac{1}{2}}\right) \frac{U_{i+1,j} - U_{i,j}}{x_{i+1} - x_i},$$

$$\int\limits_{\overrightarrow{DA}} M_2 dy = \int_{y_{j+\frac{1}{2}}}^{y_{j-\frac{1}{2}}} \frac{1}{2}\lambda^2 y \frac{\partial U}{\partial x} dy \approx -\frac{1}{2}\lambda^2 y_j \left(y_{j+\frac{1}{2}} - y_{j-\frac{1}{2}}\right) \frac{U_{i,j} - U_{i-1,j}}{x_i - x_{i-1}}.$$

For the integrals in y direction, we have

$$\begin{aligned}\int\limits_{\overrightarrow{AB}} L_1 dx &= -\int_{x_{i-\frac{1}{2}}}^{x_{i+\frac{1}{2}}} \left(a_2 - \frac{1}{2}\sigma^2 + b_2 y_{j-\frac{1}{2}}\right) U dx \\ &\approx -\frac{1}{2}\left(x_{i+\frac{1}{2}} - x_{i-\frac{1}{2}}\right)\left(a_2 - \frac{1}{2}\sigma^2 + b_2 y_{j-\frac{1}{2}}\right)\left(U_{i,j-1} + U_{i,j}\right), \\ \int\limits_{\overrightarrow{CD}} L_1 dx &= -\int_{x_{i+\frac{1}{2}}}^{x_{i-\frac{1}{2}}} \left(a_2 - \frac{1}{2}\sigma^2 + b_2 y_{j+\frac{1}{2}}\right) U dx \\ &\approx \frac{1}{2}\left(x_{i+\frac{1}{2}} - x_{i-\frac{1}{2}}\right)\left(a_2 - \frac{1}{2}\sigma^2 + b_2 y_{j+\frac{1}{2}}\right)\left(U_{i,j} + U_{i,j+1}\right),\end{aligned}$$

$$\int\limits_{\overrightarrow{AB}} L_2 dx = -\int_{x_{i-\frac{1}{2}}}^{x_{i+\frac{1}{2}}} \frac{1}{2}\sigma^2 y_{j-\frac{1}{2}} \frac{\partial U}{\partial y} dx \approx -\frac{1}{2}\sigma^2 y_{j-\frac{1}{2}} \left(x_{i+\frac{1}{2}} - x_{i-\frac{1}{2}}\right) \frac{U_{i,j} - U_{i,j-1}}{y_j - y_{j-1}},$$

$$\int\limits_{\overrightarrow{CD}} L_2 dx = -\int_{x_{i+\frac{1}{2}}}^{x_{i-\frac{1}{2}}} \frac{1}{2}\sigma^2 y_{j+\frac{1}{2}} \frac{\partial U}{\partial y} dx \approx \frac{1}{2}\sigma^2 y_{j+\frac{1}{2}} \left(x_{i+\frac{1}{2}} - x_{i-\frac{1}{2}}\right) \frac{U_{i,j+1} - U_{i,j}}{y_{j+1} - y_j}.$$

For the last integral, we have

$$\iint\limits_R (b_2 + r) U dx dy \approx \left(x_{i+\frac{1}{2}} - x_{i-\frac{1}{2}}\right)\left(y_{j+\frac{1}{2}} - y_{j-\frac{1}{2}}\right)(b_2 + r) U_{i,j}.$$

To sum up, we have for $1 \leq i \leq N_1 - 1, 1 \leq j \leq N_2 - 1$,

$$\mathcal{L}U\left(x_i, y_j, \tau_m\right) \approx \frac{1}{m(R)} \iint\limits_R \mathcal{L}U(x, y, \tau_m) dx dy \approx \mathcal{A}U_{i,j} + \mathcal{B}U_{i,j} - rU_{i,j},$$

where $m(R) = \left(x_{i+\frac{1}{2}} - x_{i-\frac{1}{2}}\right)\left(y_{j+\frac{1}{2}} - y_{j-\frac{1}{2}}\right)$ is the area of the rectangle $ABCD$ and

$$\mathcal{A}U_{i,j} = a_{i-1,j}U_{i-1,j} - a_{i,j}U_{i,j} + a_{i+1,j}U_{i+1,j},$$

$$\mathcal{B}U_{i,j} = b_{i,j-1}U_{i,j-1} - b_{i,j}U_{i,j} + b_{i,j+1}U_{i,j+1},$$

$$\begin{aligned}
a_{i-1,j} &= \frac{1}{\Delta x_i + \Delta x_{i+1}}\left[\frac{\lambda^2 y_j}{\Delta x_i} - (a_1 + b_1 y_j)\right], \\
a_{i,j} &= \frac{\lambda^2 y_j}{\Delta x_i \Delta x_{i+1}}, \\
a_{i+1,j} &= \frac{1}{\Delta x_i + \Delta x_{i+1}}\left[\frac{\lambda^2 y_j}{\Delta x_{i+1}} + (a_1 + b_1 y_j)\right], \\
b_{i,j-1} &= \frac{1}{\Delta y_j + \Delta y_{j+1}}\left[\frac{\sigma^2 y_j}{\Delta y_j} - (a_2 + b_2 y_j) + \frac{1}{2} b_2 \Delta y_j\right], \\
b_{i,j} &= \frac{\sigma^2 y_j}{\Delta y_j \Delta y_{j+1}} + \frac{1}{2} b_2, \\
b_{i,j+1} &= \frac{1}{\Delta y_j + \Delta y_{j+1}}\left[\frac{\sigma^2 y_j}{\Delta y_{j+1}} + (a_2 + b_2 y_j) + \frac{1}{2} b_2 \Delta y_{j+1}\right].
\end{aligned}$$

5.3.2 The Nodes on the Boundary $x = X_{\mathbf{min}}$

For the boundary node $(0, y_j)$, $0 \le j \le N_2$, we have by the boundary conditions (5.8) and (5.9)

$$U_{0,j}^m = \begin{cases} Ke^{-r\tau} & \text{for European put options,} \\ K - K\exp\left(X_{\min} + \frac{\rho}{\sigma} y_j\right) & \text{for American put options.} \end{cases} \tag{5.14}$$

5.3.3 The Nodes on the Boundary $x = X_{\mathbf{max}}$

For the boundary node (x_{N_1}, j), $1 \le j \le N_2 - 1$, we have by the boundary conditions (5.10)

$$U_{N_1,j}^m = 0. \tag{5.15}$$

5.3.4 The Nodes on the Boundary $y = 0$

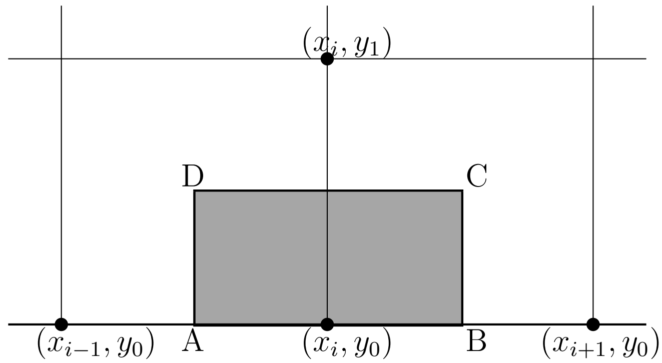

Figure 5.2: A node on the boundary $y = 0$

For the boundary node $(x_i, 0), 1 \leq i \leq N_1 - 1$, consider the dual rectangle $ABCD$, denoted by R, as shown in Figure 5.2. We recall the boundary condition (5.11).

Using the same idea as section 5.3.1

$$\begin{aligned}\iint\limits_R \mathcal{L}U\,dxdy &= \oint\limits_{\partial R}(L_1dx + M_1dy) + \oint\limits_{\partial R}(L_2dx + M_2dy) - \iint\limits_R (b_2 + r)U\,dxdy \\ &= \int\limits_{\overrightarrow{AB}}(L_1 + L_2)dx + \int\limits_{\overrightarrow{BC}}(M_1 + M_2)dy + \int\limits_{\overrightarrow{CD}}(L_1 + L_2)dx + \int\limits_{\overrightarrow{DA}}(M_1 + M_2)dy \\ &- \iint\limits_R (b_2 + r)U\,dxdy.\end{aligned}$$

For the integrals in x direction, we have

$$\int\limits_{\overrightarrow{BC}} M_1dy = \int_{y_0}^{y_{\frac{1}{2}}}(a_1 + b_1y)U\,dy \approx \frac{1}{2}\left(y_{\frac{1}{2}} - y_0\right)\left(a_1 + b_1y_{\frac{1}{4}}\right)(U_{i,0} + U_{i+1,0}),$$

$$\int\limits_{\overrightarrow{DA}} M_1dy = \int_{y_{\frac{1}{2}}}^{y_0}(a_1 + b_1y)U\,dy \approx -\frac{1}{2}\left(y_{\frac{1}{2}} - y_0\right)\left(a_1 + b_1y_{\frac{1}{4}}\right)(U_{i-1,0} + U_{i,0}),$$

$$\int\limits_{\overrightarrow{BC}} M_2dy = \int_{y_0}^{y_{\frac{1}{2}}}\frac{1}{2}\lambda^2y\frac{\partial U}{\partial x}dy \approx \frac{1}{2}\lambda^2y_{\frac{1}{4}}\left(y_{\frac{1}{2}} - y_0\right)\frac{U_{i+1,0} - U_{i,0}}{x_{i+1} - x_i},$$

$$\int\limits_{\overrightarrow{DA}} M_2dy = \int_{y_{\frac{1}{2}}}^{y_0}\frac{1}{2}\lambda^2y\frac{\partial U}{\partial x}dy \approx -\frac{1}{2}\lambda^2y_{\frac{1}{4}}\left(y_{\frac{1}{2}} - y_0\right)\frac{U_{i,0} - U_{i-1,0}}{x_i - x_{i-1}}.$$

For the integrals in y direction, we have

$$\int_{\overrightarrow{AB}} L_1 dx = -\int_{x_{i-\frac{1}{2}}}^{x_{i+\frac{1}{2}}} \left(a_2 - \frac{1}{2}\sigma^2 + b_2 y_0\right) U dx \approx -\left(x_{i+\frac{1}{2}} - x_{i-\frac{1}{2}}\right)\left(a_2 - \frac{1}{2}\sigma^2\right) U_{i,0},$$

$$\int_{\overrightarrow{CD}} L_1 dx = -\int_{x_{i+\frac{1}{2}}}^{x_{i-\frac{1}{2}}} \left(a_2 - \frac{1}{2}\sigma^2 + b_2 y_{\frac{1}{2}}\right) U dx \approx \frac{1}{2}\left(x_{i+\frac{1}{2}} - x_{i-\frac{1}{2}}\right)\left(a_2 - \frac{1}{2}\sigma^2 + b_2 y_{\frac{1}{2}}\right)(U_{i,0} + U_{i,1}),$$

$$\int_{\overrightarrow{AB}} L_2 dx = -\int_{x_{i-\frac{1}{2}}}^{x_{i+\frac{1}{2}}} \left(\frac{1}{2}\sigma^2 y_0\right) \frac{\partial U}{\partial y} dx = 0,$$

$$\int_{\overrightarrow{CD}} L_2 dx = -\int_{x_{i+\frac{1}{2}}}^{x_{i-\frac{1}{2}}} \left(\frac{1}{2}\sigma^2 y_{\frac{1}{2}}\right) \frac{\partial U}{\partial y} dx \approx \frac{1}{2}\sigma^2 y_{\frac{1}{2}}\left(x_{i+\frac{1}{2}} - x_{i-\frac{1}{2}}\right)\frac{U_{i,1} - U_{i,0}}{y_1 - y_0}.$$

For the last integral, we have

$$\iint_R (b_2 + r) U dxdy \approx \left(x_{i+\frac{1}{2}} - x_{i-\frac{1}{2}}\right)\left(y_{\frac{1}{2}} - y_0\right)(b_2 + r) U_{i,0}.$$

To sum up, we have for $1 \leq i \leq N_1 - 1$,

$$\mathcal{L}U\left(x_i, 0, \tau_m\right) \approx \frac{1}{m(R)} \iint_R \mathcal{L}U(x, y, \tau_m) dxdy \approx \mathcal{A}U_{i,0} + \mathcal{B}U_{i,0} - rU_{i,0},$$

where $m(R) = \left(x_{i+\frac{1}{2}} - x_{i-\frac{1}{2}}\right)\left(y_{\frac{1}{2}} - y_0\right)$ is the area of the rectangle $ABCD$ and

$$\mathcal{A}U_{i,0} = a_{i-1,0}U_{i-1,0} - a_{i,0}U_{i,0} + a_{i+1,0}U_{i+1,0},$$

$$\mathcal{B}U_{i,0} = b_{i,0}U_{i,0} + b_{i,1}U_{i,1},$$

$$a_{i-1,0} = \frac{1}{\Delta x_i + \Delta x_{i+1}}\left[\frac{\lambda^2 \Delta y_1}{4\Delta x_i} - \left(a_1 + b_1 \frac{\Delta y_1}{4}\right)\right],$$

$$a_{i,0} = \frac{\lambda^2 \Delta y_1}{4\Delta x_i \Delta x_{i+1}},$$

$$a_{i+1,0} = \frac{1}{\Delta x_i + \Delta x_{i+1}}\left[\frac{\lambda^2 \Delta y_1}{4\Delta x_{i+1}} + \left(a_1 + b_1 \frac{\Delta y_1}{4}\right)\right],$$

$$b_{i,0} = \frac{1}{\Delta y_1}\left[-a_2 - \frac{1}{2} b_2 \Delta y_1\right],$$

$$b_{i,1} = \frac{1}{\Delta y_1}\left[a_2 + \frac{1}{2} b_2 \Delta y_1\right].$$

5.3.5 The Nodes on the Boundary $y = Y_{\mathbf{max}}$

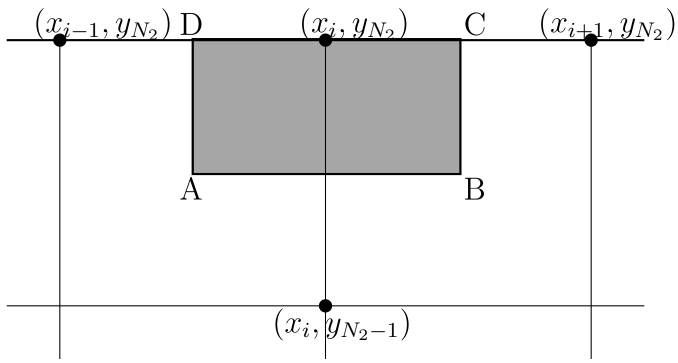

Figure 5.3: A node on the boundary $y = Y_{\text{max}}$

For boundary node $(i, N_2), 1 \le i \le N_1 - 1$, consider the dual rectangle $ABCD$, denoted by R, as shown in Figure 5.3. By the boundary condition (5.12), on the side $\overrightarrow{CD}$, we have

$$\frac{\partial U}{\partial y} = \frac{\rho}{\sigma}\frac{\partial U}{\partial x}.$$

Using the same idea as section 5.3.1

$$\begin{aligned}
\iint\limits_R \mathcal{L}U dxdy &= \oint\limits_{\partial R}(L_1 dx + M_1 dy) + \oint\limits_{\partial R}(L_2 dx + M_2 dy) - \iint\limits_R (b_2 + r)U dxdy \\
&= \int\limits_{\overrightarrow{AB}}(L_1 + L_2)dx + \int\limits_{\overrightarrow{BC}}(M_1 + M_2)dy + \int\limits_{\overrightarrow{CD}}(L_1 + L_2)dx + \int\limits_{\overrightarrow{DA}}(M_1 + M_2)dy \\
&- \iint\limits_R (b_2 + r)U dxdy.
\end{aligned}$$

For the integrals in x direction, we have

$$\int_{\overrightarrow{BC}} M_1 dy = \int_{y_{N_2-\frac{1}{2}}}^{y_{N_2}} (a_1 + b_1 y) U dy \approx \frac{1}{2}\left(y_{N_2} - y_{N_2-\frac{1}{2}}\right)(a_1 + b_1 y_{N_2})(U_{i,N_2} + U_{i+1,N_2}),$$
$$\int_{\overrightarrow{DA}} M_1 dy = \int_{y_{N_2}}^{y_{N_2-\frac{1}{2}}} (a_1 + b_1 y) U dy \approx -\frac{1}{2}\left(y_{N_2} - y_{N_2-\frac{1}{2}}\right)(a_1 + b_1 y_{N_2})(U_{i-1,N_2} + U_{i,N_2}),$$
$$\int_{\overrightarrow{BC}} M_2 dy = \int_{y_{N_2-\frac{1}{2}}}^{y_{N_2}} \frac{1}{2}\lambda^2 y \frac{\partial U}{\partial x} dy \approx \frac{1}{2}\lambda^2 y_{N_2}\left(y_{N_2} - y_{N_2-\frac{1}{2}}\right)\frac{U_{i+1,N_2} - U_{i,N_2}}{x_{i+1} - x_i},$$
$$\int_{\overrightarrow{DA}} M_2 dy = \int_{y_{N_2}}^{y_{N_2-\frac{1}{2}}} \frac{1}{2}\lambda^2 y \frac{\partial U}{\partial x} dy \approx -\frac{1}{2}\lambda^2 y_{N_2}\left(y_{N_2} - y_{N_2-\frac{1}{2}}\right)\frac{U_{i,N_2} - U_{i-1,N_2}}{x_i - x_{i-1}}.$$

For the integrals in y direction, we have

$$\int_{\overrightarrow{AB}} L_1 dx = -\int_{x_{i-\frac{1}{2}}}^{x_{i+\frac{1}{2}}} \left(a_2 - \frac{1}{2}\sigma^2 + b_2 y_{N_2-\frac{1}{2}}\right) U dx$$
$$\approx -\frac{1}{2}\left(x_{i+\frac{1}{2}} - x_{i-\frac{1}{2}}\right)\left(a_2 - \frac{1}{2}\sigma^2 + b_2 y_{N_2-\frac{1}{2}}\right)(U_{i,N_2-1} + U_{i,N_2}),$$
$$\int_{\overrightarrow{CD}} L_1 dx = -\int_{x_{i+\frac{1}{2}}}^{x_{i-\frac{1}{2}}} \left(a_2 - \frac{1}{2}\sigma^2 + b_2 y_{N_2}\right) U dx \approx \left(x_{i+\frac{1}{2}} - x_{i-\frac{1}{2}}\right)\left(a_2 - \frac{1}{2}\sigma^2 + b_2 y_{N_2}\right) U_{i,N_2},$$
$$\int_{\overrightarrow{AB}} L_2 dx = -\int_{x_{i-\frac{1}{2}}}^{x_{i+\frac{1}{2}}} \left(\frac{1}{2}\sigma^2 y_{N_2-\frac{1}{2}}\right)\frac{\partial U}{\partial y} dx \approx -\left(x_{i+\frac{1}{2}} - x_{i-\frac{1}{2}}\right)\left(\frac{1}{2}\sigma^2 y_{N_2-\frac{1}{2}}\right)\frac{U_{i,N_2} - U_{i,N_2-1}}{y_{N_2} - y_{N_2-1}},$$
$$\int_{\overrightarrow{CD}} L_2 dx = -\int_{x_{i+\frac{1}{2}}}^{x_{i-\frac{1}{2}}} \left(\frac{1}{2}\sigma^2 y_{N_2}\right)\frac{\partial U}{\partial y} dx = -\int_{x_{i+\frac{1}{2}}}^{x_{i-\frac{1}{2}}} \left(\frac{1}{2}\sigma^2 y_{N_2}\right)\frac{\rho}{\sigma}\frac{\partial U}{\partial x} dx$$
$$\approx \left(x_{i+\frac{1}{2}} - x_{i-\frac{1}{2}}\right)\left(\frac{1}{2}\rho\sigma y_{N_2}\right)\frac{U_{i+1,N_2} - U_{i-1,N_2}}{x_{i+1} - x_{i-1}}.$$

For the last integral, we have

$$\iint_R (b_2 + r) U dx dy \approx \left(x_{i+\frac{1}{2}} - x_{i-\frac{1}{2}}\right)\left(y_{N_2} - y_{N_2-\frac{1}{2}}\right)(b_2 + r) U_{i,N_2}.$$

To sum up, we have for $1 \le i \le N_1 - 1$,

$$\mathcal{L}U\left(x_i, y_{N_2}, \tau_m\right) \approx \frac{1}{m(R)} \iint_R \mathcal{L}U(x, y, \tau_m) dx dy \approx \mathcal{A}U_{i,N_2} + \mathcal{B}U_{i,N_2} - rU_{i,N_2},$$

where $m(R) = \left(x_{i+\frac{1}{2}} - x_{i-\frac{1}{2}}\right)\left(y_{N_2} - y_{N_2-\frac{1}{2}}\right)$ is the area of the rectangle $ABCD$ and

$$
\begin{aligned}
\mathcal{A}U_{i,N_2} &= a_{i-1,N_2}U_{i-1,N_2} - a_{i,N_2}U_{i,N_2} + a_{i+1,N_2}U_{i+1,N_2}, \\
\mathcal{B}U_{i,N_2} &= b_{i,N_2-1}U_{i,N_2-1} + b_{i,N_2}U_{i,N_2}, \\
a_{i-1,N_2} &= \frac{1}{\Delta x_i + \Delta x_{i+1}}\left[\frac{\lambda^2 y_{N_2}}{\Delta x_i} - (a_1 + b_1 y_{N_2}) - \frac{\rho\sigma y_{N_2}}{\Delta y_{N_2}}\right], \\
a_{i,N_2} &= \frac{\lambda^2 y_{N_2}}{\Delta x_i \Delta x_{i+1}}, \\
a_{i+1,N_2} &= \frac{1}{\Delta x_i + \Delta x_{i+1}}\left[\frac{\lambda^2 y_{N_2}}{\Delta x_{i+1}} + (a_1 + b_1 y_{N_2}) + \frac{\rho\sigma y_{N_2}}{\Delta y_{N_2}}\right], \\
b_{i,N_2-1} &= \frac{1}{\Delta y_{N_2}}\left[\frac{\sigma^2 y_{N_2}}{\Delta y_{N_2}} - (a_2 + b_2 y_{N_2}) + \frac{1}{2}b_2 \Delta y_{N_2}\right], \\
b_{i,N_2} &= \frac{1}{\Delta y_{N_2}}\left[-\frac{\sigma^2 y_{N_2}}{\Delta y_{N_2}} + (a_2 + b_2 y_{N_2}) - \frac{1}{2}b_2 \Delta y_{N_2}\right].
\end{aligned}
$$

5.3.6 Discretization of the Operator $\mathcal{L}$

Combining the discretizations in the previous subsections, we have

$$\mathcal{L}U(x_i, y_j) \approx \mathcal{L}^* U_{i,j} = \mathcal{A}U_{i,j} + \mathcal{B}U_{i,j} - rU_{i,j}$$

for $1 \le i \le N_1, 0 \le j \le N_2$, and

$$\mathcal{L}^* U_{i,j} = \begin{cases} -rU_{i,j} & \text{for European option,} \\ 0 & \text{for American option.} \end{cases}$$

for $i = 0, N_1$ and $0 \le j \le N_2$, where $U_{0,j}$ and $U_{N_1,j}$ are given by (5.14) and (5.15). Let

$$\mathcal{A}^* = \mathcal{A} - \frac{1}{2}r\mathcal{I}, \quad \mathcal{B}^* = \mathcal{B} - \frac{1}{2}r\mathcal{I},$$

where $\mathcal{I}$ is the identity operator. Then

$$\mathcal{L}^* = A^* + \mathcal{B}^*. \tag{5.16}$$

For fixed $0 \le j \le N_2$, let $\boldsymbol{U_{\cdot,j}} = [U_{0,j}, U_{1,j}, U_{2,j}, \cdots, U_{N_1,j}]^T$ and $\boldsymbol{A_j^*}$ be the matrix such that $\mathcal{A}^* \boldsymbol{U_{\cdot,j}} = \boldsymbol{A_j^*} \boldsymbol{U_{\cdot,j}}$. Then we have

$$\boldsymbol{A_j^*} = \begin{bmatrix} a^* & 0 & & & & & & \\ a_{0,j}^{-1} & a_{1,j}^{0} & a_{2,j}^{+1} & & & & & \\ & a_{1,j}^{-1} & a_{2,j}^{0} & a_{3,j}^{+1} & & & & \\ & & \ddots & \ddots & \ddots & & & \\ & & & a_{i-1,j}^{-1} & a_{i,j}^{0} & a_{i+1,j}^{+1} & & \\ & & & & \ddots & \ddots & \ddots & \\ & & & & & a_{N_1-2,j}^{-1} & a_{N_1-1,j}^{0} & a_{N_1,j}^{+1} \\ & & & & & & 0 & a^* \end{bmatrix}_{(N_1+1)\times(N_1+1)}, \tag{5.17}$$

where

$$a^* = \begin{cases} -\frac{1}{2}r & \text{for European option,} \\ 0 & \text{for American option.} \end{cases}$$

$$a_{i-1,j}^{-1} = \begin{cases} \frac{1}{\Delta x_i + \Delta x_{i+1}} \left[\frac{\lambda^2 \Delta y_1}{4 \Delta x_i} - (a_1 + b_1 \frac{\Delta y_1}{4}) \right] & \text{for } 1 \le i \le N_1 - 1, j = 0, \\ \frac{1}{\Delta x_i + \Delta x_{i+1}} \left[\frac{\lambda^2 y_j}{\Delta x_i} - (a_1 + b_1 y_j) \right] & \text{for } 1 \le i \le N_1 - 1, 1 \le j \le N_2 - 1, \\ \frac{1}{\Delta x_i + \Delta x_{i+1}} \left[\frac{\lambda^2 y_{N_2}}{\Delta x_i} - (a_1 + b_1 y_{N_2}) - \frac{\rho \sigma y_{N_2}}{\Delta y_{N_2}} \right] & \text{for } 1 \le i \le N_1 - 1, j = N_2. \end{cases}$$

$$a_{i,j}^{0} = \begin{cases} -\frac{\lambda^2 \Delta y_1}{4 \Delta x_i \Delta x_{i+1}} - \frac{1}{2}r & \text{for } 1 \le i \le N_1 - 1, j = 0, \\ -\frac{\lambda^2 y_j}{\Delta x_i \Delta x_{i+1}} - \frac{1}{2}r & \text{for } 1 \le i \le N_1 - 1, 1 \le j \le N_2 - 1, \\ -\frac{\lambda^2 y_{N_2}}{\Delta x_i \Delta x_{i+1}} - \frac{1}{2}r & \text{for } 1 \le i \le N_1 - 1, j = N_2. \end{cases}$$

$$a_{i+1,j}^{+1} = \begin{cases} \frac{1}{\Delta x_i + \Delta x_{i+1}} \left[\frac{\lambda^2 \Delta y_1}{4 \Delta x_{i+1}} + (a_1 + b_1 \frac{\Delta y_1}{4}) \right] & \text{for } 1 \le i \le N_1 - 1, j = 0, \\ \frac{1}{\Delta x_i + \Delta x_{i+1}} \left[\frac{\lambda^2 y_j}{\Delta x_{i+1}} + (a_1 + b_1 y_j) \right] & \text{for } 1 \le i \le N_1 - 1, 1 \le j \le N_2 - 1, \\ \frac{1}{\Delta x_i + \Delta x_{i+1}} \left[\frac{\lambda^2 y_{N_2}}{\Delta x_{i+1}} + (a_1 + b_1 y_{N_2}) + \frac{\rho \sigma y_{N_2}}{\Delta y_{N_2}} \right] & \text{for } 1 \le i \le N_1 - 1, j = N_2. \end{cases}$$

For fixed $0 \le i \le N_1$, let $\boldsymbol{U_{i,\cdot}} = [U_{i,0}, U_{i,1}, U_{i,2}, \cdots, U_{i,N_2}]^T$ and $\boldsymbol{B_i^*}$ be the matrix such that $\mathcal{B}^* \boldsymbol{U_{i,\cdot}} = \boldsymbol{B_i^*} \boldsymbol{U_{i,\cdot}}$. Then we have

$$\boldsymbol{B_i^*} = \begin{bmatrix} b_{i,0}^{0} & b_{i,1}^{+1} & & & & & & \\ b_{i,0}^{-1} & b_{i,1}^{0} & b_{i,2}^{+1} & & & & & \\ & b_{i,1}^{-1} & b_{i,2}^{0} & b_{i,3}^{+1} & & & & \\ & & \ddots & \ddots & \ddots & & & \\ & & & b_{i,j-1}^{-1} & b_{i,j}^{0} & b_{i,j+1}^{+1} & & \\ & & & & \ddots & \ddots & \ddots & \\ & & & & & b_{i,N_2-2}^{-1} & b_{i,N_2-1}^{0} & b_{i,N_2}^{+1} \\ & & & & & & b_{i,N_2-1}^{-1} & b_{i,N_2}^{0} \end{bmatrix}_{(N_2+1)\times(N_2+1)}, \tag{5.18}$$

where

$$b^0_{i,0} = \begin{cases} b^* & \text{for } i = 0, N_1, \\ -\frac{1}{\Delta y_1}\left[a_2 + \frac{1}{2}b_2\Delta y_1\right] - \frac{1}{2}r & \text{for } 1 \le i \le N_1 - 1. \end{cases}$$

$$b^{+1}_{i,1} = \begin{cases} 0 & \text{for } i = 0, N_1, \\ \frac{1}{\Delta y_1}\left[a_2 + \frac{1}{2}b_2\Delta y_1\right] & \text{for } 1 \le i \le N_1 - 1. \end{cases}$$

$$b^{-1}_{i,j-1} = \begin{cases} 0 & \text{for } i = 0, N_1, \\ \frac{1}{\Delta y_j + \Delta y_{j+1}}\left[\frac{\sigma^2 y_j}{\Delta y_j} - (a_2 + b_2 y_j) + \frac{1}{2}b_2\Delta y_j\right] & \text{for } 1 \le i \le N_1 - 1, 1 \le j \le N_2 - 1. \end{cases}$$

$$b^0_{i,j} = \begin{cases} b^* & \text{for } i = 0, N_1, \\ -\left[\frac{\sigma^2 y_j}{\Delta y_j \Delta y_{j+1}} + \frac{1}{2}b_2\right] - \frac{1}{2}r & \text{for } 1 \le i \le N_1 - 1, 1 \le j \le N_2 - 1. \end{cases}$$

$$b^{+1}_{i,j+1} = \begin{cases} 0 & \text{for } i = 0, N_1, \\ \frac{1}{\Delta y_j + \Delta y_{j+1}}\left[\frac{\sigma^2 y_j}{\Delta y_{j+1}} + (a_2 + b_2 y_j) + \frac{1}{2}b_2\Delta y_{j+1}\right] & \text{for } 1 \le i \le N_1 - 1, 1 \le j \le N_2 - 1. \end{cases}$$

$$b^{-1}_{i,N_2-1} = \begin{cases} 0 & \text{for } i = 0, N_1, \\ \frac{1}{\Delta y_{N_2}}\left[\frac{\sigma^2 y_{N_2}}{\Delta y_{N_2}} - (a_2 + b_2 y_{N_2}) + \frac{1}{2}b_2\Delta y_{N_2}\right] & \text{for } 1 \le i \le N_1 - 1. \end{cases}$$

$$b^0_{i,N_2} = \begin{cases} b^* & \text{for } i = 0, N_1, \\ \frac{1}{\Delta y_{N_2}}\left[-\frac{\sigma^2 y_{N_2}}{\Delta y_{N_2}} + (a_2 + b_2 y_{N_2}) - \frac{1}{2}b_2\Delta y_{N_2}\right] - \frac{1}{2}r & \text{for } 1 \le i \le N_1 - 1. \end{cases}$$

$$b^* = \begin{cases} -\frac{1}{2}r & \text{for European option,} \\ 0 & \text{for American option.} \end{cases}$$

5.4 Time Discretization: an ADI method

Applying the Crank-Nicolson scheme and introducing an auxiliary vector λ^m as in [31], we have the following full-discretization scheme

$$\frac{U^m - U^{m-1}}{\Delta\tau} = \frac{1}{2}\left(\mathcal{L}^* U^m + \mathcal{L}^* U^{m-1}\right) + \lambda^m, \tag{5.19}$$

$$\lambda^m \ge 0, \quad U^m \ge G, \quad (U^m - G)\lambda^m = 0, \tag{5.20}$$

where U^m is the approximation of $U(\tau_m)$ and $G_{i,j} = \Psi(x_i, y_j)$. The equation (5.19) can be rewritten as

$$\left(\mathcal{I} - \frac{1}{2}\Delta\tau\mathcal{L}^*\right) U^m = \left(\mathcal{I} + \frac{1}{2}\Delta\tau\mathcal{L}^*\right) U^{m-1} + \Delta\tau\lambda^m, \tag{5.21}$$

where $\mathcal{I}$ is the identity operator. In order to solve the above linear complementarity problem (LCP) by an ADI method, we have the following approximate LCP by using the technique introduced by Ikonen and Toivanen [36]

$$\left(\mathcal{I} - \frac{1}{2}\Delta\tau\mathcal{L}^*\right)\overline{U}^m = \left(\mathcal{I} + \frac{1}{2}\Delta\tau\mathcal{L}^*\right)U^{m-1} + \Delta\tau\lambda^{m-1}, \tag{5.22}$$

$$U^m - \overline{U}^m - \Delta\tau(\lambda^m - \lambda^{m-1}) = 0, \tag{5.23}$$

$$\lambda^m \geq 0, \quad U^m \geq G, \quad (U^m - G)\lambda^m = 0, \tag{5.24}$$

where $\overline{U}^m$ can be regarded as the prediction of the approximation to $U(t_m)$ and $\lambda^0 = 0$. Once $\overline{U}^m$ is obtained by solving (5.22), we can easily solve (5.23)–(5.24) to get

$$\begin{aligned} U^m &= \max\left\{\overline{U}^m - \Delta\tau\lambda^{m-1}, G\right\}, \\ \lambda^m &= \max\left\{\lambda^{m-1} + \frac{G - \overline{U}^m}{\Delta\tau}, 0\right\}. \end{aligned}$$

By Theorem 1 in [36], the truncation errors for schemes (5.22)–(5.24) and (5.19)–(5.20) are of the same order, which is at most $\mathcal{O}((\Delta\tau)^2)$. The possible irregularity of the solution with respect to time might reduce the order of accuracy.

Next we consider how to solve (5.22) by an ADI method. Since $\mathcal{L}^* = \mathcal{A}^* + \mathcal{B}^*$, equation (5.22) becomes as

$$\left(\mathcal{I} - \frac{1}{2}\Delta\tau(\mathcal{A}^* + \mathcal{B}^*)\right)\overline{U}^m = \left(\mathcal{I} + \frac{1}{2}\Delta\tau(\mathcal{A}^* + \mathcal{B}^*)\right)U^{m-1} + \Delta\tau\lambda^{m-1}.$$

By adding and subtracting the corresponding $\frac{1}{4}(\Delta\tau)^2\mathcal{A}^*\mathcal{B}^*$ term, we have

$$\begin{aligned} \left(\mathcal{I} - \frac{1}{2}\Delta\tau\mathcal{A}^*\right)\left(\mathcal{I} - \frac{1}{2}\Delta\tau\mathcal{B}^*\right)\overline{U}^m &= \left(\mathcal{I} + \frac{1}{2}\Delta\tau\mathcal{A}^*\right)\left(\mathcal{I} + \frac{1}{2}\Delta\tau\mathcal{B}^*\right)U^{m-1} \\ &\quad + \Delta\tau\lambda^{m-1} + \frac{1}{4}(\Delta\tau)^2\mathcal{A}^*\mathcal{B}^*\left(\overline{U}^m - U^{m-1}\right). \end{aligned}$$

After dropping the last term, we get

$$\left(\mathcal{I} - \frac{1}{2}\Delta\tau\mathcal{A}^*\right)\left(\mathcal{I} - \frac{1}{2}\Delta\tau\mathcal{B}^*\right)\overline{U}^m = \left(\mathcal{I} + \frac{1}{2}\Delta\tau\mathcal{A}^*\right)\left(\mathcal{I} + \frac{1}{2}\Delta\tau\mathcal{B}^*\right)U^{m-1} + \Delta\tau\lambda^{m-1}.$$

The above equation can be rewritten as

$$\begin{aligned}\left(\mathcal{I} - \frac{1}{2}\Delta\tau\mathcal{B}^*\right)\overline{U}^m = \left(\mathcal{I} + \frac{1}{2}\Delta\tau\mathcal{A}^*\right)\left(\mathcal{I} - \frac{1}{2}\Delta\tau\mathcal{A}^*\right)^{-1}\left(\mathcal{I} + \frac{1}{2}\Delta\tau\mathcal{B}^*\right)U^{m-1} \\ + \Delta\tau\left(\mathcal{I} - \frac{1}{2}\Delta\tau\mathcal{A}^*\right)^{-1}\lambda^{m-1}.\end{aligned}$$

Letting

$$\overline{U}^{m-\frac{1}{2}} = \left(\mathcal{I} - \frac{1}{2}\Delta\tau\mathcal{A}^*\right)^{-1}\left(\mathcal{I} + \frac{1}{2}\Delta\tau\mathcal{B}^*\right)U^{m-1},$$

we have the following ADI scheme to compute $\overline{U}^m$:

$$\left(\mathcal{I} - \frac{1}{2}\Delta\tau\mathcal{A}^*\right)\overline{U}^{m-\frac{1}{2}} = \left(\mathcal{I} + \frac{1}{2}\Delta\tau\mathcal{B}^*\right)U^{m-1}, \tag{5.25}$$

$$\left(\mathcal{I} - \frac{1}{2}\Delta\tau\mathcal{B}^*\right)\overline{U}^m = \left(\mathcal{I} + \frac{1}{2}\Delta\tau\mathcal{A}^*\right)\overline{U}^{m-\frac{1}{2}} + \Delta\tau\left(\mathcal{I} - \frac{1}{2}\Delta\tau\mathcal{A}^*\right)^{-1}\lambda^{m-1}. \tag{5.26}$$

To conclude this section, we formulate the following algorithm for our FV-ADI method, which has been implemented by writing a C++ package.

Algorithm 9. A FV-ADI method for the American put option under Heston model

1. Let

$$U^0_{i,j} = \Psi(x_i, y_j), \quad i = 0, \ldots, N_1, \quad j = 0, \ldots, N_2.$$
$$U^m_{0,j} = K - K\exp\left(X_{\min} + \frac{\rho}{\sigma} y_j\right), \quad m = 0, \ldots, M, \quad j = 0, \ldots, N_2.$$
$$U^m_{N_1,j} = 0, \quad m = 0, \ldots, M, \quad j = 0, \ldots, N_2.$$
$$\boldsymbol{\lambda^0} = \mathbf{0}$$

2. For $m = 1, \ldots, M$, do

   For $i = 0, \ldots, N_1$, do

   - compute $\boldsymbol{f_{i,\cdot}} = \boldsymbol{U^{m-1}_{i,\cdot}}(\boldsymbol{I} + \frac{1}{2}\Delta\tau\boldsymbol{B^*})^T$ to get the $i-$th row of $\boldsymbol{f}$

   End do

   For $j = 0, \ldots, N_2$, do

   - solve $\left(\boldsymbol{I} - \frac{1}{2}\Delta\tau\boldsymbol{A^*_j}\right)\boldsymbol{\overline{U}^{m-\frac{1}{2}}_{\cdot,j}} = \boldsymbol{f_{\cdot,j}}$ to get $\boldsymbol{\overline{U}^{m-\frac{1}{2}}_{\cdot,j}}$
   - solve $\left(\boldsymbol{I} - \frac{1}{2}\Delta\tau\boldsymbol{A^*_j}\right)\boldsymbol{\gamma_{\cdot,j}} = \boldsymbol{\lambda^{m-1}_{\cdot,j}}$ to get the j-th column of $\boldsymbol{\gamma}$
   - compute $\boldsymbol{g_{\cdot,j}} = (\boldsymbol{I} + \frac{1}{2}\Delta\tau\boldsymbol{A^*})\boldsymbol{\overline{U}^{m-\frac{1}{2}}_{\cdot,j}} + \Delta\tau\boldsymbol{\gamma_{\cdot,j}}$ to get the $j-$th column of $\boldsymbol{g}$

   End do

   For $i = 1, \ldots, N_1$, do

   - solve $\left(\boldsymbol{I} - \frac{1}{2}\Delta\tau\boldsymbol{B^*_i}\right)(\boldsymbol{\overline{U}^m_{i,\cdot}})^T = \boldsymbol{g^T_{i,\cdot}}$ to get $\boldsymbol{\overline{U}^m}$

   End do

   Let

$$U^m_{i,j} = \max\{\overline{U}^m_{i,j} - \Delta\tau\lambda^{m-1}_{i,j}, U^0\}, \quad \lambda^m_{i,j} = \max\{\lambda^{m-1}_{i,j} + \frac{U^0_{i,j} - \overline{U}^m_{i,j}}{\Delta\tau}, 0\}.$$

   for $i = 0, \ldots, N_1, \quad j = 0, \ldots, N_2$.

   End do

5.5 Numerical Results

In this section, we present numerical results to validate our C++ codes to implement Algorithm 9 and examine the rate of convergence and efficiency of our FV-ADI method.

We shall consider the options with strike price $K = \$100$ and expiration date $T = 1$ year. The values of the parameters for the Heston model are specified in Table 5.1. The six cases can be grouped according to $2\kappa\eta > \sigma^2$ (Cases A and B), $2\kappa\eta = \sigma^2$ (Cases C and D), and $2\kappa\eta < \sigma^2$ (Cases E and F). It should be pointed out that $2\kappa\eta > \sigma^2$ is called the Feller condition under which the volatility (the solution of the SDE (2.14)) is always positive ([13]). In addition, the correlations are positive for Cases A, C and E and negative for the other cases.

Case	A	B	C	D	E	F
q	0.05	0.05	0.05	0.05	0.05	0.05
κ	1.00	1.00	1.00	1.00	1.00	1.00
η	0.2	0.2	0.2	0.2	0.2	0.2
σ	0.2	0.2	$\sqrt{0.4}$	$\sqrt{0.4}$	$\sqrt{0.9}$	$\sqrt{0.9}$
ρ	0.5	-0.5	0.5	-0.5	0.5	-0.5

Table 5.1: Parameters for the Heston model for put option

We want to obtain the approximate option prices on the domain that contains $[S_{\min}, S_{\max}] \times [0, v_{\max}]$ for stock price S and volatility v, where $S_{\min}$, $S_{\max}$ and $v_{\max}$ will be set according to the actual needs. It follows from the non-linear transformations in (2.17) that the computational domain for the variational inequality problem (5.7) is $[X_{\min}, X_{\max}] \times [0, y_{\max}]$, where $y_{\max} = v_{\max}$ and

$$X_{\min} = \text{floor}\left(\ln\left(\frac{S_{\min}}{K}\right) - \max\left(0, \frac{\rho}{\sigma}v_{\max}\right)\right),$$
$$X_{\max} = \text{ceil}\left(\ln\left(\frac{S_{\max}}{K}\right) - \min\left(0, \frac{\rho}{\sigma}v_{\max}\right)\right).$$

In all numerical examples, we shall set $S_{\min} = 1$, $S_{\max} = 1000$ and $v_{\max} = 5$.

The uniform partition is used in x by setting $\Delta x = \Delta t$. The graded mesh is employed in y for interval $[0, 1]$ with 32% of the total number of nodes and the uniform partition for interval $[1, 5]$ with 68% of the total number of nodes. We illustrate the partition of the computational domain for Case A in Fig. 5.4.

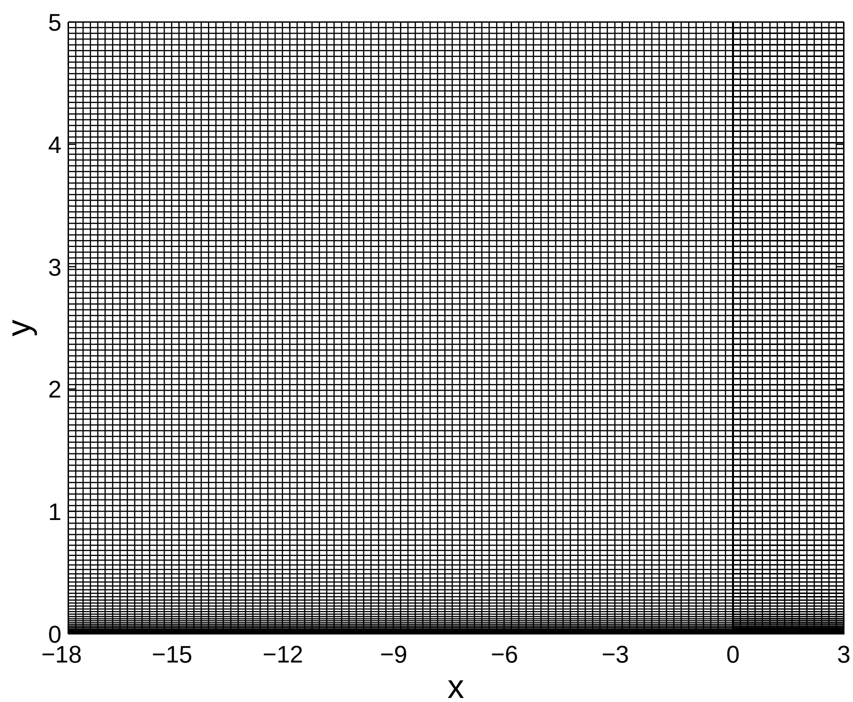

Figure 5.4: Discretization mesh

We run our programs on a PC with Intel(R) Core(TM) i7-5820K CPU @3.3GHz and

16G memory. The CPU times for Case A in Example 5.2 are given in the following table.

M	N_1	N_2	step size	CPU time
25	525	125	0.04000	0m1.858s
50	1050	250	0.02000	0m8.015s
100	2100	500	0.01000	0m41.500s
200	4200	1000	0.00500	4m9.328s
400	8400	2000	0.00250	29m4.656s
800	16800	4000	0.00125	260m27.656s

Table 5.2: The CPU times

Example 5.1. (*Validation*) In this example, we validate our C++ codes for our FV-ADI method. It is well known that the values of American put option and European put option are equal when the interest rate is zero ($r = 0$). We use our ADI method to compute the American put prices while the European put prices are computed by using numerical integration based on the Heston's formula in [33].

We display the absolute errors between the reference values and the values computed by our program for today's option prices in Tables 5.3–5.8 for asset prices $S = 80 : 5 : 120$ while the volatility is a typical value $v = 0.16$. We also plot the maximum absolute errors (MAE) for $S = 10 : 1 : 200$ and $v = [0 : 0.01 : 1, 1.25 : 0.25 : 2]$ in Fig. 5.5. It is shown that our program produces convergent sequences of the approximate option prices as the time step size decreases. We can also observe that the rate of convergence is 2 as expected and that the super-convergence occurs at some points.

S_0	Ref	M=25	M=50	M=100	M=200	M=400
80	29.85054	0.05120955	0.01269067	0.00318701	0.00079893	0.00019892
85	26.74502	0.04183880	0.01081631	0.00274977	0.00070083	0.00016184
90	23.87882	0.03817732	0.00950394	0.00242347	0.00054080	0.00014087
95	21.24947	0.03110983	0.00836335	0.00181905	0.00048654	0.00012918
100	18.85105	0.01865687	0.00493423	0.00120392	0.00029581	0.00007514
105	16.67483	0.01976479	0.00594802	0.00110563	0.00031791	0.00009123
110	14.70994	0.01841217	0.00424438	0.00122823	0.00016707	0.00005204
115	12.94395	0.01587990	0.00142789	0.00036469	0.00009805	0.00003384
120	11.36342	0.01331012	0.00183450	0.00067097	0.00021192	0.00001892

Table 5.3: The absolute errors: Case A

S_0	Ref	M=25	M=50	M=100	M=200	M=400
80	28.99942	0.08435909	0.02134354	0.00525510	0.00132428	0.00033168
85	25.94948	0.09337602	0.02274683	0.00557729	0.00138627	0.00036714
90	23.17441	0.09252513	0.02313850	0.00569280	0.00152574	0.00037244
95	20.66417	0.09627934	0.02331302	0.00614986	0.00150639	0.00036621
100	18.40459	0.10600380	0.02614307	0.00655431	0.00165116	0.00041078
105	16.37883	0.09946856	0.02370950	0.00633546	0.00154205	0.00037224
110	14.56866	0.09605189	0.02434278	0.00590746	0.00162415	0.00039523
115	12.95537	0.09400179	0.02600756	0.00649274	0.00161499	0.00039462
120	11.52050	0.09203324	0.02442909	0.00590676	0.00143069	0.00039053

Table 5.4: The absolute errors: Case B

S_0	Ref	M=25	M=50	M=100	M=200	M=400
80	30.35873	0.01146552	0.00286257	0.00074755	0.00018511	0.00004609
85	27.10850	0.00958386	0.00261187	0.00060518	0.00015687	0.00004129
90	24.06991	0.00807667	0.00234213	0.00050648	0.00014516	0.00003424
95	21.25083	0.00799582	0.00123010	0.00042663	0.00013264	0.00001971
100	18.65650	0.00326452	0.00161903	0.00044220	0.00009912	0.00002918
105	16.28917	0.00143776	0.00022331	0.00026266	0.00011091	0.00000071
110	14.14782	0.00282990	0.00168531	0.00001915	0.00005473	0.00002749
115	12.22805	0.00544611	0.00141071	0.00035889	0.00009391	0.00002089
120	10.52209	0.00723739	0.00067983	0.00049088	0.00002014	0.00002566

Table 5.5: The absolute errors: Case C

S_0	Ref	M=25	M=50	M=100	M=200	M=400
80	27.85898	0.02777764	0.00756279	0.00174577	0.00043790	0.00010893
85	24.72579	0.03333746	0.00761086	0.00170611	0.00047349	0.00010618
90	21.93416	0.02665749	0.00890817	0.00208209	0.00046546	0.00010291
95	19.46937	0.03327126	0.00724237	0.00158146	0.00056782	0.00013470
100	17.30640	0.03056834	0.00644426	0.00157497	0.00040954	0.00009555
105	15.41497	0.02366643	0.00661857	0.00140930	0.00052111	0.00012007
110	13.76349	0.02148121	0.00755193	0.00165662	0.00034488	0.00009214
115	12.32153	0.02112664	0.00537457	0.00126829	0.00035586	0.00007612
120	11.06117	0.02083894	0.00460881	0.00157878	0.00033658	0.00007078

Table 5.6: The absolute errors: Case D

S_0	Ref	M=25	M=50	M=100	M=200	M=400
80	30.45936	0.00392613	0.00099924	0.00029043	0.00006599	0.00002427
85	27.07738	0.00221526	0.00069900	0.00019699	0.00005042	0.00001316
90	23.89063	0.00072293	0.00039320	0.00002659	0.00000052	0.00000282
95	20.91583	0.00086218	0.00036702	0.00002590	0.00003908	0.00000218
100	18.16891	0.00757869	0.00105941	0.00006331	0.00008200	0.00000860
105	15.66366	0.00995982	0.00141597	0.00010930	0.00013887	0.00001972
110	13.41003	0.00562558	0.00054272	0.00071235	0.00010537	0.00000580
115	11.41225	0.00207529	0.00150489	0.00000527	0.00018626	0.00002700
120	9.66736	0.00158195	0.00263193	0.00026566	0.00004216	0.00001374

Table 5.7: The absolute errors: Case E

S_0	Ref	M=25	M=50	M=100	M=200	M=400
80	27.15882	0.02023512	0.00641775	0.00149440	0.00033288	0.00007425
85	23.86274	0.03010901	0.00692433	0.00150614	0.00030779	0.00008202
90	20.96071	0.01963132	0.00796429	0.00179218	0.00037148	0.00007228
95	18.44960	0.02618924	0.00494498	0.00127605	0.00028369	0.00008891
100	16.30081	0.02794540	0.00556526	0.00103173	0.00039462	0.00007543
105	14.47135	0.01719641	0.00407220	0.00104849	0.00023544	0.00007080
110	12.91428	0.01323280	0.00685797	0.00162911	0.00037148	0.00007805
115	11.58531	0.01208901	0.00408051	0.00071725	0.00025836	0.00004534
120	10.44577	0.01151331	0.00285281	0.00069075	0.00017204	0.00004149

Table 5.8: The absolute errors: Case F

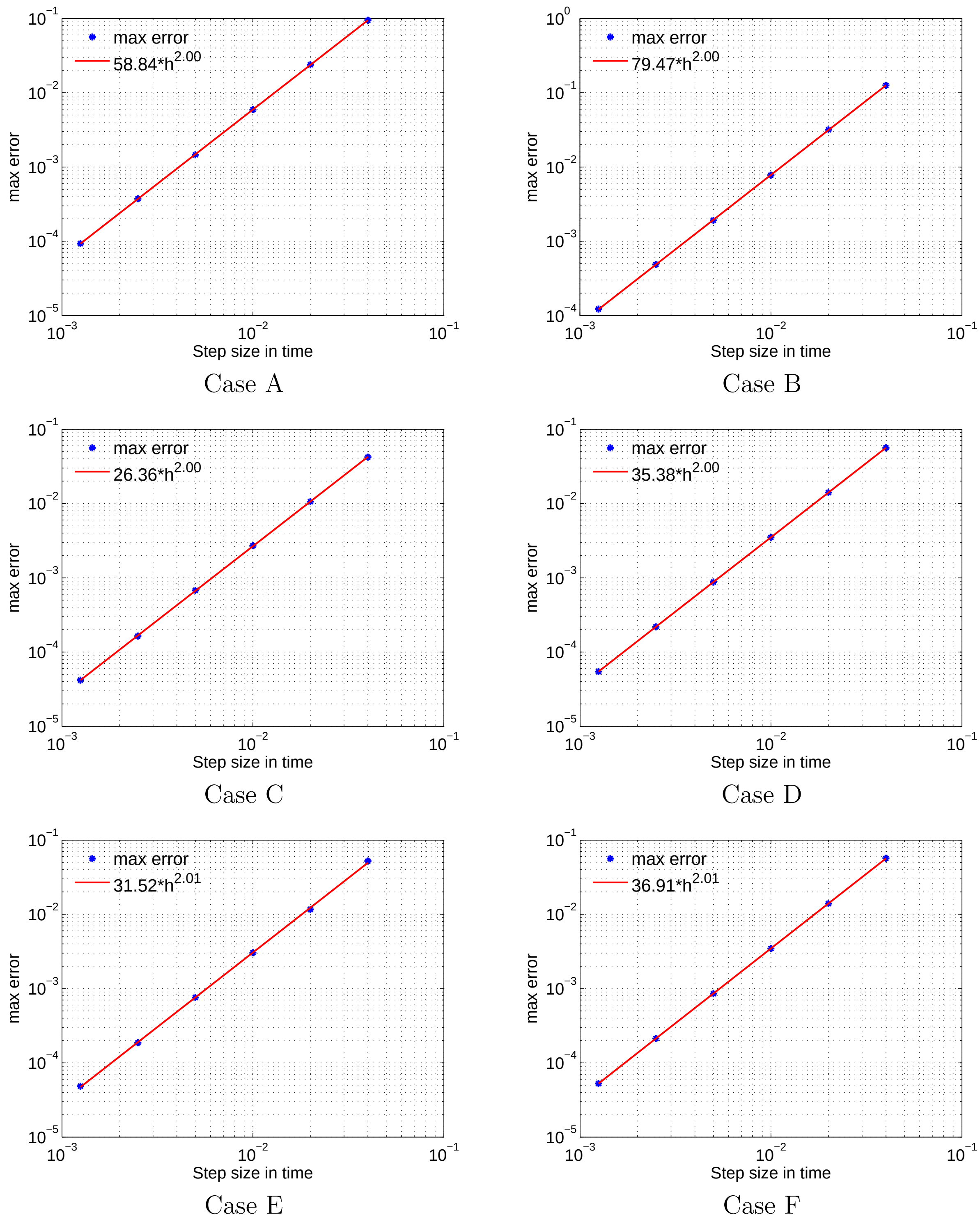

Figure 5.5: The rates of convergence for maximum absolute errors (validation)

Example 5.2. (*The American put options*) In this example, we consider the American put option problems when $r = 0.1 > 0$. Since there is no analytic solutions, we investigate the rate of convergence by examining the errors between the approximate solutions to the variational inequality problem (5.7) when the number of time steps is M and $2M$. The errors are computed on the domain $[X_{\min} + 1, X_{\max} - 1] \times [0, 1]$. We plot the maximum absolute errors (MAE), root mean square errors (RMSE) and L_2 errors (L2E) in Figs. 5.6–5.8 when time $t = T$. We can observe that the RMSE and L2E rates of convergence are almost 2 for Cases A and B, while the MAE rates of convergence are 1.24 and 2.13, respectively. By checking the data, we have found that the maximum absolute errors occur near the early exercise boundary for Case A. Since the initial value as well as the constrain function (the payoff function) is only in H^1, we should not expect that the exact solution to the variational inequality problem (5.7) would have the desired regularity for the MAE and RMSE estimates. The same observations can be made for Cases C, D, E, and F when Feller condition is not satisfied. We also notice that the convergency is better when the correlation is negative. In fact, the correlation between stock price S and volatility v is also negative in the real financial market ([14][43]).

We also plot the option prices as the functions of S and v when time $t = 0, 0.5T, 0.75T, 0.99T$ in Figs. 5.9–5.14. The payoff function is also plotted for comparison. Their joint part is the exercise region. As shown in these figures, the surfaces of option prices will converge to the payoff surface as time is approaching to T. In addition, the projections of the boundary lines of the two surfaces on the Sv-plain are the early exercise boundaries, which are displayed in Fig. 5.15.

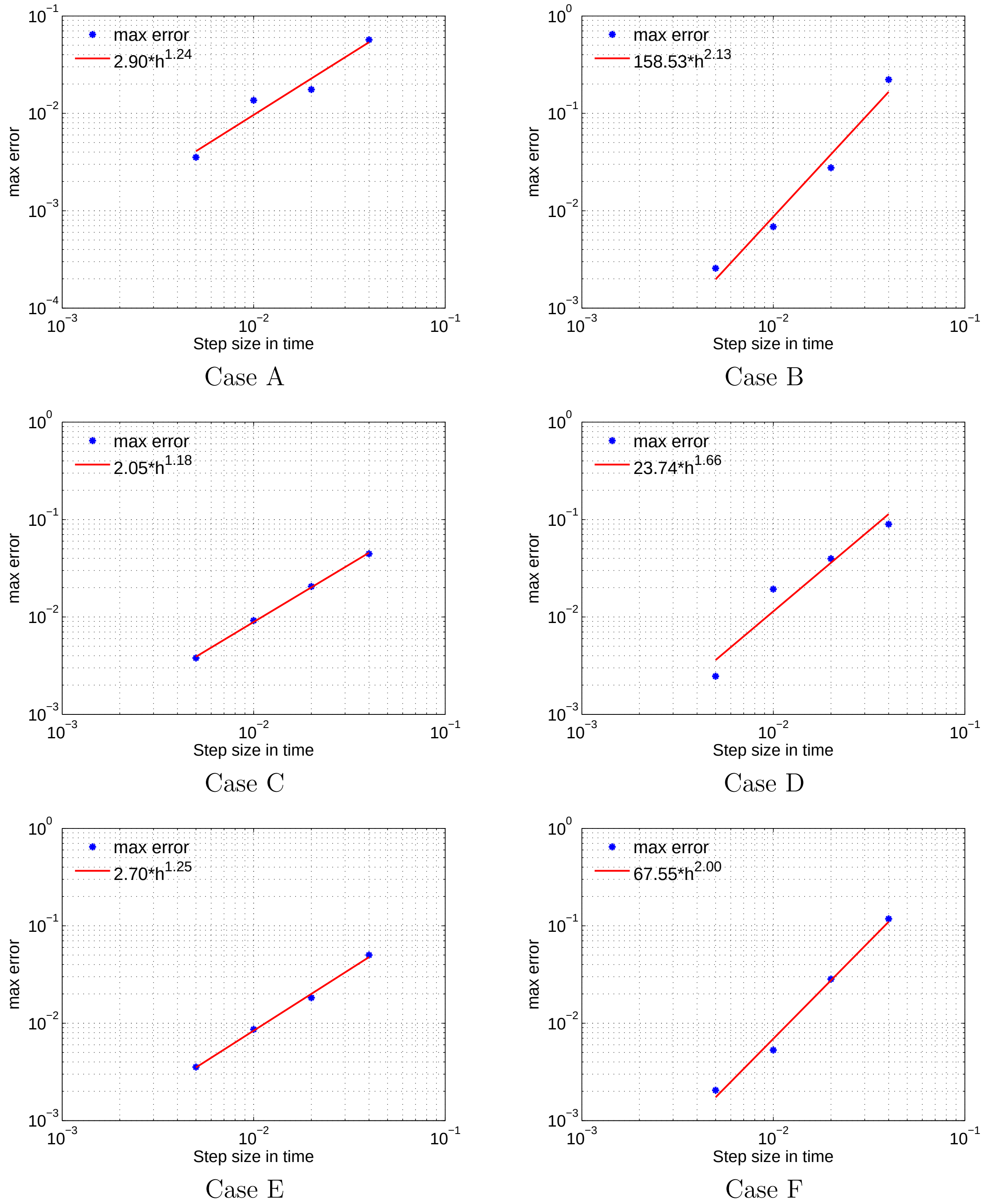

Figure 5.6: The rates of convergence for maximum absolute errors

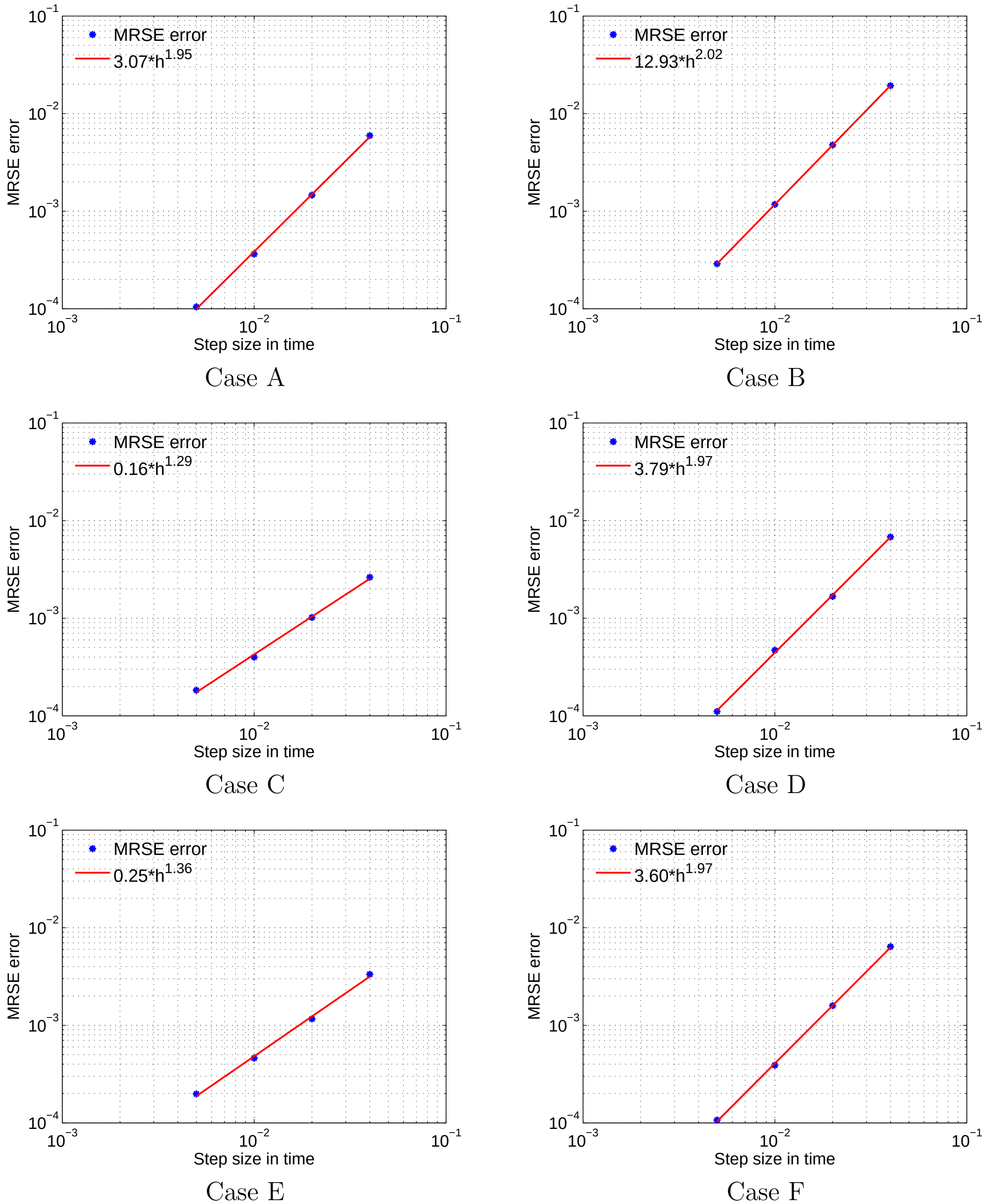

Figure 5.7: The rates of convergence for the root mean square errors

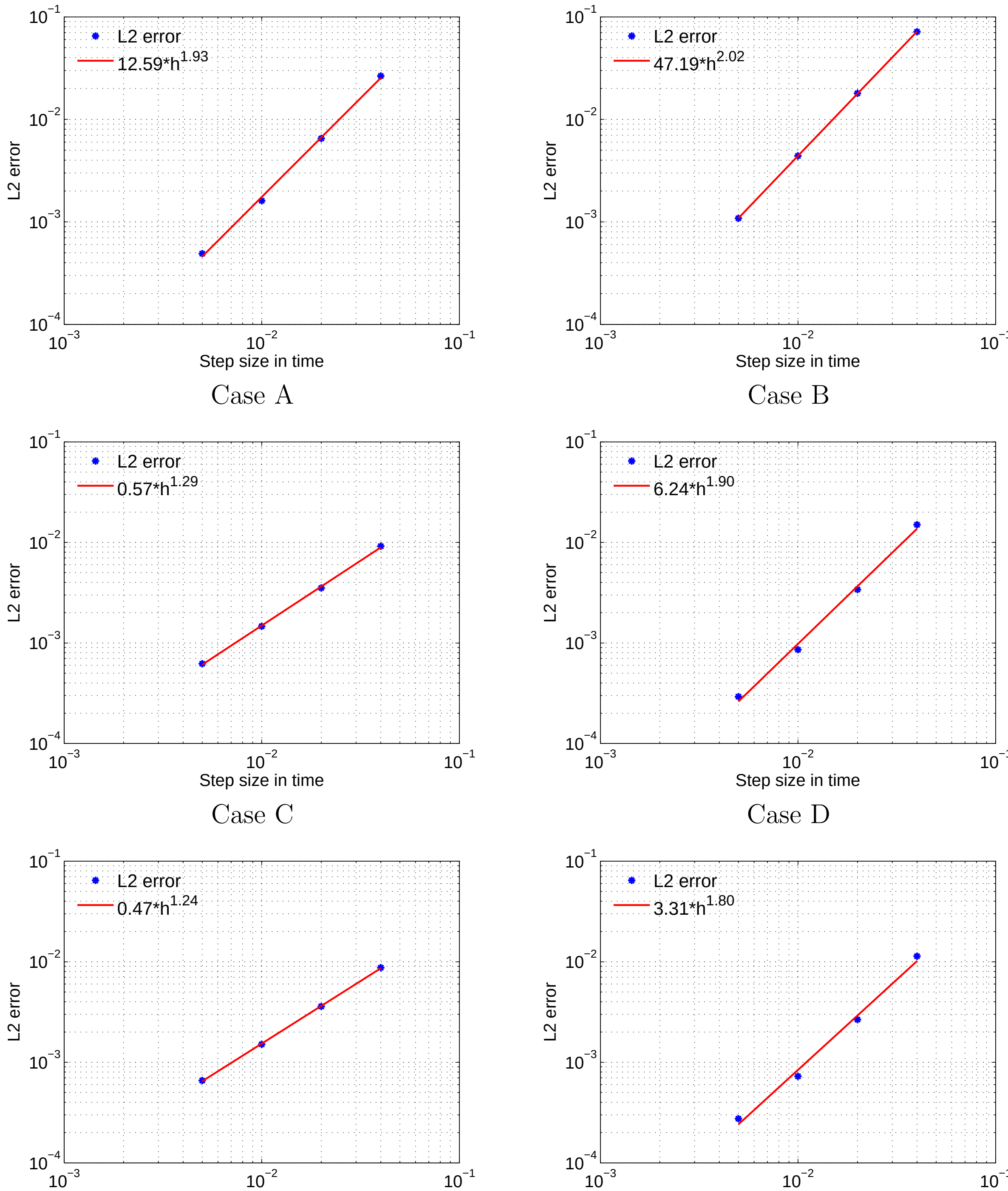

Case A

Case B

Case C

Case D

Case E

Case F

Figure 5.8: The rates of convergence for the L_2 errors

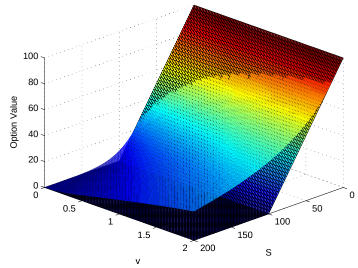

(a) $t = 0$

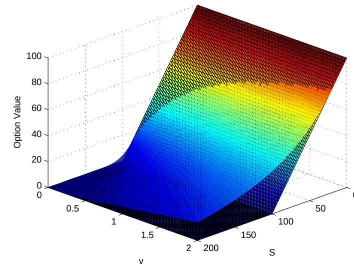

(b) $t = 0.5T$

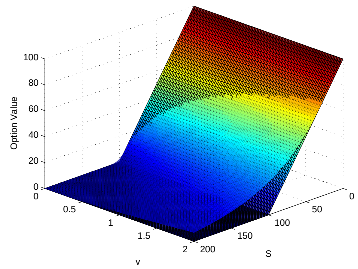

(c) $t = 0.75T$

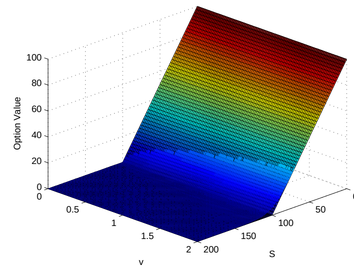

(d) $t = 0.99T$

Figure 5.9: The American put option prices: Case A

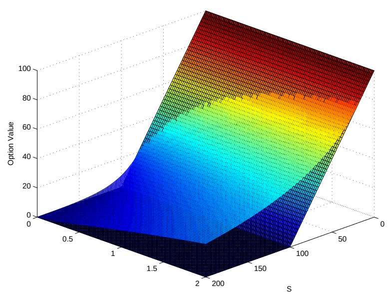

(a) $t = 0$

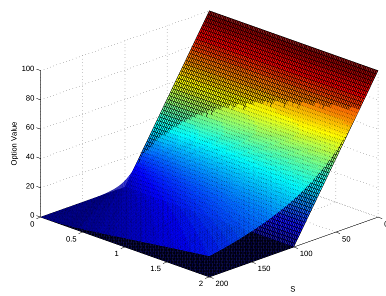

(b) $t = 0.5T$

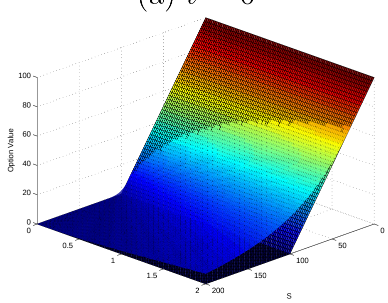

(c) $t = 0.75T$

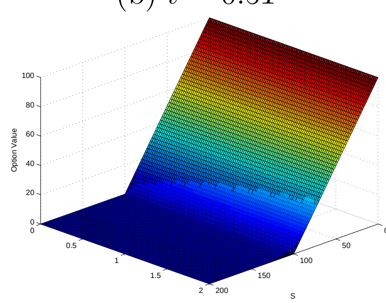

(d) $t = 0.99T$

Figure 5.10: The American put option prices: Case B

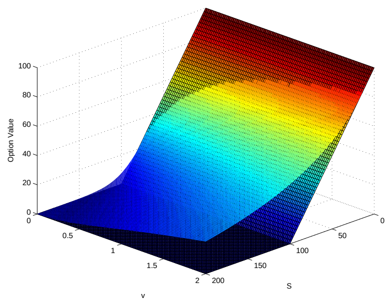

(a) $t = 0$

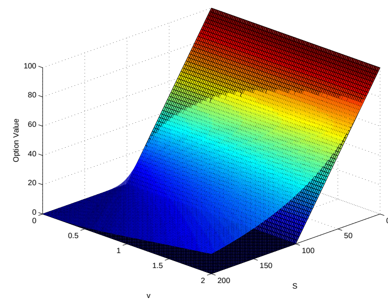

(b) $t = 0.5T$

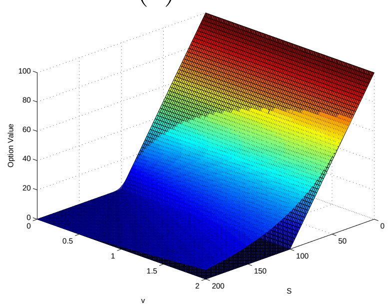

(c) $t = 0.75T$

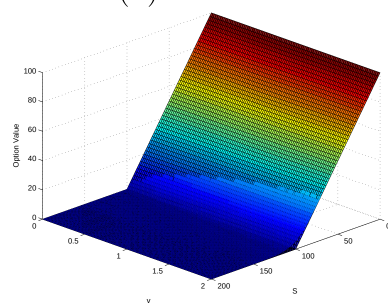

(d) $t = 0.99T$

Figure 5.11: The American put option prices: Case C

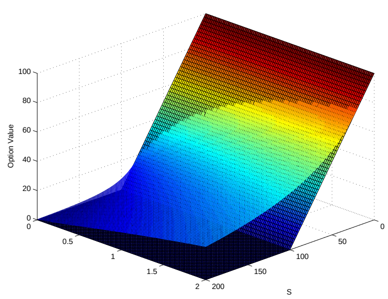

(a) $t = 0$

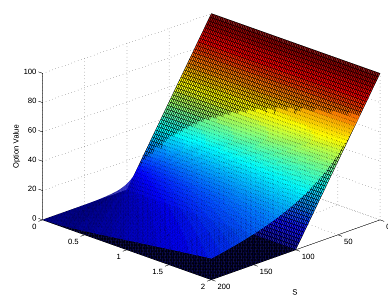

(b) $t = 0.5T$

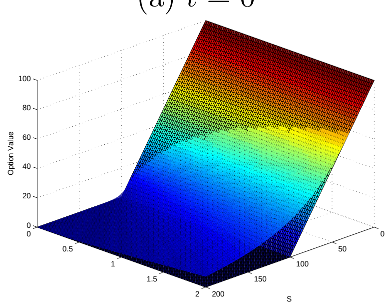

(c) $t = 0.75T$

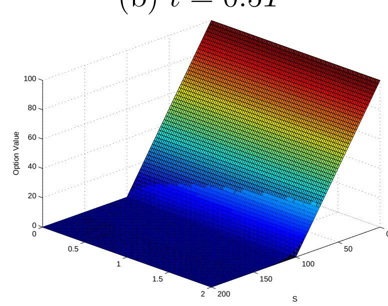

(d) $t = 0.99T$

Figure 5.12: The American put option prices: Case D

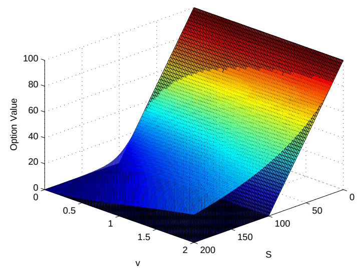

(a) $t = 0$

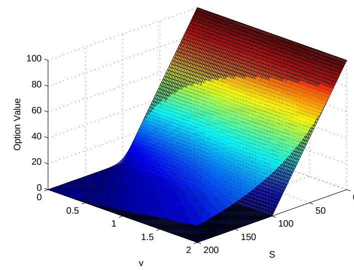

(b) $t = 0.5T$

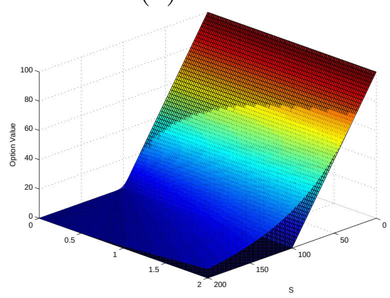

(c) $t = 0.75T$

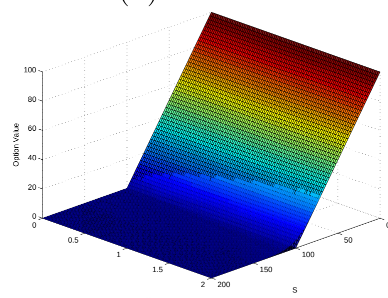

(d) $t = 0.99T$

Figure 5.13: The American put option prices: Case E

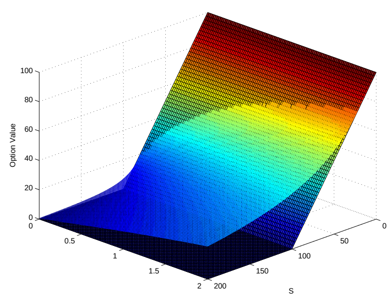

(a) $t = 0$

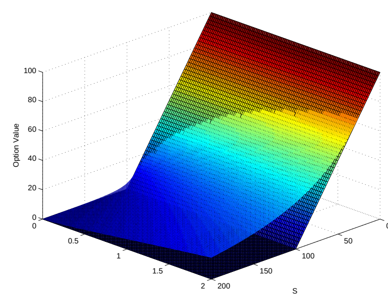

(b) $t = 0.5T$

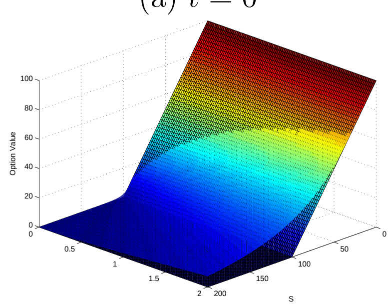

(c) $t = 0.75T$

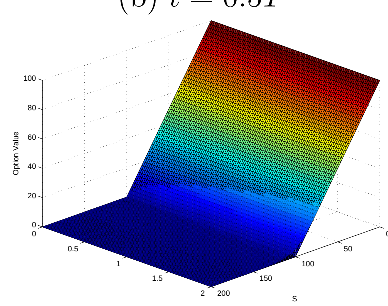

(d) $t = 0.99T$

Figure 5.14: The American put option prices: Case F

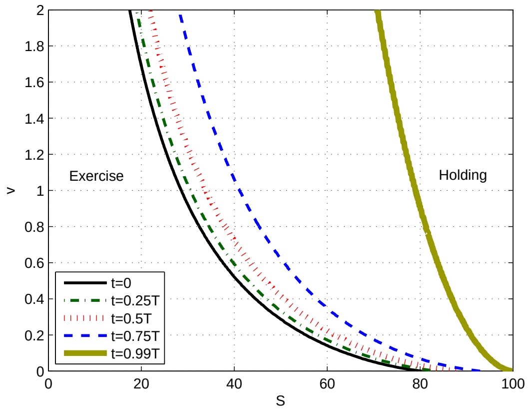

Case A

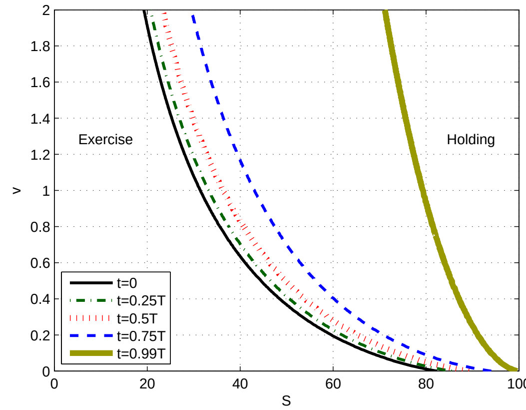

(b) Case B

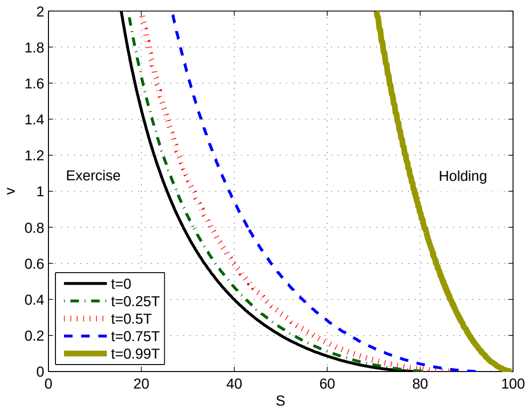

ase C

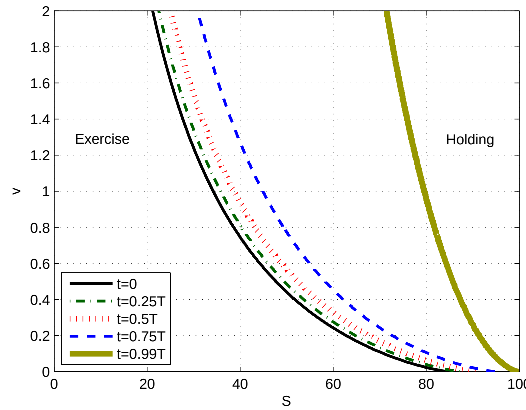

Case D

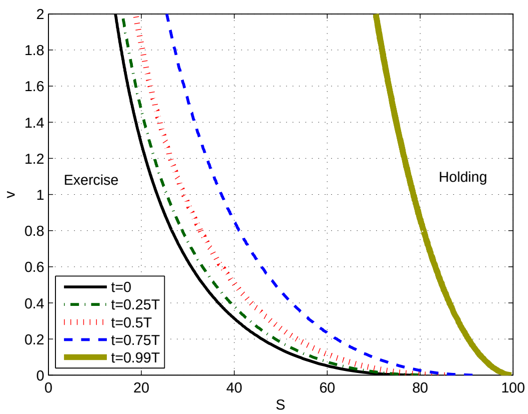

Case E

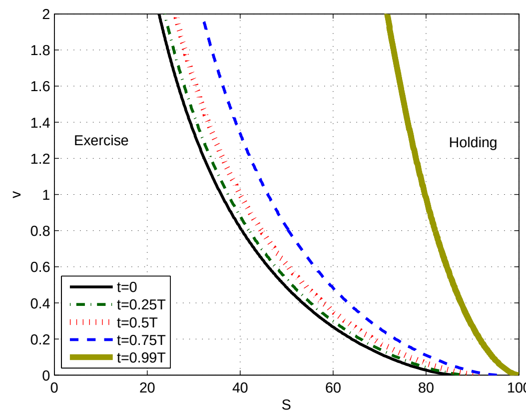

Case F

Figure 5.15: The early exercise boundaries for the American put options

Example 5.3. (*Comparison*) In this example, we compare the approximate option prices computed by our method and the others in the literatures. We consider two sets of the parameters in Table 5.9 as in [31]. The parameters of Case G satisfies the Feller condition ($2\kappa\eta > \sigma^2$) while Case H fails the condition.

Case	G	H
K	10	100
r	0.10	0.04
q	0.0	0.0
T	0.25	0.25
κ	5.00	1.15
η	0.16	0.0348
σ	0.9	0.39
ρ	0.1	-0.64

Table 5.9: Parameters for the Heston model for comparison

Here we choose the number of the steps such that the mesh size is 0.01 which is compatible to those in the reference papers. The approximate option prices are given in Tables 5.10–5.11 and Tables 5.12. The values in the first row are obtained by our method (FVADI). The other values are from Table 2-4 in [31] and the references therein. All the approximate option prices are compatible. However, the validations of the schemes are not carried out in the other papers as in our Example 5.1. Hence, we believe that our C++ codes should provide more accurate results.

S	8	9	10	11	12
FVADI	2.0000	1.1078	0.5200	0.2136	0.0821
Haentjens & Hout [31]	2.0000	1.1081	0.5204	0.2143	0.0827
Zvan, Forsyth & Vetzal [62]	2.0000	1.1076	0.5202	0.2138	0.0821
Ikonen & Toivanen [36]	2.0000	1.1076	0.5199	0.2135	0.0820
Persson & Von Sydow [52]	1.9998	1.1085	0.5195	0.2150	0.0822
Oosterlee [50]	2.00	1.107	0.517	0.212	0.0815
Clarke & Parrott [12]	2.0000	1.1080	0.5316	0.2261	0.0907
Vellekoop & Nieuwenhuis [59]	1.9968	1.1076	0.5202	0.2134	0.0815

Table 5.10: The American option prices for Case G: $v = 0.0625$

S	8	9	10	11	12
FVADI	2.0787	1.3339	0.7960	0.4483	0.2428
Haentjens & Hout [31]	2.0788	1.3339	0.7962	0.4486	0.2433
Zvan, Forsyth & Vetzal [62]	2.0784	1.3337	0.7961	0.4483	0.2428
Ikonen & Toivanen [36]	2.0785	1.3336	0.7959	0.4482	0.2427
Persson & Von Sydow [52]	2.0784	1.3333	0.7955	0.4479	0.2426
Oosterlee [50]	2.0790	1.3340	0.7960	0.4490	0.2430
Clarke & Parrott [12]	2.0733	1.3290	0.7992	0.4536	0.2502

Table 5.11: The American option prices for Case G: $v = 0.25$

S	90	100	110
FVADI	10.0042	3.2096	0.9288
Haentjens & Hout [31]	10.0039	3.2126	0.9305
Fang & Oosterlee [24] ,	9.9958	3.2079	0.9280

Table 5.12: The American option prices for Case H: $v = 0.0348$

CHAPTER 6

CONCLUSION

In this dissertation, we introduce a general transformation to decouple correlated stochastic processes governed by a system of stochastic differential equations and apply the new transformation to some popular two-factor models such as the two-asset model, the stochastic volatility model, and the stochastic interest rate models. The transformed stochastic processes are uncorrelated and result in simpler and more effective numerical implements. This transformation can extended to higher dimensional cases.

In Chapter 3, we develop a mixed Monte Carlo/analytic method for the European options under two-factor models (two-asset model, stochastic volatility model, stochastic interest rate models). A control variates technique based on the formulation is also applied. Numerical results show that the new method is very accurate and efficient.

In Chapter 4, we develop a lattice method for the European and American options under the two-asset model and the stochastic interest rate models. The numerical results show that the lattice method is convergent linearly as expected. We also examine the properties of the early exercise regions for the American options numerically.

In chapter 5, we develop a finite volume - alternating direction implicit method for American option under the Heston model (stochastic volatility). We validate the scheme, check the convergence and accuracy with several sets of parameters, and compare our result with other researches. We can conclude that our method is accurate and efficient.

For the future work, we will focus on the following topics:

1. Study the finite volume-ADI method to the option problems under the other two-factor models.

2. Apply the proposed methods in Chapters 3 and 4 to the stochastic volatility jump model (the Bates model [3]):

$$\frac{dS(t)}{S(t)} = (r-q)dt + \sqrt{v(t)}dW_2(t) + dZ(t),$$
$$dv(t) = \kappa\left[\eta - v(t)\right]du + \sigma\sqrt{v(t)}dW_1(t).$$

3. Consider the following popular three-factor models:

- The Fong-Vasicek model:

$$\frac{dS(t)}{S(t)} = (r(t)-q)dt + \sigma dW_1(t),$$
$$dr(t) = \kappa_r(\theta_r - r(t))dt + \sqrt{v(t)}dW_2(t),$$
$$dv(t) = \kappa_v(\theta_v - v(t))dt + \delta\sqrt{v(t)}dW_3(t).$$

- The stochastic interest rate and volatility model:

$$\frac{dS(t)}{S(t)} = (r(t)-q)dt + \sqrt{v(t)}dW_1(t),$$
$$dv(t) = \kappa\left[\eta - v(t)\right]du + \sigma\sqrt{v(t)}dW_2(t),$$
$$dr(t) = \kappa_r(\theta_r - r(t))dt + \delta dW_3(t).$$

- The interest rate swap model:

$$
\begin{aligned}
dr_d &= \lambda_d(\theta_d - r_d)dt + \sigma_d r_d^{\alpha} dW_1(t), \\
dr_f &= \lambda_f(\theta_f - r_f)dt + \sigma_d r_f^{\beta} dW_2(t), \\
\frac{dX}{X} &= (r_d - r_f)dt + \sigma_X dW_3(t).
\end{aligned}
$$

APPENDIX: THE ANALYTIC FORMULAS FOR $\widetilde{V}$

We first consider the spread option. Its payoff function is

$$\Phi\left(S_1(T), S_2(T)\right) = (S_1(T) - S_2(T) - K)^+.$$

Then (3.4) becomes

$$\begin{aligned}
\widetilde{V}\left(\widetilde{S}_2, z, t, T\right) &= \mathbb{E}\left[e^{-(T-t)r}\left(z - z^{\alpha}\widetilde{S}_2(T) - K\right)^+ \middle| \widetilde{S}_2(t) = \widetilde{S}_2\right] \\
&= z^{\alpha}\mathbb{E}\left[e^{-(T-t)r}\left(z^{-\alpha}(z-K) - \widetilde{S}_2(T)\right)^+ \middle| \widetilde{S}_2(t) = \widetilde{S}_2\right] \\
&= \begin{cases} 0, & \text{if } z - K < 0, \\ z^{\alpha}\mathbb{E}\left[e^{-(T-t)r}\left(\widetilde{K} - \widetilde{S}_2(T)\right)^+ \middle| Y(t,T), \mathcal{F}_t\right], & \text{if } z - K \geq 0, \end{cases} \\
&= \begin{cases} 0, & \text{if } z - K < 0, \\ z^{\alpha}e^{-r(T-t)}\widetilde{K}N(-d_2) - z^{\alpha}e^{-q(T-t)}\widetilde{S}_2N(-d_1), & \text{if } z - K \geq 0, \end{cases}
\end{aligned} \tag{6.1}$$

where

$$\begin{aligned}
\widetilde{K} &= z^{-\alpha}(z - K), \\
d_1 &= \frac{\ln(\frac{\widetilde{S}_2}{\widetilde{K}}) + \left(r - \tilde{q} + \frac{1}{2}\tilde{\sigma}^2\right)(T-t)}{\tilde{\sigma}\sqrt{T-t}}, \\
d_2 &= d_1 - \tilde{\sigma}\sqrt{T-t}.
\end{aligned}$$

It should be pointed out that the spread option becomes the exchange option when $K = 0$, which can be evaluated by the Margrabe's formula [46].

Next, we consider the classic two-assets call options. For the corresponding put options, the put-call parity can be applied. We have the following four payoff functions

$$\text{Call on max: } \Phi_1(S_1, S_2) = (\max(S_1, S_2) - K)^+ .$$

$$\text{Call on min: } \Phi_2(S_1, S_2) = (\min(S_1, S_2) - K)^+ .$$

$$\text{Maximum call: } \Phi_3(S_1, S_2) = \max\left((S_1 - K_1)^+, (S_2 - K_2)^+\right).$$

$$\text{Minimum call: } \Phi_4(S_1, S_2) = \min\left((S_1 - K_1)^+, (S_2 - K_2)^+\right).$$

The first two options are just the special cases of the last two options. Indeed, we have

$$\Phi_1(S_1, S_2) = (\max(S_1, S_2) - K)^+ = \max\left((S_1 - K)^+, (S_2 - K)^+\right),$$

$$\Phi_2(S_1, S_2) = (\min(S_1, S_2) - K)^+ = \min\left((S_1 - K)^+, (S_2 - K)^+\right).$$

Notice that

$$\begin{aligned}\Phi_3(S_1, S_2) &= \max\left((S_1 - K_1)^+, (S_2 - K_2)\right) \\ &= \left(S_2 - K_2 - (S_1 - K_1)^+\right)^+ + (S_1 - K_1)^+.\end{aligned}$$

We have for the maximum call option

$$\begin{aligned}\widetilde{V}\left(\widetilde{S}_2, z, t, T\right) &= \mathbb{E}\left[e^{-(T-t)r}\left(\left(z^\alpha \widetilde{S}_2(T) - K_2 - (z - K_1)^+\right)^+ + (z - K_1)^+\right) \middle| \widetilde{S}_2(t) = \widetilde{S}_2\right] \\ &= z^\alpha \mathbb{E}\left[e^{-(T-t)r}\left(\widetilde{S}_2(T) - \widetilde{K}\right)^+ \middle| \widetilde{S}_2(t) = \widetilde{S}_2\right] + e^{-r(T-t)}(z - K_1)^+,\end{aligned}$$

where

$$\widetilde{K} = z^{-\alpha}\left(K_2 + (z - K_1)^+\right).$$

Hence, we have by the Black-Scholes formula

$$\widetilde{V}\left(\widetilde{S}_2, z, t, T\right) = z^\alpha e^{-q(T-t)} \widetilde{S}_2 N(d_1) - z^\alpha e^{-r(T-t)} \widetilde{K} N(d_2) + e^{-r(T-t)}(z - K_1)^+,$$

where

$$\begin{aligned}d_1 &= \frac{\ln(\frac{\widetilde{S}_2}{\widetilde{K}}) + \left(r - \tilde{q} + \frac{1}{2}\tilde{\sigma}^2\right)(T - t)}{\tilde{\sigma}\sqrt{T - t}}, \\ d_2 &= d_1 - \tilde{\sigma}\sqrt{T - t}.\end{aligned}$$

Notice that

$$\begin{aligned}\Phi_4(S_1,S_2) &= (S_1-K_1)^+ + (S_2-K_2)^+ - h_3(S_1,S_2)\\ &= (S_2-K_2)^+ - \left(S_2-K_2-(S_1-K_1)^+\right)^+.\end{aligned}$$

We have for the minimum call option

$$\begin{aligned}&\widetilde{V}\left(\widetilde{S}_2,z,t,T\right)\\ =&\mathbb{E}\left[e^{-(T-t)r}\left(\left(z^\alpha\widetilde{S}_2(T)-K_2\right)^+ - \left(z^\alpha\widetilde{S}_2(T)-K_2-(z-K_1)^+\right)^+\right)\middle|\widetilde{S}_2(t)=\widetilde{S}_2\right]\\ =&z^\alpha\left(\mathbb{E}\left[e^{-(T-t)r}\left(\widetilde{S}_2(T)-\widetilde{K}_2\right)^+\middle|\widetilde{S}_2(t)=\widetilde{S}_2\right]-\mathbb{E}\left[e^{-(T-t)r}\left(\widetilde{S}_2(T)-\widetilde{K}_1\right)^+\middle|\widetilde{S}_2(t)=\widetilde{S}_2\right]\right),\end{aligned}$$

where

$$\widetilde{K}_1 = z^{-\alpha}\left(K_2+(z-K_1)^+\right),\ \widetilde{K}_2 = z^{-\alpha}K_2.$$

Hence, we have by the Black-Scholes formula

$$\widetilde{V}\left(\widetilde{S}_2,z,t,T\right) = z^\alpha\left(e^{-q(T-t)}\widetilde{S}_2\left(N(d_1)-N(d_3)\right)-e^{-r(T-t)}\left(\widetilde{K}_2N(d_2)-\widetilde{K}_1N(d_4)\right)\right),$$

where

$$\begin{aligned}d_1 &= \frac{\ln\left(\frac{\widetilde{S}_2}{\widetilde{K}_2}\right)+\left(r-\tilde{q}+\frac{1}{2}\tilde{\sigma}^2\right)(T-t)}{\tilde{\sigma}\sqrt{T-t}},\\ d_2 &= d_1-\tilde{\sigma}\sqrt{T-t},\\ d_3 &= \frac{\ln\left(\frac{\widetilde{S}_2}{\widetilde{K}_1}\right)+\left(r-\tilde{q}+\frac{1}{2}\tilde{\sigma}^2\right)(T-t)}{\tilde{\sigma}\sqrt{T-t}},\\ d_4 &= d_3-\tilde{\sigma}\sqrt{T-t}.\end{aligned}$$

BIBLIOGRAPHY

[1] W. Allegretto, Y. Lin, H. Yang, Finite element error estimates for a nonlocal problem in American option valuation, *SIAM J. Numer. Anal.*, **39** , pp. 834-857 (2001).

[2] K.I. Amin, R.A. Jarrow, Pricing options on risky assets in a stochastic interest rate economy, *Mathematical Finance*, **2(4)**, 217-237 (1992).

[3] D. Bates, Jump and stochastic volatility: exchange rate processes implicit in deutsche mark options, *Review of Financial Studies*, **9**, 69-107 (1996).

[4] N. Beliaeva, S. Nawalkha, A simple approach to pricing American options under the Heston stochastic volatility model. *Journal of Derivatives*, **17(4)**, 25-43 (2010).

[5] F. Black, M. Scholes, The pricing of options and corporate liabilities, *Journal of Political Economy*, **81(3)**, 637-54 (1973).

[6] P.P. Boyle, Options: A Monte Carlo approach, *Journal of Financial Economics*, **4(3)**, 323-338 (1977).

[7] P.P. Boyle, J. Evnine, S. Gibbs, Numerical evaluation of multivariate contingent claims, *Review of Financial Studies*, **2**, 241-250 (1989).

[8] P.P. Boyle, M. Broadie, P. Glasserman, Monte Carlo methods for security pricing, *Journal of Economic Dynamics & Control*, **21(8-9)** 1267-1321 (1997).

[9] M.J. Brennan, E.S. Schwartz, Finite difference method and jump processes arising in the pricing of contingent claims, *Journal of Financial and Quantitative Analysis*, **13**, 461-474 (1978).

[10] M. Broadie, J. Detemple, The valuation of American options on mutiple assets, *Mathematical Finance*, **7(3)**, 241-286 (1997).

[11] P. Carr, M. Chesney, American put call symmetry, preprint, (1996).

[12] N. Clarke, K. Parrott, Multigrid for American option pricing with stochastic volatility, *Applied Mathematical Finance*, **5(3)**, 177-195 (1999).

[13] J.C. Cox, J.E. Ingersoll, S.A, Ross. A Theory of the term structure of interest rates, *Econometrica*, **53**, 385-408 (1985).

[14] R. Cont, Empirical properties of asset returns: stylized facts and statistical issues, *Quantitative Finance*, **1**, 223-236 (2001).

[15] J.C. Cox, S.A. Ross, M. Rubinstein, Option pricing: A simplified approach, *Journal of financial Economics*, **7(3)**, 229-263 (1979).

[16] A. Cozma, C. Reisinger, A mixed Monte Carlo and partial differential equation variance reduction method for foreign exchange options under the Heston-Cox-Ingersoll-Ross model, *Journal of Computational Finance*, **20(3)**, 109-149 (2017).

[17] M. Curran, Valuing asian and portfolio options by conditioning on the geometric mean price, *Manag. Sci.*, **40**, 1705-1711 (1994).

[18] D.M.Dang, C.C.Christara, K.R.Jackson, Pricing multi-asset American options on Graphics Processing Units using a PDE approach, *High Performance Computational Finance (WHPCF)*, IEEE Workshop (2010).

[19] J. Detemple, American options: Symmetry properties, *Option pricing, interest rates and risk management*, Cambridge University Press, Cambridge, UK, 67-104, (2001).

[20] J. Detemple, *American-style derivatives: Valuation and computation*, Chapman & Hall/CRC, Taylor & Francis Group, 2006.

[21] J.N. Dewynne, S.D. Howison, I. Rupf, P. Wilmott, Some mathematical results in the pricing of American options, *European Journal of Applied Mathematics*, **4**, 381-398 (1993).

[22] R.F. Donnelly, S. Jaimungal, D. Rubisov, Valuing GWBs with stochastic interest rates and volatility, *Quantitative Finance* (2012).

[23] H. Fang, European option pricing formula under stochastic interest rate, *Progress in Applied Mathematics*, **4(1)**, 14-21 (2012).

[24] F. Fang, C.W. Oosterlee, A Fourier-based valuation method for Bermudan and barrier options under Heston model, *SIAM J. Finan. Math.*, **2**, 439-463 (2011).

[25] N.P. Firth, High dimensional American options, *Ph.D thesis*, Brasenose College, University of Oxford, (2005).

[26] H.G. Fong, O.A. Vasicek, Fixed income volatility management, *Journal of Portfolio Management*, summer, 41-46 (1991).

[27] A. Gamba, L. Trigeorgis, An improved binomial lattice method for mmulti-dimensional options, *Applied Mathematical Finance*, **14**, 453-475 (2007).

[28] P. Glasserman, *Monte Carlo Methods in Financial Engineering*, Springer-Verlag, New York, 2004.

[29] L.A. Grzelak, C.W. Oosterlee, On the Heston model with stochastic interest rates, *SIAM J. Finan. Math.*, **2(1)**, 255-286 (2011).

[30] S.T. Haentjens, K.J. in 't Hout, ADI finite difference schemes for the Heston-Hull-White PDE, *The Journal of Computational Finance*, **16**, 83-110 (2012).

[31] S.T. Haentjens, K.J. in 't Hout, ADI schemes for pricing American options under the Heston model, *Appl. Math. Finan.*, **22**, 207-237 (2015).

[32] A. Harel, G. Harpaz, J.C. Francis, Pricing futures on geometric indexes: a discrete time approach, *Rev. Quant. Financ. Account.*, **28**, 227-240 (2007).

[33] S. Heston, A closed-form solution for options with stochastic volatility with applications to bond and currency options, *Review of Financial Studies*, **6**, 327-343 (1993).

[34] J. Hull, *Options, Futures, and Ohter Derivatives (8th edition)*, Prentice Hall, 2011.

[35] W. Hundsdorfer, J. Verwer, *Numerical Solution of Time-Dependent Advection-Diffusion-Reaction Equations*, Springer Berlin Heidelberg, 2003.

[36] S. Ikonen, J. Toivanen. Operator splitting methods for pricing American options under stochstic volatility, *Numer. Math.*, **113** 299-324 (2009).

[37] H. Johnson, Options on the maximum or the minimum of several assets, *Journal of Financial and Quantitative Analysis*, **22(3)**, 277-283 (1987).

[38] Y. Kim, N. Kunitomo, Pricing options under stochastic interest rates: A new approach, *Asia-Pacific Financial Markets*, **6**, 49-70 (1999).

[39] N.V. Krylov, *Controlled diffusion processes*, Springer, New York, 1980.

[40] Y.K. Kwok, *Mathematical Models of Financial Derivatives, 2nd edition*, Springer Finance, 2008.

[41] P. Kovalov, V. Linetsky, M. Marcozzi, Pricing multi-asset American options: A finite element method-of-lines with smooth penalty, *J Sci Comput*, **33**, 209-237 (2007).

[42] D.P. Leisen, Stock evolution under stochastic volatility: A discrete approach, *Journal of Derivatives*, Winter, 9-27 (2000).

[43] S. Levendorskii, Efficient pricng and reliable calibration in the Heston model, *Int. J. Theor. Appl. Finan.*, **15**, 1250050 (2012).

[44] G. Loeper, O. Pironneau, A mixed PDE/Monte-Carlo method for stochastic volatility models, *C. R. Acad. Sci. Paris*, **I 347**, 559-563 (2009).

[45] F.A. Longstaff, E.S. Schwartz, Valuing American options by simulation: A simple least-squares approach, *Revieiw of Financial Studies*, **14**, 113-147 (2001).

[46] W. Margrabe, The value of an option to exchange one asset for another, *The Journal of Finance*, **33**, 177-186 (1978).

[47] A. Medvedev, O. Scaillet, Pricing American options under stochastic volatility and stochastic interest rates, *Journal of Financial Economics*, **98(1)**, 145-159 (2010).

[48] R. Merton, Theory of rational option pricing, *Bell Journal of Economics and Management Science*, **4(1)**, 141-183 (1973).

[49] R. Merton, Option pricing when underlying stock returns are discontinuous, *J. Financial Economics*, **3**, 125-144 (1976).

[50] C. W. Oosterlee, On multigrid for linear complementarity problems with application to American-style options, *Elec. Trans. Numer. Anal.*, **15**,165-185 (2003).

[51] D.W. Peaceman, H.H. Rachford Jr, The numerical solution of parabolic and elliptic differential equations, *Journal of the Society for Industrial and Applied Mathematics*, **3(1)**, 28-41 (1955).

[52] J. Persson, L. von Sydow, Pricing American options using a space-time adaptive finite difference method, *Math. Comp. Simul.*, **80**, 1922-1935 (2010).

[53] P. Ritchken, R. Trevor, Pricing Options under generalized GARCH and stochastic volatility process, *Journal of Finance*, **54(N1)**, 377-402 (1999).

[54] S.E. Shreve, *Stochastic Calculus for Finance II Continuous-Time Models (2nd edition)*, Springer Finance, 2004.

[55] H. Stoll, The relationship between put and call option prices, *Journal of Finance*, **24(5)**, (1969)

[56] R. M. Stulz, Options on the minimum or the maximum of two risky assets,*Journal of Financial Economics*, **10**, 161-185 (1982).

[57] D. Tavella, C. Randall, *Pricing Financial Instruments: The Finite Difference Method*, John Wiley & Sons, New York, 2000.

[58] O. Vasicek, An equilibrium characterization of the term structure, *J. Financial Economics*, **5**, 177-188 (1977).

[59] M. Vellekoop, H. Nieuwenhuis, A tree-based method to price American options in the Heston model, *J. Comp. Finan.*, **13**, 1-21 (2009).

[60] S. Villeneuve, Exercise regions of American options on several assets, *Finance and S-tochastics*, **3(3)**, 295-322 (1999).

[61] S. Villeneuve, A. Zanette, Parabolic ADI methods for pricing American options on two stocks, *Math. Oper. Res.*, **27**, 121-149 (2002).

[62] R. Zvan, P.A. Forsyth, K.R. Vetzal. Penalty methods for American options with stochastic volatility, *Journal of Computational and Applied Mathematics*, **91**, 199-218 (1998).

CURRICULUM VITAE

Graduate College
University of Nevada, Las Vegas

Jiacheng Cai

Degrees:
Bachelor of Science - Mathematics, 2011
University of Science and Technology of China, China

Dissertation Title:
Numerical Methods for Option Pricing under the Two-Factor Models

Dissertation Examination Committee:
Chairperson, Hongtao Yang, Ph.D.
Committee Member, Michael Marcozzi, Ph.D.
Committee Member, Monika Neda, Ph.D.
Committee Member, Pengtao Sun, Ph.D.
Graduate Faculty Representative, Jianzhong Zhang, Ph.D.